Purification, Identification and Characterization of Mammalian Endoribonucleases that Degrade *c-myc* mRNA *in vitro*

Tavish Richard MacKay Barnes

B.Sc., University of Northern British Columbia, 2005

Thesis Submitted in Partial Fulfillment of

The Requirements for the Degree of

Master of Science

in

Mathematical, Computer and Physical Sciences

(Chemistry)

The University of Northern British Columbia

May 2007

Your file Votre référence
ISBN: 978-0-494-48825-6
Our file Notre référence
ISBN: 978-0-494-48825-6

Abstract

Tavish Barnes

There is increasing evidence that mammalian endoribonucleases play a significant role in the degradation of messenger RNA (mRNA) and are key players in the regulation of gene expression particularly under conditions of cellular stress.

The main goal of this thesis was to re-purify and conclusively identify the mammalian hepatic-derived endoribonuclease(s) and the proteins that co-purified with endonucleolytic activity against *c-myc* CRD RNA *in vitro*. The first aim of this investigation was to purify and identify enzyme(s) responsible for endoribonucleolytic activity. The second aim of this study was to further characterize the endoribonuclease(s) and to confirm the identity of the enzyme(s) by immunodepleting native endoribonuclease activity. The third aim of this study was to test the recombinant 35 kDa endoribonuclease (APEI) for endoribonuclease activity. This study demonstrated that recombinant APEI does possess endoribonuclease activity and cleaves specifically at dinucleotide UA 1751 of *c-myc* CRD RNA.

TABLE OF CONTENTS

CHAPTER 2 – Purification and Identification of Two Distinct Mammalian Hepatic Endoribonucleases with the Ability to Degrade *c-myc* CRD RNA *in vitro*

CHAPTER 3 – Identification and Characterization of the 35 kDa and 17 kDa Hepatic Endoribonucleases

List of Tables

List of Figures

Acknowledgements

There are numerous people who I would like to thank for contributing to both my personal growth and the development of my skills as a biochemist while completing my MSc. at UNBC. First and foremost, I would like to acknowledge my mom Janice Barnes and dad Harvey Barnes. They have given me unwavering love and support throughout my academic endeavors and life adventures. I would like to thank my supervisor Dr. Chow Lee for his insights, and encouragement throughout my research and while writing this thesis. I would like to thank Dan Sparanese who provided great friendship and many hours of knowledge during the first year of my MSc research. Many thanks to Tyler Bassett, Ric Bennett, Stephanie Sellers and all other members of the Lee lab for their support and camaraderie throughout my MSc.

I would like to thank the members of my supervisory committee, Dr. Stephen Rader and Dr. Brent Murray for providing their insights throughout the course of my studies. I would also like to extend my gratitude to Dr. Andrea Gorrell for patiently providing guidance and technical support.

All of these individuals and numerous others not mentioned here have made my time at UNBC most memorable and rewarding.

Relevant Academic Discussions

Articles

Barnes TR, and Lee CH. (2007) Identification of APE1 as the Novel Mammalian Endoribonuclease that Cleaves *c-myc* CRD RNA *In Vitro* (*Manuscript in preparation)*

Barnes TR, and Lee CH. (2007) Mammalian endoribonucleases: Multifunctional proteins with Diverse Roles in RNA Metabolism and Messenger RNA Decay. *Federation of European Biochemical Societies (Submitted)*

Abstracts

Barnes TR, and Lee CH. Purification and characterization of a novel 35 kDa RNase 1-like endonuclease that cleaves *c-myc* mRNA *in vitro.* American Association for Cancer Research Annual Meeting, Los Angeles CA (2007)

CHAPTER 1

Introduction

1.1 Messenger RNA Regulation and Gene Expression- An Overview

The many complexities involved in the processes required for gene expression necessitates an understanding of a diverse set of cellular pathways. One such gene regulatory pathway is the process of mRNA (messenger RNA) degradation. Identifying the mechanisms and players involved in the regulation of mRNA decay has become paramount in our understanding of gene expression. The control of gene expression occurs at various levels including: transcriptional, post-transcriptional and translational levels. Cytosolic levels of mRNA transcripts are generally believed to be an indicator of gene expression levels; moreover, the longer an mRNA persists in the cytosol, the higher the levels of protein expression (Dodson and Shapiro 2002). The stability of different mRNAs within a cell can vary by orders of magnitude and thus contribute greatly to differential gene product levels (Parker and Song 2004). The stability of individual mRNAs can be regulated in response to a variety of stimuli, allowing for rapid alterations in gene expression (Parker and Song 2004; Wilusz and Wilusz 2004; Khodursky and Bernstein 2003; Brewer 2002; Guhaniyogi and Brewer 2001).

A number of elements contribute to the stability of a given mRNA. The m^7G (methyl guanosine) cap at the 5' termini of the mRNA and the poly (A) tail at the 3' termini of the transcript provide the basic level of transcript stability. Specific *cis* elements also contribute to mRNA transcript stability. Stability elements of many mRNAs are located within the 3'-untranslated region (3'-UTR) of the transcript. It has become increasingly clear that higher-order structures of RNA and *trans*-acting proteins,

such as RNA-binding proteins, ribonucleases and RNA helicases are the critical determinants of mRNA longevity; moreover, *cis*-determinants, *trans*-acting factors, and a variety of secondary structural features inherent in the transcript determine the accessibility for cleavage by cellular exonucleases and endoribonucleases (Dodson and Shapiro 2002; Coburn and Mackie 1999; Mackie 1998). The following review sections will examine the various pathways involved in the control and processes governing mRNA degradation. Specific emphasis will be given to the family of endoribonuclease proteins that initiate mRNA degradation from within the sequence. These review sections will serve as a framework for the investigations within this thesis. Specifically, this thesis aims at identifying and exploring the properties of a novel mammalian endoribonuclease that possesses the ability to degrade *c-myc* mRNA *in vitro*.

1.2 Generalized Mechanisms and Pathways of Messenger RNA Decay

The core mRNA degradation pathways and quality control mechanisms governing RNA decay and processing have been well-characterized in bacteria, lower eukaryotes (predominantly using *Saccharomyces sereviciae*) and higher eukaryotes-albeit to a lesser extent. Core mRNA degradation events can be classified into a defined number of pathways. Consequently, the mRNA regulatory functions involved in gene expression within the cell direct the initial events of mRNA degradation into one of these defined pathways (see Figure 1). The major degradation pathways appear to be as follows: deadenylation-dependent removal of the poly (A) tail at the 3' terminus of the mRNA transcript followed by 3'-5' exonucleolytic decay, deadenylation-dependent removal of the poly (A) tail followed by decapping and 5'-3' exonucleolytic decay, deadenylation-independent 5' decapping and 5'-3' exonucleolytic degradation, nonsense-mediated

decay, and endoribonucleolytic degradation (Figure 1) (Parker and Song 2004; Guhaniyogi and Brewer 2001). In addition, there exists several decay pathways in what are termed mRNA-surveillance mechanisms (Garneau *et al.* 2007) (Figure 2). A more detailed account of each of these pathways will be discussed shortly.

The enzymes that are responsible for cleavage of mRNA *in vivo* and *in vitro* can be classified into two broad categories; the exoribonucleases and the endoribonucleases. The exoribonucleases cleave between consecutive nucleotides, starting at either the 5'- or the 3' end of an RNA strand (Gerlt 1993). In contrast, endoribonucleases are capable of cleaving the internal phosphodiester bonds in an RNA strand (Gerlt 1993). Exoribonucleases generally do not recognize specific RNA targets but degrade any RNA that is single-stranded. In contrast, endoribonucleases differ greatly among each other in their individual substrate specificities. Furthermore, endonucleases possess diverse functionality in the processing of RNA. Their function ranges from the generation of 3' ends of mRNAs to processing tRNAs, microRNA's, small nuclear RNAs and nucleolar RNAs. Endoribonuclease recognition of RNA sequences displays a range of specificity (Dodson and Shapiro 2002). For example, RNases T2 and V1 exhibit cleavage of the bonds between nucleotides in a single- or double-stranded configuration, respectively; thus exhibit little sequence specificity (Lockard and Kumar 1981). RNase 1 and RNase T1 exhibit some degree of sequence specificity as they cleave 3' to single-stranded pyrimidines and G-residues, respectively (Czaja *et al.* 2004; Thompson *et al.* 1995). In addition, more complex recognition determinants are required for cleavage. Bacterial RNase E cleaves single-stranded regions near the 5'-terminus (close to the translation initiation site). It specifically cleaves upstream of 5' secondary structural features of

target mRNA and generates fragments that can be degraded by 3'-5' exonucleases and by RNase E itself (Coburn and Mackie 1998). In addition, studies have shown that RNase E preferentially cleaves 5' to AU dinucleotides within A/U-rich regions (Coburn and Mackie 1998; Mackie 1998).

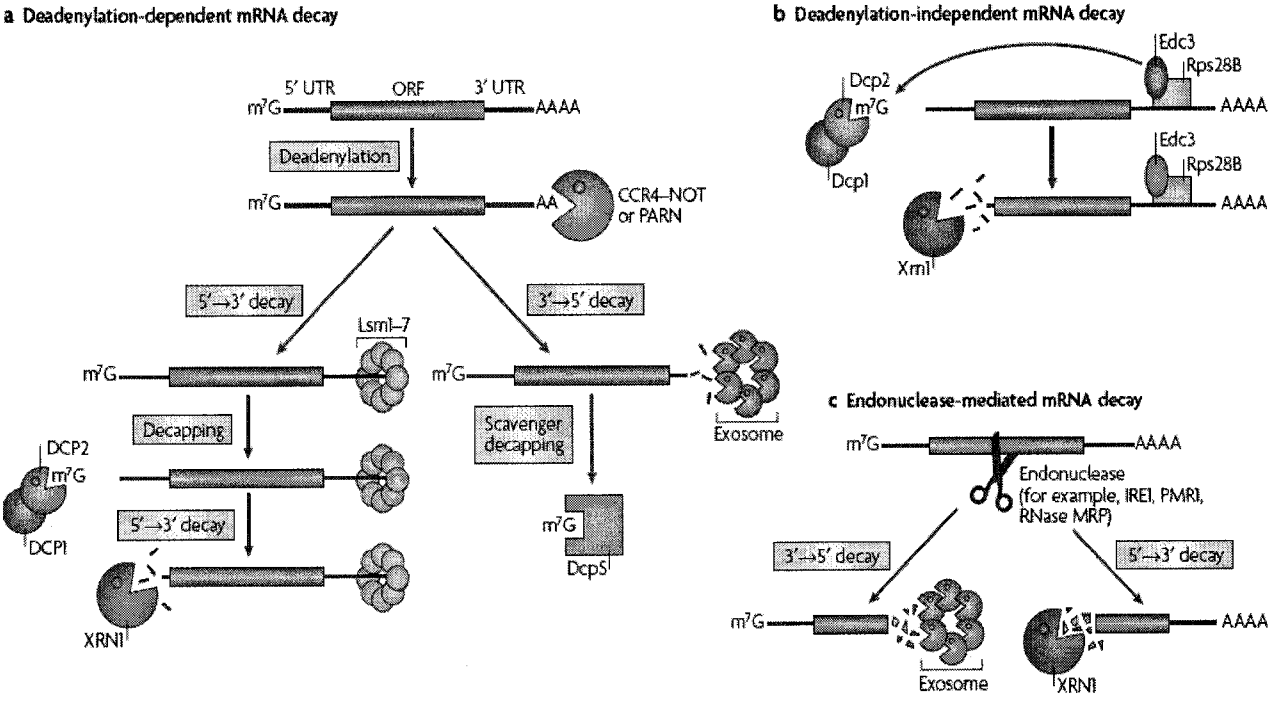

Figure 1: A schematic representation of the normal pathways of mRNA degradation in yeast (Garneau *et al.* 2007)

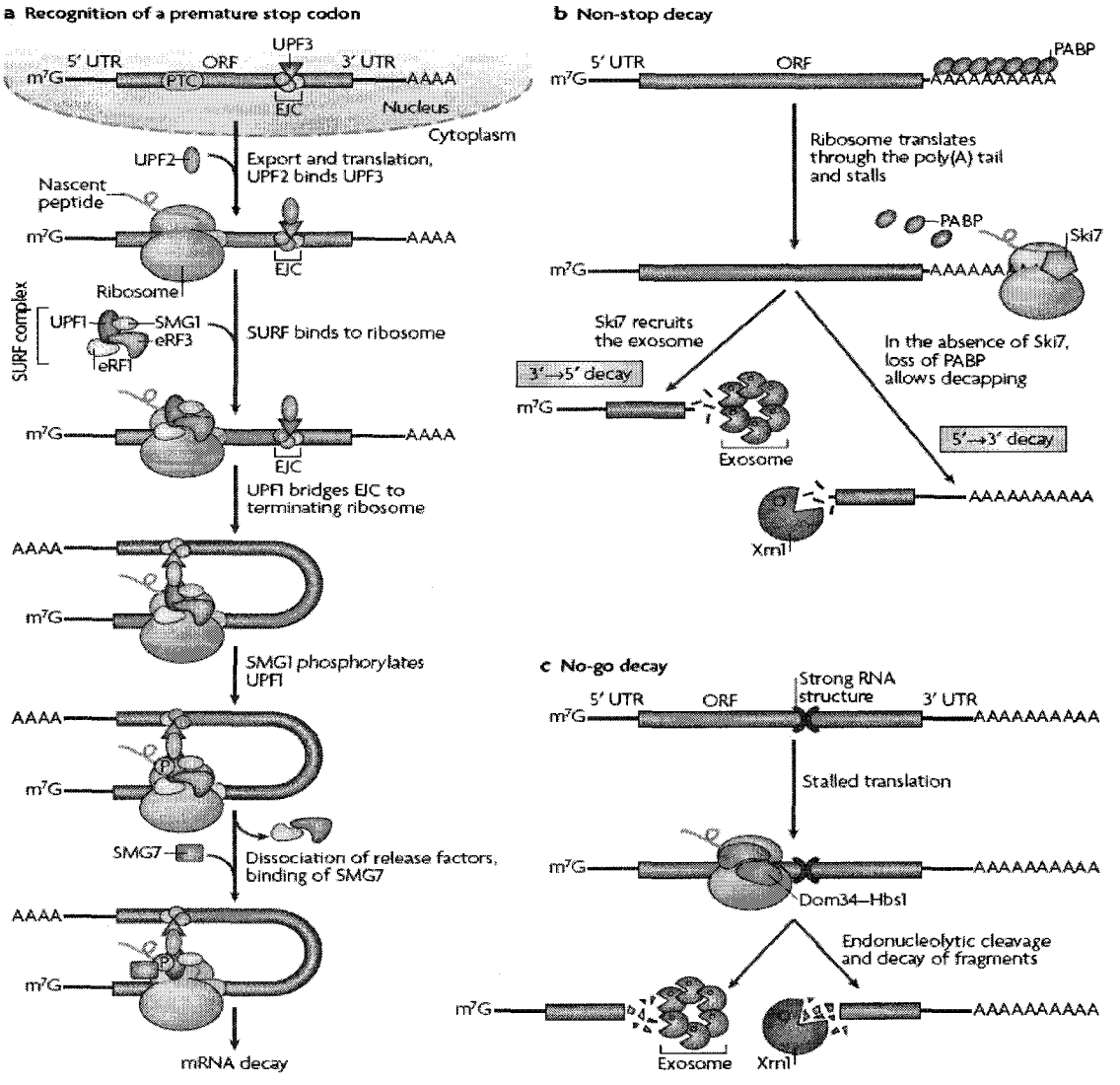

Figure 2: A schematic representation of the specialized surveillance mechanisms of mRNA degradation in yeast (Garneau *et al.* 2007)

1.2.1 Messenger RNA Decay in Prokaryotes (Bacteria)

A significant amount of research within the field of prokaryotic mRNA turnover has been based on studies using the simple bacteria *Escherichia coli* as the primary model organism. Initially it was believed that the processes that operated within these systems would be true of any organism. However, it is now abundantly clear that there are many

differences between the mechanistics of mRNA metabolism in prokaryotes and that of eukaryotic cells. Prokaryotic mRNA is accessible to the protein synthetic machinery as soon as it is transcribed from DNA. Since translation and transcription occur somewhat simultaneously, bacterial mRNA is utilized very rapidly. This process is highly efficient since many genes can be transcribed together in a single polycistronic mRNA, consequently mRNAs generally have relatively short half-lives. Bacterial RNA transcripts initially possess a triphosphate at the 5' end and a stem-loop structure at the 3' end. In *E. coli*, the degradation of most mRNAs is thought to begin with internal cleavage by RNase E, an endonuclease that cuts RNA in single-stranded regions that are AU-rich (Mudd *et al.*1990; Babitzke and Kushner 1991; Melefors and von Gabain 1991; Taraseviciene *et al.* 1991; McDowall *et al.* 1994). Less frequently, mRNA decay in *E. coli* starts with cleavage by another endonuclease, such as RNase III, RNase G, or RNase P (Schmeissner *et al.* 1984; Portier *et al.* 1987; Umitsuki *et al.* 2001; Li and Altman 2003). The transcript is no longer protected by the 3' stem-loop, and the resulting endonuclease-mediated cleavage products with monophosphorylated 5' termini are rapidly degraded by 3' exonucleases (Mackie 1998; Feng and Cohen 2000). The downstream endonuclease-mediated cleavage products can also undergo further endonucleolytic cleavage as RNase E exhibits a strong preference for monophosphorylated RNA substrates (Mackie 1998; Feng and Cohen 2000). Intriguingly, RNase E has been shown to function within a large multiprotein complex termed the RNA degradosome (Regonesi *et al.* 2006). In addition to RNase E, the degradosome contains the exoribonuclease polynucleotide phosphorylase (PNPase), an RNA helicase RhlB, and enolase that functions within the glycolytic pathway (Jain 2002;

Kushner 2002). A number of other endoribonucleases also participate in the mRNA decay processes although their involvement is believed to be considerably less important. These include RNase G, a known homolog of RNase E (Li and Deutscher 1994), RNase III which acts on double stranded RNA substrates (Li and Deutscher 1994), RNase P which acts predominantly on tRNA precursors but has been shown to possess the ability to cleave several polycistronic operon mRNAs *in vitro* in *E. coli* (Li and Deutscher 1994) and several bacterial toxins such as RelE, MazF, Kid and PemK (Li and Deutscher 1994; Zhang *et al.* 2004). The major endoribonucleases present in *E. coli* are shown in Table 1. 5'-3' exonucleases are not thought to participate in bacterial mRNA degradation, as no such ribonucleases have been identified in any prokaryotic organism (Deana and Belasco 2005). There are, however, three major 3'-5' exoribonucleases in *E. coli*: PNPase, RNase II, and oligoribonuclease as shown in Table 1, that appear to be involved in mRNA decay (Li and Deutscher 1994). RNase II, is a hydrolytic enzyme that removes nucleoside monophosphates from an RNA (Li and Deutscher 1994). PNPase is a phosphorolytic enzyme that utilizes inorganic phosphate to remove nucleotides from RNA ends, yielding nucleoside diphosphates (Carpousis *et al.* 1994; Blum *et al.* 1997). Oligoribonuclease functions to degrade small oligonucleotide substrates (4-7 nt) to mononucleotides and has been shown to be essential for cell viability (Yu and Deutscher 1995; Ghosh and Deutscher 1999). Additionally, the enzyme RNase R has been implicated in exoribonucleolytic decay of repetitive extragenic palindromic (REP) sequences in prokaryotic and eukaryotic systems (Cheng and Deutscher 2005; Baker and Condon 2004; Deutscher 2003).

Table 1: A summary of the major mRNA degrading endo- and exo-ribonucleases present in *E. coli*. (Steege 2000)

Enzyme	Gene	Monomer size (kDa)	Electrophoretic mobility (kDa) on SDS-PAGE	Subunit structure	Reference
		A. Endoribonucleases			
RNase E	*rne*	118	180	dimer ?	Coburn et al., 1999
RNase G	*rng (cafA/mre)*	55	55	?	
RNase III	*rnc*	25	25	α2 dimer	Dunn, 1976
		B. 3′ → 5′ Exoribonucleases			
RNase II	*rnb*	72.5	72.5	monomer	Gupta et al., 1977
Polynucleotide phosphorylase	*pnp*	77	85	α3 trimer	Portier, 1975; Soreq & Littauer, 1977
Oligoribonuclease	*orn*	20.7	20	α2 dimer	Ghosh & Deutscher, 1999; Zhang et al., 1998

1.2.2 Messenger RNA Decay in Lower Eukaryotes (*Saccharomyces cerevisiae*)

Much of our current knowledge of eukaryotic mRNA decay systems stems from research using yeast, specifically, *Saccharomyces cerevisiae*. In contrast to prokaryotic mRNA turnover, transcription in eukaryotes occurs in the nucleus and translation generally occurs in the cytoplasm, a circumstance that imposes spatial barriers between the transcription and translation processes. These barriers are further enhanced by the necessity of splicing intervening sequences from most eukaryotic transcripts prior to translation. As a result, the primary transcripts, which generally code for a single protein, must be processed and translocated across the nuclear membrane prior to translation and as such, these mRNAs have relatively long half-lives. The predominant mechanism of mRNA decay in yeast involves deadenylation (shortening of poly (A) tail) with the primary deadenylase composed of nine proteins termed CCR4-NOT or with a secondary deadenylase Poly(A) ribonuclease enzyme (PARN). The deadenylation process is then followed by decapping with Dcp1p, Dcp2p and subsequent 5'-3' exoribonuclease decay of the transcript by the exoribonuclease Xrn1p (Parker and Song 2004). More recently, a

10-12 multisubunit complex of 3'-5' exoribonucleases, termed the exosome, was discovered and appears to be involved in the cytosolic 3'-to-5' degradation of mRNA and in the 3' processing of noncoding RNAs in the nucleus (Garneau *et al.* 2007). Following 3'-5' exonucleolytic decay, the 5' oligonucleotide cap is hydrolyzed by the scavenger decapping enzyme DcpS (Parker and Song 2004; Liu *et al.* 2002). Several accessory proteins are also required for efficient decapping. After the mRNA has been deadenylated, a complex of Sm-like (Lsm 1-7) proteins associates with the 3' end of the mRNA (Tharun *et al.* 2000; Tharun and Parker 2001). Other proteins, namely Lsm 16 (also termed enhancer of decapping-3 or EDC3), Lsm 14, Poly(A) binding protein-1 (Pbp1), Pat1, and the DExD/H-box RNA helicase Dhh1 are known to help mediate the decapping process (Garneau *et al.* 2007; Coller *et al.* 2001; Bonnerot *et al.* 2000). The deadenylation-dependent and deadenylation independent mRNA decay pathways are summarized in Figure 1 (a and b). Endoribonucleolytic decay represents an additional method of mRNA degradation (see Figure 1-c)

There are several other specialized 'surveillance' mRNA degradation pathways in yeast. A summary of these pathways is shown in Figure 2 (a,b and c). The first such pathway termed nonsense-mediated decay (NMD) is activated by the presence of a premature stop codon (nonsense termination codon) within an otherwise normal open reading frame. The premature stop codons can be created through mutation, frame-shifts, incomplete translation initiation and incorrect 3' UTRs (Garneau *et al.* 2007). Once detected, these incorrect transcripts are degraded by several pathways; however, much remains to be discovered about these pathways. The next surveillance type pathway is termed nonstop decay (NSD). mRNAs that do not possess translation termination codons

results in the ribosome proceeding onto the poly(A) tail, thereby displacing the poly(A)-binding protein and stalling at the 3' end of the transcript (Garneau *et al.* 2007). As shown in Figure 2 (b), there are two proposed pathways for decay of such mRNAs. The first pathway which is conserved in yeast and mammalian cells degrades mRNAs 3'-5' with the cytoplasmic exosome (van Hoof *et al.* 2002, Frischmeyer *et al.* 2002; Garneau *et al.* 2007) and the second pathway, found solely in yeast, utilizes a 5'-3' decay mechanism (Garneau *et al.* 2007). The third mRNA surveillance decay pathway is no-go decay (NGD). As outlined in Figure 2 (c), this pathway is initiated as a result of ribosomal stalling and is believed to be triggered by the associated translation initiation complex (Doma and Parker 2006). The mRNA is subsequently endonucleolytically cleaved near the stall site. The mRNA fragments are released and subsequently degraded by the exosome and by Xrn1 (Doma and Parker 2006).

1.2.3 Messenger RNA Decay in Higher Eukaryotes (Mammalian Cells)

By and large, homologous degradation pathways and enzymes are present in lower eukaryotes (yeast) and in higher eukaryotes (Tucker and Parker, 2000). Deadenylation followed by 3'-5' exonucleolytic degradation catalyzed by a putative complex of exonucleases (exosome) and 5' decapping followed by 5'-3' exonucleolytic degradation are relatively well established mRNA degradative pathways in mammalian cells. In support of the exosome-mediated degradation pathway, the mammalian exosome has been purified and its composition is very similar to its yeast counterpart (Mukherjee *et al.* 2002). Also, the recent discovery of a mammalian homolog to yeast decapping enzymes (Lykke-Andersen 2002) and the 5'-3' exonuclease Xrn1 (Bashkirov 1997) suggests that decapping followed by 5'-3' degradation are evolutionarily conserved

mechanisms. In addition, there are other known specialized degradation pathways similar to their yeast counterparts including: nonsense mediated decay (NMD) nonstop decay (NSD), no-go decay (NGD) and endonucleolytic cleavage. While many of the endonucleolytic decay pathways remain poorly characterized, there has been substantial *in vivo* evidence of decay products for specific mRNA transcripts.

1.3 RNA-Binding Proteins

In order to fully understand the interactions between RNA and RNA-binding proteins, one must be somewhat familiar with the basic structural features inherent in RNA-binding proteins. The specific interaction of a protein with RNA occurs through various peptide motifs in the protein, termed RNA-binding domains. Often these are structural features of the folded protein. The binding domains enable the protein to recognize and bind to target areas in an RNA molecule. Often, RNA-binding proteins contain multiple copies of these domains. Furthermore, RNA binding can be determined via cooperative interaction of two or more domains (Perez-Canadillas and Varani 2001; Deo *et al.* 1999). The multiple interactions of repeat domains within an RNA-binding protein or the interaction with various types of domains in other RNA-binding proteins permits great diversity in RNA molecule recognition. Ultimately, this translates into a greater variety of biological function (Maris *et al.* 2005; Siomi *et al.* 1997).

There are three general categories of eukaryotic RNA-binding protein domains. The most extensively characterized single stranded RNA-binding domain is the ribonucleoprotein (RNP) motif, also referred to as RNA-binding domain (RBD) or RNA recognition motif (RRM) (Perez-Canadillas and Varani 2001; Maris *et al.* 2005; Siomi *et al.* 1997). RRM's are frequently found in proteins that function in post-transcriptional

regulation of RNA (Maris *et al.* 2005; Siomi *et al.* 1997). The second domain termed hnRNP K homology domain or K-homology domain (KH) is one of the most commonly identified motifs found in RNA-binding proteins. KH domains have been associated with a wide variety of cellular functions including nuclear localization (Nielsen *et al.* 1999), nuclear export (Nielsen *et al.* 1999) and post-transcriptional mechanisms governing mRNA stability (Ioannidis *et al.* 2004). The third major RNA-binding domain found in eukaryotic cells is the double stranded RNA-binding domain (dsRBD). The dsRBD functions in binding to double stranded regions of structured RNA molecules (Chang *et al.* 2005; Chen 2005). The dsRBD motif is found in both eurkaryotic and prokaryotic systems, and has been implicated in a variety of RNA metabolic processes including RNA localization (Chang *et al.* 2005; Chen 2005; Siomi 1997).

In addition to the motifs found within RNA binding proteins, specific secondary structural conformations can be adopted by single stranded RNA. These conformations are often required for protein recognition and include regions of base-pairing (Watson-Crick) interspersed among regions that form single stranded loops (hairpin and internal), bulges and helical junctions (Chen and Varani 2005). It should be noted, however, that the study of protein-RNA binding *in vitro* as a model for mechanisms *in vivo* is difficult and is complicated by the secondary structures adopted by single-stranded RNA *in vivo* and by the structural alteration as a result of the binding of additional proteins or ligands *in vivo* (Perez-Canadillas and Varani 2001; Chen and Varani 2005).

In summary, our knowledge of the fundamental mechanisms and basic principles involved in protein-RNA interaction provide the underlying foundation for many areas of study within the field of RNA metabolism including the field of mRNA decay.

1.3.1 mRNA Stability and RNA-Binding Proteins

The 3' UTR of mRNA transcripts has a major role in controlling their stability (Guhaniyogi and Brewer, 2001). Several proteins that bind the 3' UTR of mRNA's *in vivo* such as AUF 1 (Brewer 1991), Aldolases A and C (Canete-Soler *et al.* 2005) and HADHB (Adams *et al.* 2003) are known to function as mRNA-destabilizing factors. In addition, there are numerous 3' UTR mRNA-binding proteins such as GAPDH (Nagy and Rigby 1995), HuD, HuC (Levine *et al.* 1993), HuR (Ma *et al.* 1996; Levy *et al.* 1998), αCP (Wilson and Brewer 1999; Kiledjian *et al.* 1997), IRE-BP (Rouault and Klausner, 1997), and vigilin (Cunningham *et al.* 2000; Kruse *et al.* 2003). These proteins are proposed to specifically bind AU-rich elements (AREs) within the 3' UTR of specific mRNAs and prevent ARE-mediated decay (Park-Lee *et al.* 2003).

The interaction between RNA-binding proteins and the 5' UTR of select mRNAs has been shown to influence their stability *in vivo*. Examples include: nucleolin and YB-1 proteins which bind to and stabilize the JNK-response element (JRE) in the 5' UTR of IL-2 mRNA (Chen *et al.* 2000) and the IL-1α protein which binds to the 5' UTR and stabilizes KC mRNA (Tebo *et al.* 2000).

In addition to 3' UTR- and 5' UTR-binding proteins, there are proteins which bind to the coding regions or instability (decay) elements of several mRNAs. A complex of proteins including AUF1, NSAP1, PABP, Unr and hnRNP-R bind to and function to destabilize c-fos mRNA (Schiavi *et al.* 1994; Chen *et al.* 1992). The coding region of *c-myc* mRNA, which will be the focus of this thesis, is bound by a protein termed CRD-BP (Prokipcak *et al.* 1994). The binding of CRD-BP is hypothesized to stabilize *c-myc* mRNA by protecting it from cleavage by cellular ribonucleases (Prokipcak *et al.* 1994).

In fact, this hypothesis has been directly demonstrated and confirmed *in vitro* (Sparanese and Lee, 2007).

1.4 The *c-myc* Proto-Oncogene

Rapid advances in understanding of cellular genetics have enabled a greater depth of understanding into the mechanisms that govern cancer cell biology. Proto-oncogene refers to a sequence of DNA that has been altered or mutated from its original form. Generally, they code for proteins that are involved in normal cellular growth and proliferation. Consequently, they promote specialization and division of normal cells. A change in their genetic sequence can result in uncontrolled cell growth, ultimately causing the formation of a cancerous tumor (Varmus 1984).

In humans, proto-oncogenes can be transformed into oncogenes in three ways: point mutation (alteration of a single nucleotide base pair), translocation (in which a segment of the chromosome breaks off and attaches to another chromosome), or amplification (increase in the number of copies of the proto-oncogene). Oncogenes were first discovered in certain retroviruses and were later identified as cancer-causing agents in many animals (Varmus 1984). The *myc* gene was first discovered in Burkitt's lymphoma patients whom exhibit chromosomal translocations; most often involving VIII. Subsequent cloning of the break point of the fusion chromosomes revealed a gene that was similar to avian myelocytomatosis viral oncogene (*v-myc*). Thus, the newly discovered cellular gene was named *c-myc* (Varmus 1984). It is roughly estimated that the *c-myc* proto-oncogene influences the expression of at least 10% of all human genes (Levens 2003). The c-Myc protein or the *c-myc* gene is overexpressed in a wide variety of human cancers with 80% of breast cancers, 70% of colon cancer, 90% of

gynecological cancers, 50% of hepatocellular carcinomas and a variety of hematological tumors possessing abnormal myc expression. On the basis of these frequencies, it is estimated that approximately 100,000 US cancer deaths per year are associated with changes in the *c-myc* gene or its expression (Gardner *et al.* 1998). Given that alterations in the expression of the c-*myc* gene may contribute to one-seventh of U.S. cancer deaths, it continues to be a target for the development of specific anti-cancer therapies.

1.4.1 The Functional Importance of the *c-myc* Gene in Mammalian Cells

The *c-myc* gene codes for the protein c-Myc that functions as a transcription factor by heterodimerizing with a partner protein, termed Max, to regulate gene expression. Thus it acts as a regulator of cell proliferation, differentiation and apoptosis (Levens 2003). In fact, *c-myc* is expressed in almost all proliferating normal cells, and its repression is required for terminal differentiation of many cell types (Levens 2003). Deregulated expression of *c-myc* prevents differentiation of many cell types, can induce apoptosis, can induce genomic instability, and is associated with many tumor phenotypes (Felsher and Bishop 1999a). Mutations, amplification, chromosomal rearrangements, and translocation of this gene in addition to mRNA stabilization have been associated with a variety of hematopoietic tumors, leukemias and lymphomas, including Burkitt lymphoma (Hermeking 2003). Regardless of the mechanism by which the *c-myc* gene is activated, the final outcome is the overexpression of *c-myc* mRNA and the associated higher level of c-Myc protein.

The ultimate function of the c-Myc protein is largely influenced by its interaction with numerous networks of proteins (Atchley and Fernandes 2005). A variety of cellular responses are generated by the expression and suppression of different overlapping

subsets of target genes (Hoffman *et al.* 2002). Moreover, the final cellular response to c-Myc is most probably situation-specific and is dictated by the expression of numerous other genes including oncogenes and tumor suppressor genes (Hoffman *et al.* 2002). Although the c-Myc protein is responsible for the activation of several growth-promoting genes in a variety of cancers, the precise mechanisms by which these transformations occur remain somewhat unclear (Levens 2003).

1.5 *c-myc*, mRNA-Binding Proteins and mRNA-Degrading Enzymes

The complexity of mRNA metabolism from post-transcriptional maturation to degradation of messenger RNA (mRNA), requires specific RNA-protein interactions. In addition, these RNA-protein interactions must occur with a high level of specificity to ensure the correct control and sequence of events leading to the decay or the stabilization of the mRNA transcript. In light of these critical interactions, considerable research has focused on the proteins and associated factors that bind or interact with the instability elements present in mRNA transcripts. The following sections will address the interactions between RNA-binding proteins, RNA-degrading enzymes and the *c-myc* mRNA transcript.

1.5.1 *c-myc* mRNA Stability and Degradation

c-myc gene expression is regulated at many levels including: transcriptional initiation (Brewer 2003; Lee *et al.* 2003), translational elongation (Lemm and Ross 2002) and post-transcriptional processes (Yeilding *et al.* 1996). Furthermore, there is widespread evidence that mRNA stability plays a critical role in the regulation of *c-myc* gene expression (Brawerman 1987; Ross 1995). The stability of *c-myc* mRNA, like many other mRNAs is believed to be a result of several factors including the presence of

cis-acting adenosine and uridine (AU)-rich instability elements (AREs) inherent in the 3' untranslated regions (3'UTRs) of the RNA sequence, *trans*-acting regulatory factors such as RNA-binding proteins, and the presence of exo- and endo-ribonucleases that function to degrade the mRNA transcripts (Ross 1995).

The half-life of *c-myc* mRNA is also controlled by multiple instability elements located within both the 249-nucleotide coding region instability determinant known as the coding region determinant (CRD) and the 3' untranslated region (3' -UTR) (Bremer *et al.* 2003; Doyle *et al.* 2000; Brewer 1999) as shown in Figure 3. Highly unstable transcripts such as *c-myc* generally contain one to three AUUUA elements spaced throughout the 3'-UTR (Jones *et al.* 1987; Langa *et al.* 2001; Brewer 2003). In addition, ARE's are often targeted and bound by proteins that trigger the removal of the poly(A) tail and the 5' cap structure. Consequently, the mRNA transcripts become susceptible to exonucleolytic degradation (Park *et al.* 2000; Brewer 2003).

In vitro and *in vivo* evidence has shown that the CRD region of the *c-myc* mRNA transcript plays a fundamental role in destabilizing *c-myc* mRNA during translation (Lemm and Ross 2002). Evidence from these studies suggests that pausing of the ribosome during translation due to the presence of rare codons in a region upstream of the CRD results in rapid decay of the *c-myc* transcript (Lemm and Ross 2002). Interestingly, *in vivo* experiments have shown that removing the 3'- or 5'-UTR of *c-myc* mRNA has little effect on stability thus lending further support for the notion that the CRD plays an important role in regulating *c-myc* stability (Bonnieu *et al.* 1988; Laird-Offringa *et al.* 1991). Furthermore, the sequence spanning the CRD has been shown to be an essential regulator of mRNA stability *in vivo*. Firstly, when the CRD region of *c-myc* was inserted

into the coding region of the stable globin mRNA, it became rapidly destabilized (Ross and Herrick 1994). Secondly, several studies have shown that the CRD was required to post-transcriptionally down-regulate *c-myc* mRNA during differentiation of C2 myoblasts (Kren *et al.* 1996). Thirdly, cell-free mRNA decay experiments using polysome extracts and a 180nt RNA sense strand for *c-myc* CRD was sufficient to induce endonucleolytic cleavage within the CRD region and an 8-fold increase in *c-myc* mRNA destabilization (Berstein *et al.* 1992). In addition, this increase in *c-myc* mRNA destabilization was highly specific as experiments using competitor RNA corresponding to other areas of *c-myc* mRNA did not result in transcript destabilization (Berstein *et al.* 1992).

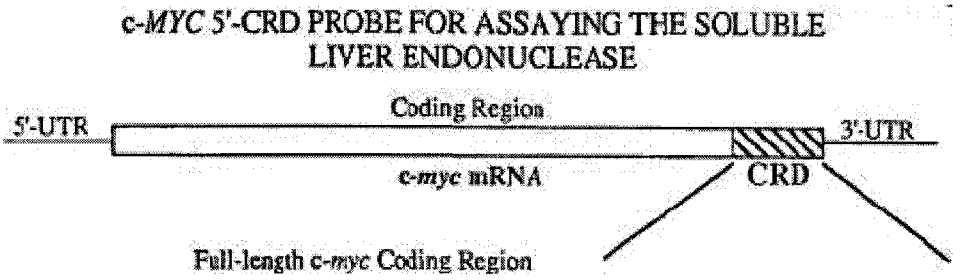

Figure 3: Human *c-myc* mRNA with 3'-, 5'-UTRs and the full length CRD (nts 1705-1886) regions highlighted (Lee *et al.* 1998)

Endoribonuclease-mediated decay *in vivo* (Hanson and Schoenberg 2001) and *in vitro* (Wennborg *et al.* 1995; Tourriere *et al.* 2001; Tourriere *et al.* 2003; Lee *et al.* 1998; Bergstrom *et al.* 2006) of *c-myc* mRNA has also been shown to occur in a stem-loop structure within nucleotides 1705-1790 of the CRD region (Lemm and Ross 2002). Therefore, *c-myc* mRNA degradation can occur *in vivo* via two pathways: deadenylation followed by 3'-5' exonucleolytic decay starting in the AU-rich region of the 3' UTR (Brewer 1999; Doyle *et al.* 2000; Bremer *et al.* 2003) or endonucleolytically within the

CRD at the carboxyl terminal end of the coding region shown in Figure 3 (Hanson and Schoenberg 2001; Wennborg *et al.* 1995; Tourriere *et al.* 2001; Tourriere *et al.* 2003; Lee *et al.* 1998; Bergstrom *et al.* 2006).

1.5.2 *c-myc* mRNA and the Coding Region Determinant Binding Protein (CRD-BP)

The CRD region of the *c-myc* mRNA transcript is the target of a 68-kDa RNA-binding protein known as the coding region determinant binding protein (CRD-BP). CRD-BP contains two RNA recognition motifs and four hnRNP K homology domains (Lemm and Ross 2002). The proposed model functions such that under normal cellular conditions when CRD-BP is bound to c-*myc* mRNA, the CRD of the mRNA is shielded from endonucleolytic attack (Bernstein *et al.* 1992; Doyle *et al.* 1998; Prokipcak *et al.*1994). In this case, the mRNA transcript is degraded only by an ARE-dependent deadenylation pathway (Brewer and Ross 1988). When the CRD-BP dissociates from the *c-myc* mRNA, the CRD is believed to be exposed and susceptible to endonucleolytic attack (Bernstein *et al.* 1992). The transcript is then rapidly degraded by endonucleolytic cleavage within this CRD region. Additionally, direct *in vitro* evidence in support of this shielding hypothesis has recently been demonstrated (Sparanese and Lee, 2007).

Several *in vivo* observations support the hypothesis that CRD-BP binds to and protects *c-myc* mRNA. Firstly, the overexpression of CRD-BP in colorectal cancer is associated with a slight elevation in *c-myc* mRNA levels (Ross *et al.* 2001). Secondly, a decrease in *c-myc* mRNA levels were observed in MCF-7 cells (Ioannidis *et al.* 2005) and colorectal cells (Noubissis *et al.* 2006) following downregulation of CRD-BP. Finally, the addition of sense RNA corresponding to *c-myc* CRD in cells was shown to result in an increased decay of *c-myc* mRNA (Coulis *et al.* 2000). In contrast to the

aforementioned supporting evidence for the CRD-BP-*c-myc* CRD shielding hypothesis, two recent studies do not support this hypothesis. For example, transgenic mice over expressing CRD-BP in mammary tissue, did not exhibit elevated levels of *c-myc* mRNA (Tessier *et al.* 2004). In addition, knockdown of CRD-BP in a K562 cell line, had no effect on levels of *c-myc* mRNA (Liao *et al.* 2004).

1.6 Mammalian Endoribonucleases

Many of the mRNA-degrading pathways characterized to date in mammalian cells involve cellular exoribonucleases; however, there is substantial evidence for the functional involvement of endoribonucleases within mammalian mRNA degradation pathways; the CRD region of *c-myc* mRNA is a prime example (Bernstein *et al.* 1992; Doyle *et al.* 1998; Prokipcak *et al.*1994). Several of the known mammalian proteins that possess endoribonucleolytic function are shown in Table 2. *In vivo* evidence of mRNA decay products has been documented for several transcripts such as: transferrin receptor (Cairo *et al.* 1994), insulin-like growth factor-II (van Dijk *et al.* 2000), avian apo-very low density lipoprotein II (Binder *et al.* 1989), *Xenopus* Xlhbox2B mRNA, *Xenopus* β-globin (Bremer *et al.* 2003), albumin (Cunningham *et al.* 2000), *c-myc* (Lee *et al.* 1998; Bergstrom *et al.* 2006), vitellogenin (Cunningham *et al.* 2000), hepatitis B virus (Hou *et al.* 2005), and α-globin (Liu and Kiledjian 2000), cytokine groα (Stoeckle 1992), and several maternal homeodomain proteins (Brown and Harland 1990; Brown *et al.* 1993). Although most proteins with endoribonucleolytic properties exibit some degree of substrate specificity, few of the endoribonucleases characterized in mRNA decay pathways have been shown to target specific transcripts *in vivo* (Dodson and Shapiro 2002). One of the major challenges remains identifying and assessing the significance of

Table 2: A summary of mammalian endoribonucleases that have been characterized

Mammalian Endoribonucleases	Size	Cellular Location of Action	Activation Signal	Cleavage Specificity	Reference
PMR-1	60 kDa	RNP complex, sequestered to polysomes	Estrogen	ss **UG** dinucleotides ss AY**UGA** (Y= C or U)	Cunningham *et al.* 2001a; Stevens *et al.* 2002; Bremer *et al.* 2003; Chernokalskaya *et al.* 1998
ErEN	40kDa (denaturing conditions)	Non-Polysomal, Precise location unknown	ATP-dependent, Deadenylation of mRNA transcript	dinucleotides 63-64-**CU** in **CU**- rich regions	Wang and Kiledjian 2000a; Wang and Kiledjian 2000b
ARD-1/NIPP-1	ARD-1: 13.3kDa NIPP-1: 38.5kDa	Polysomes	-	ss AREs	Claverie-Martin *et al.* 1997; Chang *et al.* 1999
RNase L	741 kDa	Cytoplasm/ER	INF, 2-5A	ss **UA** and **UU** dinucleotides	Zhou *et al.* 1993; Mishra 2001
IRE-1	110 kDa	ER membrane	Unfolded/ proteins in ER lumen	ss **GC**, **GA**, **UG**, **AC**, **CU** dinucleotides	Tirasophon *et al.* 2000; Lee *et al.* 2002; Hollien and Weissman 2006
RasGAP-associated G3BP	52 kDa	Cytoplasm	Phosphorylation -Dependent	ss **CA** dinucleotides	Tourriere *et al.* 2001; Barnes *et al.* 2002; Gallouzi *et al.* 1998
Aldolase A, Aldolase C	~ 40 kDa	Neuronal RNP complex	Unidentified	**UG** dinucleotides	Canete-Soler *et al.* 2005
Argonaute 2	130 kDa	RISC complex	Unidentified	3' UTR AREs	Hammond *et al.* 2001; Liu *et al.* 2004
Dicer	218 kDa	RISC complex	ds RNAs in RNAi pathway miRNAs	None	Fortin *et al.* 2002; Nicholson and Nicholson 2002; Doi *et al.* 2003; Zhang *et al.* 2004a
RNase A Family					
*pt RNase 1	~13 kDa	Extracellular	unknown	ss **UA, CA, CC, UG;** preference for poly(C) over poly(U)	Barnard 1969; Sorrentino and Libonati 1994
**npt RNase 2 Eosinophil-Derived Neurotoxin (EDN)	***12-17 kDa	Eosinophils, spleen, liver, placenta, and kidney tissues urine	unknown	Preference for poly **(U)** over poly **(C)**	Sorrentino 1998
npt RNase 3 Eosinophil Cationic Protein (ECP)	***12-17 kDa	Granulocytes Exibits neurotoxicity	unknown	Preference for poly **(U)** over poly **(C)**	Barker *et al.* 1989; Sorrentino *et al.* 1992
pt/npt RNase 4	***12-17 kDa	Pancreas, liver, lung, skeletal muscle, heart, kidney tissues	unknown	Predominantly poly**(U)**	Hofsteenge *et al.* 1998
Angiogenin/RNase 5	***12-17 kDa	Human plasma	unknown	Weak activity against ss **UA, CA,**	Shapiro *et al.* 1986; Saxena *et al.* 1992 Riordan 1997
npt RNase 6	***12-17 kDa	Primarily lung tissue	unknown	unknown	Rosenberg and Dyer 1996
npt RNase 7 and 8	***12-17 kDa	Primarily liver	unknown	unknown	Zhang *et al.* 2003

* pt refers to pancreatic-type, with homology to bovine pancreatic RNase
** npt refers to nonpancreatic-type
***unglycosylated state

these enzymes within the context of normal cell function. With these challenges in mind, the following sections endeavor to explore the features of known mammalian endoribonucleases. In addition, the structural and functional similarities and the cellular distribution of bi- or multi-functional proteins that possess documented endoribonucleolytic activity will be highlighted.

1.6.1 The Diversity of Mammalian Endoribonuclease Proteins and their Role in RNA Processing

Research continues to uncover and highlight the importance of endoribonuclease-mediated mRNA decay pathways. Endonucleolytic RNA cleavage pathways characterized to date have largely been represented as site-specific mechanisms for fine tuning levels of specific mRNA transcripts, under specialized cellular conditions of stress (Dodson and Shapiro 2002). Perhaps the most striking feature of recent studies is the diversity of proteins responsible for RNA degradation and their site-specific distribution within the mammalian cell. In fact endoribonucleases are present in a wide range of locals within the cell, including the nucleolus, nucleus, cytosol, endoplasmic reticulum, polysomes, and specialized foci such as stress granules and processing bodies (Dodson and Shapiro 2002; Yang and Schoenberg 2004; Tourriere *et al.* 2001). In addition, there are secreted extracellular members and non-secretory cytoplasmic members of the RNase A superfamily; however, the extent to which this group of endoribonucleases functions in mRNA remains uncertain. Current belief is that the primary mechanistic regulation of endoribonuclease enzymes occurs by one of two methods; regulating the access to mRNA transcripts with *trans*-acting RNA-binding proteins such as CRD-BP and by the sequence specificity of the endoribonuclease itself (Dodson and Shapiro 2002). In contrast to decapping and exonuclease degradation where the mRNA is no longer

engaged by translating ribosomes, endonuclease-mediated mRNA degradation requires that either the endonuclease proteins that promote cleavage be targeted to the site of function or that the endonuclease proteins reside in the location of function (ie. within an mRNP complex) (Dodson and Shapiro 2002; Yang and Schoenberg 2004; Hollien and Weissman 2006).

1.6.2 Mammalian Endoribonucleases that function in mRNA Decay *in vitro* and *in vivo*

i) PMR-1

Polysomal ribonuclease 1 (PMR 1) is a well-characterized endoribonuclease belonging to the peroxidase gene family, that is capable of initiating the destabilization of albumin mRNA (Bremer *et al.* 2003; Yang *et al.* 2004; Yang and Schoenberg 2004). In addition, estrogen stimulation in *Xenopus* hepatocytes activates a pathway in which PMR1 functions to destabilize certain serum protein mRNAs via endonucleolytic cleavage (Chernokalskaya *et al.* 1998; Cunningham *et al.* 2001a; Stevens *et al.* 2002; Yang and Schoenberg 2004). There is, however, some uncertainty as to whether PMR1 is latent in ribonuclear protein (RNP) complexes associated with polysomes or recruited to an appropriate RNP complex bound to the polysome. Recent evidence suggests the latter as PMR1 is uniformly distributed throughout the cytoplasm, on polysomes and does not co-localize in cytoplasmic processing bodies with proteins such as human Dcp1 (Yang and Schoenberg 2004). Additionally, it has been shown that PMR 1 requires phosphorylation-dependent activation which may be required for targeting PMR 1 to polysomes (Peng and Schoenberg 2007). In the 'recruitment' model of PMR 1 activation, the binding of one or more specific proteins to a substrate mRNA (e.g., albumin) generates a platform for the binding of PMR1 to the larger complex of proteins

present on the actively- translating RNP complex (Chernokalskaya *et al.*, 1997). PMR 1 can then gain access to the mRNA substrate. Studies have revealed that vitellogenin mRNA is selectively stabilized relative to albumin mRNA (Cunningham *et al.* 2001a). The mechanism by which this occurs is believed to involve binding of the protein vigilin in the 3'UTR binding site of vitellogenin mRNA (Cunningham *et al.* 2000). When the vigilin protein is bound, cleavage of vitellogenin mRNA is effectively blocked from PMR 1 (Cunningham *et al.* 2000). In the absence of vigilin, PMR 1 cleaves vitellogenin mRNA within the 3'UTR region *in vivo* and *in vitro* (Cunningham *et al.* 2000). Evidence has shown that the 3'UTR of vitellogenin mRNA binds the vigilin protein with a ~30 fold higher affinity as compared to albumin mRNA containing known PMR 1 recognition sequences (Cunningham *et al.* 2000).

Specific domains of PMR1 in both the C-terminal and N-terminal domains are necessary for targeting to polysomes and a loss of the targeting domains has been shown to result in stabilization of several mRNAs (Yang and Schoenberg 2004). Additionally, it has been suggested that PMR 1 may function in the NMD pathway. Nonsense-containing β-globin mRNA exhibits endonuclease-mediated decay in erythroid cells *in vivo* and the cleavage products are similar to those generated by PMR1 *in vitro* (Bremer *et al.*, 2003; Stevens *et al.*, 2002). *In vitro* studies have also shown that PMR 1 generates cleavage products with free 3′ ends; ideal substrates for subsequent degradation by the exosome (Chernokalskaya *et al.*, 1997).

PMR 1 may also be implicated in signal transduction mechanisms in response to extracellular stimuli (Chernokalskaya *et al.*1998; Peng and Schoenberg 2007). In support of this notion, increasing estrogen levels have not been sufficient to directly stimulate

PMR1 activity, consequently, researchers have hypothesized that a signal transduction mechanism is required from the estrogen receptor to activate PMR1 present in an mRNP complex (Chernokalskaya *et al.* 1998). Recently, it has been shown that phosphorylation of a tyrosine residue at position 650 in the C-terminal portion of the protein by the tyrosine kinase c-Src activates the endonuclease activity of PMR 1 and is required for efficient targeting of PMR 1 to polysomes (Peng and Schoenberg 2007). A summary of RNA cleavage specificities, cellular location and properties of PMR 1 are shown in Table 2.

ii) RNase L

RNase L is a 740 kDa endoribonuclease that has been shown to target and endonucleolytically cleave single stranded mRNA, rRNA and viral RNAs (Silverman 2003) and is believed to play a role in interferon-inducible antiviral defense (Li *et al.* 2000). RNase L catalytic activity necessitates activation. When there is no activating stimulus present, the RNase L protein exists in a latent, catalytically inactive monomeric form and is bound by an inhibitory protein (RLI) (Bisbal *et al.* 1995). However, upon binding 5'-triphosphorylated-2'-5'-A synthetase molecules, the protein forms a dimerized structure that activates the cytosolic endoribonucleolytic domain (Zhou *et al.* 1993). In mammalian cells, activation of the RNase L protein leads to cell death via an apoptotic pathway (Pandey and Rath 2004). A summary of RNA cleavage specificities, cellular location and properties of RNase L are shown in Table 2.

iii) IRE-1

In a somewhat analogous oligomerization-based mechanism, similar to the type I growth factor receptors that require dimerization/oligomerization for activation, the

endoplasmic reticulum located Inositol-Requiring type 1 transmembrane protein (IRE 1) requires activation of its respective kinase and endoribonuclease domains for RNase activity (Niwa *et al.* 1999, Tirasophon *et al.* 2000; Lemmon and Schlessinger 1994; Wrana *et al.* 1994). IRE 1 possesses a lumenal stress sensor domain, a hydrophobic transmembrane anchor sequence, and cytosolic kinase/endoribonuclease domain. IRE-1 was initially discovered in yeast (*S. cerevisiae*) in a stress-induced pathway termed the unfolded protein response (UPR). The UPR is responsible for transmitting information about the status of protein folding in the lumenal portion of the ER to the cytoplasm and nucleus (Dong *et al.* 2001: Yin-Liu and Kaufman 2003). In mammalian cells, IRE 1 induces the synthesis of chaperone proteins that assist in the refolding and assembly of misfolded proteins within the ER (Pillai 2005). Misfolded proteins can result from a number of different causes of ER stress including: viral infection, heat shock, and nutrient deprivation (Kaufman 2002; Sitia and Braakman 2003).

The mechanism of activation of IRE 1 in mammalian cells is hypothesized to occur such that the ER lumenal sensory domains, normally bound by the ER chaperone Bip, are released from Bip when misfolded proteins are present. This promotes dissociation of Bip from IRE 1 and allows Bip to associate with misfolded proteins. The release of Bip results in the oligomerization and activation of the IRE 1 kinase and endoribonuclease domains (Yin-Liu and Kaufman 2003; Shamu and Walter 1996; Pillai 2005). The activation of the endoribonucleolytic domain of IRE 1 is believed to promote splicing and activation of the XBP1 gene (Yin-Liu and Kaufman 2003; Shamu and Walter 1996; Pillai 2005). In support of this theory in vertebrate cells, IRE 1 lies upstream of X-box–binding protein 1 (*XBP1* mRNA), the vertebrate homolog of *HAC1*

mRNA in yeast. Studies suggest that XBP1 orchestrates the transcriptional activation of target genes that include ER chaperones and enzymes that facilitate this mechanism of protein folding (Yin-Liu and Kaufman 2003; Shamu and Walter 1996; Pillai 2005).

Research has added additional insight into the critical role of IRE 1 in localized mRNA processing events. Based on studies utilizing S2 cells from *Drosophila*, novel IRE 1-targeted mRNA substrates have been discovered (Hollien and Weissman 2006). The substrate mRNAs appear to be specifically targeted based on their localization to the ER membrane and on the secondary structure of the mRNA itself (Hollien and Weissman 2006). It is still not yet known whether IRE 1 mediates all of the observed endonucleolytic cleavages and it has been proposed that a second ribonuclease by itself or in combination with IRE 1 may be responsible for some of these observed mRNA decay events.

iv) RasGAP-Associated G3BP

RasGAP-associated G3BP is a 52 kDa single strand-specific endoribonuclease exhibiting no sequence homology with other known mammalian endoribonucleases. G3BP was initially characterized with the ability to cleave within the 3'UTR of *c-myc* mRNA *in vitro* (Barnes *et al.* 2002; Guitard *et al.* 2001; Tourriere *et al.* 2001). Interestingly, it has been shown *in vitro* that G3BP requires phosphorylation-dependent activation for endonucleolytic function (Gallouzi *et al.* 1998; Tourriere *et al.* 2001; Irvine *et al.* 2004; Zekri *et al.* 2005). Gene knockout animal model studies involving G3BP have resulted in both embryonic lethality and growth retardation (Zekri *et al.* 2005).

v) ErEN

Erythroid enriched endoribonuclease (ErEN) was discovered and characterized as a part of a 160 kDa multiprotein complex which possessed the ability to cleave within the 3' UTR of α-globin mRNA *in vivo* and *in vitro* (Rodgers *et al.* 2002; Wang and Kiledjian 2000). Subsequent studies utilizing denaturing gel filtration have shown that ErEN is a 40 kDa protein requiring ATP for endoribonucleolytic activity (Wang and Kiledjian 2000b; Rogers *et al.* 2002). ErEN appears to be poly (A) tail-dependent in that it requires deadenylation of the mRNA transcript prior to cleavage within the 3' UTR of α-globin mRNA (Rodgers *et al.* 2002; Wang and Kiledjian 2000).

vi) ARD-1/NIPP-1

ARD-1 (Activator of RNA Decay) was initially found in humans as a a cDNA sequence that possessed the ability to reverse the pleiotropic effects of temperature-sensitive and deletion mutations in the *E. coli rne* gene (Claverie-Martin *et al.* 1997; Chang *et al.* 1999). Studies have shown that human ARD-1 protein is a 13.3 kDa single-strand-specific endoribonuclease that cleaves RNA in much the same fashion as bacterial RNase E; moreover, it cleaves at similar sites and produces cleavage products with 5'-phosphates (Claverie-Martin *et al.* 1997). It has also been shown to function as a domain of the NIPP-1 protein (Claverie-Martin *et al.* 1997).

NIPP-1 (Nuclear Inhibitor of Protein Phosphatase 1) isolated from bovine cells is a 38.5 kDa protein that was found to contain a peptide sequence at its carboxyl terminal region with homology to that of human ARD-1 cDNA (Claverie-Martin *et al.* 1997; Chang *et al.* 1999). It has now been established that in human cells, ARD-1 and NIPP-1 are isoforms, encoded by a single gene and are produced by alternatively splicing

precursor mRNA (Chang *et al.* 1999). Recent studies have shown that both ARD-1 and NIPP-1 contain lysine-rich regions in their carboxy-terminal regions that associate with AU rich sequences and promote endoribonucleolytic cleavage within these areas (Parker *et al.* 2002; Chang *et al.* 1999).

vii) Argonaute 2

The field of RNA interference in mammalian cells has also served as a reminder of the complexity and importance of the spatial localization of mRNA processing events required for correct protein expression. Argonaute 2 (Ago 2) is a member of a larger complex which is made up of Dicer and TAR RNA-binding protein (TRBP) located within the RNA-induced silencing complex (RISC) and is believed to be the enzyme required for endonucleolytic cleavage of the target mRNA (Martinez and Tuschl 2004; Liu *et al.* 2004). Ago 2 contains an N-terminal PAZ domain, two middle domains and a fourth C-terminal PIWI domain. These domains are believed to interact and form a supportive structure required for efficient cleavage of the mRNA transcript (Liu *et al.* 2004; Parker *et al.* 2004). The N-terminal PAZ domain is believed to function in RNA-binding (Parker *et al.* 2004) whereas the C-terminal PIWI domain, based on structural similarity with RNase H, is believed to be the catalytic domain required for endoribonucleolytic cleavage (Parker *et al.* 2004). Ago 2 exhibits several distinct cellular locales including cytoplasmic P-bodies. The widespread distribution of Ago 2, including known RNA decay centers may indicate that it functions in overlapping RNA degradation pathways (Sen and Blau 2006; Jing *et al.* 2005). RNA cleavage specificities and a summary of the properties of Ago 2 are shown in Table 2.

viii) Dicer

Dicer is a large 218 kDa endoribonuclease belonging to the RNase III family of endoribonucleases (Fortin *et al.* 2002). Dicer cleaves without sequence specificity, double stranded RNA substrates into smaller 21-23 nucleotide segments which are referred to as siRNAs (small interfering). Dicer also functions in the excision of microRNAs (miRNAs) from hairpin precursors (Fortin *et al.* 2002; Nicholson and Nicholson 2002; Doi *et al.* 2003; Zhang *et al.* 2004a). In mammalian cells, Dicer 1 gene (*Dcr1*) has been discovered which encodes a Dicer-like protein that is essential for the viability of cells (Zhang *et al.* 2004a). RNA cleavage specificities, cellular location and properties of Dicer are shown in Table 2.

ix) RNase A superfamily

This family of proteins includes eight known members (1-8) in human cells which are grouped into four RNase families based on structural, catalytic and biological characteristics (Sorrentino and Libonati 1997). In fact, the RNase A superfamily of endoribonucleases have been the subject of some of the most intensive biochemical studies dating back over 50 years (Sorrentino and Libonati 1997). During the mid-1980s, a group of human RNases garnered interest based on some of the properties that they were found to possess (reviewed in Beintema *et al.* 1988; Benner and Allemann 1989; D'Alessio 1993). Subsequent studies have shown that several RNase A proteins possess special biological actions such as neurotoxicity, angiogenic activity, immunosuppressivity and antitumor activity (reviewed in Beintema *et al.* 1988; Benner and Allemann 1989; D'Alessio 1993). RNA-cleavage specificities and general properties of this group of enzymes are shown in Table 2.

1.7 Research Objectives

Mammalian endonuclease-mediated mRNA degradation pathways identified to date include the RNAi pathway, the ER stress response, no-go decay and the decay of several specific mRNA transcripts; however, the identity of many of the endoribonucleases responsible for these decay products have yet to be conclusively identified. In addition, there remains significant debate as to the precise role of endonucleolytic degradation in controlling basal mRNA levels in mammalian cells. One of the major questions that remains is whether endonucleolytic cleavage events play a significant role in controlling mRNA abundance under normal cellular conditions as opposed to specialized conditions such as cellular stress. Given their role in a seemingly diverse set of mRNA degradation pathways, the numerous requirements for functional or structural activation, the lack of primary amino acid sequence homology among endoribonucleases, and the difficulties associated with detecting endonucleolytic mRNA decay products *in vivo*, it is not surprising that identifying novel members of this family of mammalian enzymes poses many challenges.

Recently, a mammalian endoribonuclease was purified and biochemical characterization was subsequently undertaken (Bergstrom *et al.* 2006). The endoribonuclease was originally isolated in high salt ribosomal salt washes from rat liver tissue. Fractions from the heparin-sepharose column containing peak endonuclease activity were pooled and analyzed on an SDS-PAGE gel using silver stain. Five clear proteins of sizes ranging from 15-35 kDa co-purified with endonuclease activity. The major component of this enzyme complex was tentatively identified as a 35 kDa protein; however, the amino acid sequence and identity of the endoribonuclease has not been

determined. Given the lack of mammalian endoribonucleases identified and characterized to date, the identity of this endoribonuclease is of paramount importance for advancing our knowledge of endoribonucleases that function within the field of mRNA degradation.

In order to fully understand the biological role of the endoribonuclease that had been purified it was necessary to re-purify and definitively identify this enzyme. In light of these gaps in our understanding of this endoribonuclease, the main objective of this thesis was to re-purify, identify and further characterize all of the major proteins that co-purified with endoribonucleolytic activity against the CRD region of *c-myc* mRNA.

The first aim of this research was to re-purify the native enzyme and the associated proteins from juvenile rat liver tissue that co-purified with endoribonucleolytic activity. The purification scheme was designed such that one pH precipitation step and five separate liquid column chromatography steps were used. The resulting eluted fractions from the final gel filtration purification column were resolved on a Coomassie Blue-stained SDS-PAGE gel. SDS-PAGE gel slices containing each of the proteins were sent to the Proteomics Centre at the University of Victoria for protein identification using LC-MS Mass Spectrometry. The results obtained were expected to definitively identify the 35 kDa protein and the four co-purified proteins.

The second aim of this research was to confirm the identity of the protein(s) responsible for endoribonucleolytic activity against the CRD region of *c-myc* RNA. Given the strong probability that the novel mammalian endoribonuclease being studied formed a complex with the co-purified proteins, the identity and a test designed to assess potential *in vitro* interactions among the co-purified proteins was performed. The techniques employed for this were Western blotting and immunoprecipitation

experiments. Ultimately, the immunoprecipitation experiments were performed in an attempt to immuno-deplete native endoribonucleolytic activity. The second aim was also to understand the kinetics of the native enzyme(s); namely V_{max} and K_m values. In order to accomplish this, a 17 base pair (mer) synthetic oligonucleotide substrate with a single incorporated ribonucleotide site was designed to rapidly assess the catalytic capabilities of the native enzyme.

The third aim of this research was designed to generate the recombinant form of the mammalian endoribonuclease(s) and if necessary generate recombinant forms of the co-purified proteins. The final portion of this research utilized RNA sequencing gels in an attempt to map the cleavage sites of the recombinant form of the endoribonuclease against the CRD of *c-myc* RNA.

CHAPTER 2

Purification and Identification of Two Distinct Mammalian Hepatic Endoribonucleases with the Ability to Degrade *c-myc* CRD RNA *in vitro*

This chapter describes and discusses the approach taken to purify two mammalian endoribonuclease proteins isolated from juvenile rat liver tissue. It includes the steps required to generate the *in vitro* transcribed *c-myc* CRD RNA substrate that was used to assay endoribonuclease activity throughout the purification. This chapter also presents the results of each step in the purification, discusses the observed results, and identification of protein bands as determined by mass spectrometry.

2.1 Methodology

2.1.1 Isolation of Polysomes and Preparation of Ribosomal Salt Wash from Rat Liver Tissue

95 juvenile frozen rat livers (approximately 175g each) from male Sprague-Dawley rats purchased from Harlan Bioproducts (Madison, Wisconsin) were placed in liquid nitrogen, crushed using a pestle, re-suspended in Buffer A (buffer contents listed in Table 3) and homogenized at 14,000 rpm for 2-3 min with a Polytron 3000 (Brinkmann). All procedures were performed on ice unless otherwise indicated. The slurry was further hand-homogenized with 20 strokes to ensure adequate cell breakage. Approximately two livers were re-suspended and homogenized in 50 mL of Buffer A (buffer contents listed in Table 3). The tissue extract was centrifuged at 12,500 rpm for 10 min at 4°C. The supernatant was carefully removed and the pelleted cellular debris discarded. The supernatant was then placed in 10 mL of Buffer B (30% sucrose w/v) (buffer contents listed in Table 3). This solution was then placed into SW28 Beckman ultracentrifuge

tubes and centrifuged at 27,000 rpm for 90 min at 4°C. The supernatant was subsequently removed, and the polysome-enriched pellet was re-suspended in 35 ml of Buffer A. This mixture was transferred to a 50 mL Falcon tube.

Five ml of Buffer C was added to the 35ml of isolated polysomes in each 50 mL Falcon tube. The tubes were gently inverted 10 times. This mixture was then placed into SW28 Beckman ultracentrifuge tubes each containing 10 mL of Buffer B (30% sucrose w/v) and centrifuged at 27,000 rpm for 90 min at 4°C. The supernatant, termed Ribosomal Salt Wash (RSW) was subsequently removed and placed in 50 mL Falcon tubes. A total volume of 9 L of RSW (10 g of protein) was isolated and refrigerated at 4°C.

Table 3: Reagents and composition utilized in the preparation and purification of rat liver tissue extract

Reagent	Composition
Buffer A	1mM potassium acetate (KOAc) (Fisher Scientific, New Jersey NY), 1.5 mM magnesium acetate (MgOAc) (Fisher Scientific, New Jersey NY), 2mM DTT, 10% (v/v) glycerol, 0.1mM ethylene glycol tetraacetic acid (EGTA) (EM Sciences Darmstadt, Germany), 10mM Tris-Cl, pH 7.4
Buffer B	1 mM potassium acetate (KOAc) (Fisher Scientific, New Jersey NY), 1.5mM magnesium acetate (MgOAc) (Fisher Scientific, New Jersey NY), 2mM DTT, 10% (v/v) glycerol, 0.1 mM ethylene glycol tetraacetic acid (EGTA) (EM Sciences Darmstadt, Germany), 10mM Tris-Cl pH 7.4, 30% w/v sucrose
Buffer C	4M potassium acetate (KOAc) (Fisher Scientific, New Jersey NY), 1.5mM magnesium acetate (MgOAc) (Fisher Scientific, New Jersey NY), 2mM DTT, 10% (v/v) glycerol, 0.1mM ethylene glycol tetraacetic acid (EGTA) (EM Sciences Darmstadt, Germany), 10mM Tris-Cl pH 7.4, 30% w/v sucrose

2.1.2 Non-Chromatographic Protein Purification

The RSW was subjected to a pH-dependent protein precipitation step to remove bulk, non-soluble proteins. All procedures were performed on ice unless otherwise indicated. The pH of the RSW was lowered to 5.0 using a solution of 1M hydrocholoric

acid (HCL) (BDH Toronto, Ontario). The RSW was subsequently centrifuged at 18,000 rpm for 25 min at 4°C. The supernatant was carefully removed, and the pH was re-adjusted to 7.0 using a solution of 1M sodium hydroxide (NaOH). The final solution was then placed in 50 ml Nalgene tubes and frozen at -20°C for storage.

2.1.3 Plasmid Digestion

Prior to plasmid digestion, stock solutions of 10 mg/mL Proteinase K (EM Sciences, Darmstadt, Germany) and a 10 X Proteinase K buffer (100 mM Tris-Cl pH 8.0, 50 mM ethylenediamine tetra-acetic acid (EDTA) pH 8.0 (Sigma-Aldrich, St. Louis, MO), 500 mM sodium chloride (NaCl) (Sigma-Aldrich, St. Louis, MO) were prepared. The plasmid construct used in this study was pUC19-CRD-*myc*-1705-1886. Plasmid digestion was performed using a single restriction enzyme, *EcoRI* (New England Biolabs). Approximately 7.0 µg of pUC19-CRD-*myc*-1705-1886 plasmid in a 10 µL reaction mixture was subjected to restriction enzyme digest (1U/ µL) at 37°C for 60 min. Immediately following plasmid digestion, the mixture was treated with 0.5 % sodium dodecyl sulfate (SDS) (EM Sciences, NJ) and 50 µg/mL diluted aliquot of Proteinase K solution in 10X Proteinase K buffer. This mixture was subsequently incubated at 50 °C for 30 min.

Following incubation with Proteinase K, 90 µL of Milli-Q-ddH_2O was added. The mixture was then subjected to a standard phenol/chloroform extraction, followed by ammonium acetate/isopropanol precipitation. One half volume of phenol (Sigma) and one half volume of chloroform: isoamyl alcohol ($CHCl_3$: IAA) (49:1) (Fluka) was added and vortexed thoroughly. After the mixture was centrifuged at 13,200 rpm for 2.5 min the top aqueous layer was extracted and placed in a fresh eppendorf tube. One full

volume of $CHCl_3$: IAA was then added and the mixture was vortexed thoroughly and centrifuged at 13,200 rpm for 2.5 min. The aqueous top layer was again extracted and transferred to a fresh eppendorf tube. This procedure was repeated once again. The DNA was precipitated by adding 1/10 volume of 7.5 M ammonium acetate and 1 volume of isopropanol (Sigma). Following centrifugation at 13,200 rpm for 45 min at 1°C, the supernatant was removed and the pellet was washed once with 200 µl of isopropanol. The supernatant was again removed and the pellet was air dried for 10 min prior to resuspension in 25 µL of nuclease-free water (Ambion).

The resuspended DNA was quantified using an ND-1000 UV-Spectrophotometer (NanoDrop Wilmington, Delaware). DNA concentrations were determined at 260nm using the following relationship: DNA concentration (µg/ml) = (OD_{260}) x (dilution factor) x (50 µg DNA/ml)/ (1 OD_{260} unit). The digested products were resolved in a 50 mL 2% agarose (Invitrogen) gel containing 1 µL of a 10 mg/mL stock ethidium bromide solution. Agarose gels were resolved at 30 mA in 1x TBE buffer (buffer composition shown in Table 4) for approximately 60 min and visualized by UV-transillumination using a ChemiImager™ System (Alpha Innotech Corporation, San Leandro, CA).

Table 4: Reagents and composition utilized in the generation of unlabeled and 5'-radiolabeled *c-myc* CRD RNA

Reagent	Composition
1x TBE	0.9M Tris-Cl/Boric acid (Sigma), 0.01M EDTA pH 8.3 (Sigma)
1x MOPS	0.2M MOPS (Sigma), 50mM sodium acetate (NaOAc) (Sigma), 10mM EDTA (Sigma)
RNA Loading Dye	50% formamide, 2% formaldehyde, 1x MOPS, 0.05 mg/mL bromophenol blue (Sigma), 0.05 mg/mL xylene cyanol (Sigma) and 0.01M EDTA pH 8.0 (Sigma)
Formamide Loading Dye	80% formamide, 0.05 mg/mL bromophenol blue (Sigma), 0.05 mg/mL xylene cyanol (Sigma), 0.01 M EDTA pH 8.0 (Sigma)
Urea/Phenol Loading Dye	9M Urea (Fisher Scientific), 10% Phenol v/v, 0.05 mg/mL bromophenol blue (Sigma), 0.05 mg/mL xylene cyanol (Sigma) and 0.01M EDTA pH 8.0 (Sigma)
Probe Elution Buffer	100mM Tris-Cl (pH 7.5), 0.5M EDTA (Sigma), ½ volume phenol (Sigma), ½ volume chloroform: isoamyl alcohol (49:1) (Fluka)

2.1.4 Generation of Unlabeled *c-myc* CRD RNA

Generation of RNA was accomplished from linearized plasmid using either T7 or SP6 RNA polymerase-mediated *in vitro* transcription kits (MEGAscript, Ambion, Austin, TX). Transcription reactions were carried out in a final volume of 20 µL. The reaction mixture typically contained 1.5 µg of linearized plasmid, 5mM ATP, CTP, GTP and UTP, respectively, 20 mM DTT (Promega Madison, WI), 1X reaction buffer (Ambion), 1 µL/40U RNasin (Promega, Madison, WI), and 4 µL/40 units of SP6 or T7 polymerase enzyme (Ambion). *In vitro* reactions were incubated at 37°C for approximately 90 min. Following the incubation period, 2U of TURBO DNase 1 (Ambion) was added to the reaction mixture and incubated at 37°C for 15 min. The RNA was isolated using a standard phenol/chloroform extraction and ammonium acetate/isopropanol precipitation.

The RNA pellet was air dried for 10 min and resuspended in 25 µL of diethylpyrocarbonate (DEPC) (Sigma) Milli-Q-ddH_2O. The RNA was quantified by measuring the absorbance at a wavelength of 260 nm on a UV/Visible Spectrophotometer (Biochrom, Ultrospec 1000). RNA concentration was determined using the relationship RNA (µg/mL) = (OD_{260}) x (dilution factor) x (40 µg RNA/mL)/ (1 OD_{260} unit). The purity of the RNA was also examined by assessing the A_{260} : A_{280} ratio using the ND-1000 UV-Spectrophotometer (NanoDrop Wilmington, Delaware). The quality of the RNA product was also assessed using a 50 mL, 2% agarose (Invitrogen) gel containing 37% formaldehyde (v/v) (Sigma) and 1 µL of a stock 10 mg/mL solution of ethidium bromide. Approximately 500 ng of RNA was mixed with RNA loading dye (composition shown in Table 4), and electrophoresed at 35 mA in 1x MOPS buffer (buffer composition shown in Table 4) for approximately 90 min. The agarose gels containing the RNA were visualized by UV-transillumination using a ChemiImager™ System (Alpha Innotech Corporation, San Leandro, CA).

2.1.5 Preparation of 5'-Radiolabeled *c-myc* CRD RNA

c-myc CRD RNA (nts 1705-1886) was subsequently dephosphorylated at the 5' terminus. A typical dephosphorylation reaction contained 7 µg of RNA, 10 U (1 µL = 1U) alkaline phophatase from calf intestine (Roche Diagnostic Inc., Montreal), 2.5 µL of a 10x dephosphorylation buffer, 10mM DTT and 40 U (40U/ µL) of RNasin (Promega). The volume of the reaction mixture was brought up to 50 µL by adding DEPC (Sigma)-treated Milli-Q-ddH_2O. The mixture was incubated at 37°C for 60 min. The dephophorylated RNA was isolated using a standard phenol/chloroform extraction and ammonium acetate/isopropanol precipitation. RNA pellets were air dried for 10 min and

re-suspended in 25 μL of nuclease-free water (Ambion). The RNA was subsequently quantified using the ND-1000 UV-Spectrophotometer (NanoDrop Wilmington, Delaware).

5'-γ^{32}P-radiolabeling of *c-myc* CRD (nts 1705-1886) RNA transcripts were carried out using the following conditions. Approximately 8 μg of dephosphorylated RNA was phosphorylated using 3 μL of 100 mM DTT, 80 U RNasin (80U/ μL) (Promega), 5 μL of a 10 X reaction buffer (New England Biolabs), 60 μCi (6 μL) γ^{32} P-ATP (Amersham Biosciences), and 40U (10 U/ μL) T4 Polynucleotide Kinase (PNK) (New England Biolabs). The reaction was incubated for 60 min at 37°C and the RNA was isolated using a standard phenol/choloroform extraction and ammonium acetate/isopropanol precipitation.

The RNA pellet was air dried for 10 min and resuspended in 20 μL of formamide loading dye (composition shown in Table 4), loaded onto an 8% denaturing polyacrylamide/ 7M urea (Fisher Scientific) gel and electrophoresed at 30 mA in 1x TBE running buffer for approximately 60 min. The RNA bands that were separated within the gel were visualized using a Cyclone Storage Phophor Screen System (Packard, Meriden, CT). The screen was then visualized with a Cyclone PhopholImager (Packard, Meriden, CT) and OptiQuant software. A full-sized image of the audioradiographed gel containing the visible RNA bands was printed and placed below the gel. The appropriate bands were excised and the gel slices were placed into 1.5 mL eppendorf tubes containing probe elution buffer (composition of probe elution buffer shown in Table 4). The gel slices were incubated at 60°C for 5 hrs and vortexed periodically (45 min intervals).

RNA was recovered following the elution by way of standard phenol/chloroform extraction and ammonium acetate/isopropanol precipitation. The RNA pellet was air dried for 10 min and resuspended in 50 μL of nuclease-free water (Ambion). The radioactivity of the RNA measured in counts per minute (cpm) was assessed using a Packard 1600 TR liquid scintillation analyzer. The 5'- γ ^{32}P-radiolabeled *c-myc* CRD was further diluted into working aliquots of 50,000 cpm and stored at -20 °C.

2.1.6 Performing Endoribonuclease Assays using 5'-Radiolabeled *c-myc* CRD RNA

To assess the enzyme activity of the purified endoribonuclease, a standard *in vitro* endoribonuclease assay was performed. The reaction mixture used for the standard assay consisted of final concentrations of 10 mM Tris (pH 7.5), 2mM MgOAc, 50 mM KOAc, 0.1mM spermidine (Sigma), 2mM DTT, 0.5U RNasin (40U/ μL). DEPC-treated Milli-Q-ddH_2O was added to ensure that the appropriate final reaction mixture volume was attained. 18 μL of the reaction mixture was aliquoted into 20 separate 1.5 mL eppendorf tubes.

The appropriate amount of enzyme was added to the bottom of each tube containing 18 μL of reaction mixture. 4 μL of DEPC-treated H_2O was placed in the tube serving as negative control (in place of the enzyme). 1 μL of 30 000 cpm, 5'-γ^{32}P-radiolabeled *c-myc* CRD RNA was added to the side of the tubes containing the reaction mixture and the tubes were pulsed to ensure the aliquot of radiolabeled RNA entered the enzyme/reaction mixture at the bottom of the tube. The reactions were incubated in a heat block at 37°C for 5 min unless otherwise stated. The reaction was terminated by placing the tubes in a heat block at 100°C for 3 min followed by the addition of 4 μL of urea/phenol loading dye (contents of dye shown in Table 4). The samples in the tubes

were then loaded onto an 8% or 12%/7M urea denaturing polyacrylamide gel. The gel was electrophoresed at 30 mA for 60 min in 1X TBE buffer (until the primary dye front, bromophenol blue approached the bottom of the glass plates). Following electrophoresis, the gel plates were separated and the gel was transferred to filter paper and placed in a gel dryer (LABCONCO, Kansas City, MI) for approximately 45-60 min. The dried gel was exposed to a phosphor image storage screen overnight and the image was subsequently visualized using the Cyclone PhosphoImager and Optiquant software.

2.1.7 Protein Purification Utilizing Column Chromatography

It should be noted that prior to each step in the chromatographic sequence of purification, the quantity of protein was determined using the Bradford Assay methodology. All column chromatographic purifications were performed using an ISCO Model 160 Gradient Former and a Foxy^R Jr. Fraction Collector (ISCO, Lincoln NB, USA).

2.1.7.1 Ion Exchange Chromatography

Cellulose-Phophate Matrix

The post-pH precipitated RSW, pH 7.0 samples were dialyzed in dialysis Buffer A (composition shown in Table 5) for 12 hrs using SnakeSkin^R Pleated Dialysis Tubing (PIERCE, Rockford, IL) with a 10,000 molecular weight cutoff. This was performed to remove high salt concentrations prior to loading onto the column matrix to ensure that proteins would bind efficiently. The cellulose phosphate column matrix (Sigma) (bed volume 900 mL) was equilibrated with 3 column volumes of Buffer D (buffer composition shown in Table 5). Approximately 1.5-2.0 g of RSW proteins were then loaded onto a 100cm x 5.0 cm, XK 50 chromatographic column (Amersham Pharmacia

Biotech.Quebec) at a flow rate of 1.8 mL/min. The column was washed until the absorbance at 280 nm (A280) as measured by the UV chart recorder unit (UA-6 UV/Vis Spectrophotometer, ISCO) returned to base line (2 column volumes Buffer D). Bound proteins were then eluted in 1.5 column volumes of Buffer E using a linear gradient from 0.1 to 0.75 M KCl. A total of 80, 15 mL fractions were collected. A 4 μL aliquot of a subset of fractions were assayed for the presence of endonuclease activity as previously described (section 2.1.6). Given the large quantity of protein that was purified, 20 separate cellulose phosphate matrix-based chromatography runs were performed using the 100cm x 5.0 cm, XK 50 column. Column runs were highly reproducible.

2.1.7.2 Affinity Chromatography

Reactive Green-19 Dye Matrix

The post-phosphocellulose pooled fractions with peak endonuclease activity were dialyzed in dialysis Buffer A (composition shown in Table 5) for 12 hrs using SnakeSkin^{R} Pleated Dialysis Tubing (PIERCE, Rockford, IL) with a 10,000 molecular weight cutoff. Again, this was performed to remove high salt concentrations prior to loading onto the column matrix to ensure that proteins would bind efficiently. The reactive green matrix (Sigma) (bed volume 160 mL) was equilibrated with 3 column volumes of Buffer F (buffer composition shown in Table 5). Approximately 2 mg of post-phosphocellulose protein with peak endonuclease activity were then loaded onto a XK 26, 70cm x 2.6 cm chromatographic column (Amersham Pharmacia Biotech.) at a flow rate of 1.25 mL/min. The column was washed until the absorbance at 280 nm (A280) returned to base line (2 column volumes Buffer F). Bound proteins were then eluted in 1.5 column volumes of Buffer G using a linear gradient from 0.1 to 0.75 M KCl.

A total of 140, 2.5 mL fractions were collected. 10 separate reactive green-19 columns were run. A 2.5 µL aliquot of a subset of fractions were assayed for the presence of endonuclease activity as previously described (section 2.1.6). Column runs were highly reproducible.

Affi-Gel Heparin Matrix

Pooled post-Reactive Green-19 fractions with maximum endonuclease activity were dialyzed in dialysis Buffer B (composition shown in Table 5) for 12 hours using SnakeSkin^R Pleated Dialysis Tubing (PIERCE, Rockford, IL) with a 10,000 molecular weight cutoff. The Affi-gel/heparin gel matrix (Biorad) (bed volume 120 mL) was equilibrated with 3 column volumes of Buffer F (buffer composition shown in Table 5). Approximately 1 mg of proteins were loaded onto a XK 26, 70cm x 2.6 cm chromatographic column (Amersham Pharmacia Biotech.,Quebec) at a flow rate of 1.5 mL/min. The column was washed until the absorbance at 280 nm (A280) returned to base line (2 column volumes Buffer F). Bound proteins were then eluted in 1 column volume of Buffer G using a linear gradient from 0.1 to 0.75 M KCl. A total of 120, 1.5 mL fractions were collected. 8 separate AffiGel-Heparin columns were run. Column runs were highly reproducible. A 1.5 µL aliquot of each was assayed for the presence of endonuclease activity as previously described (section 2.1.6).

Heparin-Sepharose Matrix

Pooled post-AffiGel-Heparin fractions with maximum endonuclease activity were dialyzed in dialysis Buffer B (composition shown in Table 5) for 12 hrs using SnakeSkin^R Pleated Dialysis Tubing (PIERCE, Rockford, IL) with a 10,000 molecular weight cutoff. The pre-packed 5 mL HiTrap Heparin-Sepharose HP column (Amersham

Biosciences) equilibrated with 10 column volumes of Buffer F. Approximately 0.50 mg of proteins were loaded at a flow rate of 1.2 mL/min onto the column. The column was washed until the absorbance at 280 nm (A280) returned to base line (4 column volumes Buffer F). Bound proteins were then eluted in three column volumes of Buffer G using a linear gradient from 0.1 to 0.75 M KCl. A total of sixty, 0.5 mL fractions were collected. The post heparin-sepharose fractions with maximum endonuclease activity were pooled. Three separate column runs were performed and each was highly reproducible. One µL aliquot of each fraction was assayed for the presence of endonuclease activity as previously described (section 2.1.6).

2.1.7.3 Gel Filtration Chromatography

The gel filtration column was equilibrated with 5 column volumes of Buffer F (composition shown in Table 5). The column was calibrated with molecular weight standards using a flow rate of 1.0 mL/min and a total column/elution volume of 100 mL as follows: 1.80 mL of Buffer F (Table 4) was used to dilute 0.2 mL (0.5 mg/mL) *BSA* 0.2 mL (4.0 mg/mL) *Ovalbumin*, 0.200 (4.0 mg/mL) *Carbonic Anhydrase*, 0.2 mL (6.0 mg/mL) *Myoglobin*, 0.2 mL (6.0 mg/mL) *Cytochrome C*. *BSA* (66 kDa) eluted at volume (V_e) of 40.6-42.2 mL, *Ovalbumin* (49 kDa) V_e of 43.5-45.6 mL, *Carbonic Anhydrase* (29 kDa) V_e of 52.4-55.2 mL, *Cytochrome C* (Dimeric form, 24.8kDa) V_e 60.8-63.6mL, *Myoglobin* (17 kDa) V_e of 66.5-70.5 mL, *Cytochrome C* (monomeric form, 12.5 kDa) V_e of 72.8-78.4 mL.

Approximately 3.0 mL of pooled post heparin-sepharose sample exhibiting peak endonuclease activity was placed in 1.0 mL aliquots using 1.5 mL eppendorf tubes and centrifuged at 10, 400 rpm for 10 min. The sample was again pooled and loaded onto a

Superdex 75 Hi Load16/60 prep grade gel filtration column (GE Healthcare) at a flow rate of 1.0 mL/min. A total of two hundred fractions of 0.5 ml were collected in microcentrifuge tubes (total of 100 mL column/elution volume). A 4 µL aliquot of each fraction was assayed for the presence of endonuclease activity as previously described (section 2.1.6).

Table 5: Reagents and composition utilized in the chromatographic purification of two mammalian endoribonucleases.

Reagent	Composition
Buffer D: Potassium phosphate binding/wash buffer	50 mM KCl (Fisher Scientific), 100 mM K_2HPO_4/ $KHPO_4$ (Sigma) pH 7.0
Buffer E: Potassium phosphate elution buffer	1M KCl (Fisher Scientific), 100 mM K_2HPO_4/ $KHPO_4$ (Sigma) pH 7.0
Buffer F: TEA binding/wash buffer	50 mM KCl (Fisher Scientific), 50 mM Triethanolamine (TEA) (Sigma), pH 7.4
Buffer G: TEA elution buffer	1M KCl (Fisher Scientific), 100 mM Triethanolamine (TEA) (Sigma), pH 7.4
Dialysis Buffer A	25 mM KCl (Fisher Scientific), 100 mM K_2HPO_4/ $KHPO_4$ (Sigma) pH 7.0
Dialysis Buffer B	25 mM KCl (Fisher Scientific), 50 mM Triethanolamine (TEA) (Sigma), pH 7.4

2.1.8 SDS-PAGE/Silver Stain Analysis of Post Heparin-Sepharose and Gel Filtration Elution Fractions.

Following purification using heparin-sepharose and gel filtration column chromatography steps, and after the routinely performed standard endoribonuclease assay, elution fractions were frequently concentrated by pooling and subjecting them to a standard acetone precipitation procedure. In brief, an equal volume of ice-cold acetone (-20°C) was added to the tubes containing the protein sample. Tubes were placed in -20°C for 60 min and centrifuged at 13,200 rpm for 45 min. The acetone was removed and the protein pellets were air-dried for 10 min. The protein pellets were re-suspended and pooled in 10 µL of Milli-Q-dd H_2O and 10 µL of 1X SDS loading dye (composition shown in Table 6). The 20 µL mixture was boiled for 5 min, allowed to cool to room

temperature and loaded onto a sodium dodecyl sulphate 15% polyacrylamide, 19:1 acrylamide/N,N'–methylenebisacrylamide (Invitrogen) gel (SDS PAGE gel). The samples were electrophoresed at 120V until the bromophenol blue dye front reached the bottom of the gel. The gel was then fixed with gently shaking for twenty minutes in a solution of 100 mL methanol, 20 mL acetic acid, 20 mL of Bio-Rad fixative enhancer concentrate, and 60 mL of Milli-Q-dd H_2O. The gels were subsequently rinsed twice for 10 minute intervals in Milli-Q-dd H_2O. As per BioRad Silver Stain Plus protocol, 35 mL of Milli-Q-dd H_2O, 5.0 mL of Bio-Rad silver complex solution, 5.0 mL of Bio-Rad reduction moderator solution, 5.0 mL of Bio-Rad image developing reagent, and 50 mL of Bio-Rad development accelerator solution were mixed thoroughly in a 250 mL Erlenmeyer flask and added to the gels. The gels were allowed to stain with gentle shaking for 10-15 min at room temperature. Once the desired staining was achieved, the gel was placed in a 5% acetic acid solution and fixed with gentle shaking for 20 min. The gel was then rinsed with Milli-Q-dd H_2O for 5 minutes and visualized using the ChemiImager™ System.

2.1.9 Determining Specific Activity of Endoribonuclease Activity

One unit (U) of enzyme was defined as the quantity of post heparin-sepharose partially purified enzyme required to cleave 25% of the 5'- γ ^{32}P-radiolabeled *c-myc* CRD RNA input probe to decay product in the standard endoribonuclease assay reaction as described in section 2.1.6.

Post-gel filtration purified native endoribonuclease samples corresponding to 17 kDa and 35 kDa respectively, were assigned units of enzyme activity based on comparative ratio of their endonuclease activities against *c-myc* CRD RNA. 1U of 17

kDa enzyme was defined as 1 μL of post gel filtration-purified sample (elution volume 65-80mL) in a standard endoribonuclease assay (described in section 2.1.6). 1U of 35 kDa enzyme was defined as 5 μL of post gel filtration-purified sample (elution volume 30-40 mL) in a standard endoribonuclease assay (described in section 2.1.6)

The yield of the enzyme, shown in Table 7, was calculated by dividing the *activity* in each step of the purification by the *activity* present in the initial sample of RSW. The *fold* purification as shown in Table 6 was calculated by dividing the *specific activity (units/mg)* in each step of the purification by the *specific activity (units/mg)* of the initial starting sample of RSW.

2.1.10 Sample Preparation and SDS-PAGE/Coomassie Staining for the First LC/MS/MASS Spectrometry Analysis

Approximately 20 mL (0.3 mg) of post-Heparin/Sepharose purified protein was utilized for MASS Spectrometry Analysis. The 20 mL volume was measured into forty, 0.5 mL aliquots and pipetted into forty separate eppendorf tubes which had been thoroughly rinsed with methanol to avoid keratin protein contamination. The tubes were then subjected to a standard acetone precipitation procedure as previously described in section 2.1.8. The protein pellets were re-suspended and pooled in 10 μL of Milli-Q-dd H_2O and 10 μL of 1X SDS loading dye (composition shown in Table 6). The 20 μL mixture was boiled for 5 min, allowed to cool to room temperature and loaded onto a sodium dodecyl sulphate 15% polyacrylamide, 19:1 acrylamide/N,N'–methylenebisacrylamide (Invitrogen) gel (SDS PAGE gel). The samples were electrophoresed at 120V until the bromophenol blue dye front reached the bottom of the gel. The gel was subsequently stained for 3 hrs with gentle shaking in a solution of Coomassie Brilliant Blue G dye (composition shown in Table 6). The gel was then de-

stained (composition of de-stain shown in Table 6) with gentle shaking for 1 hr. The appropriate bands were excised from the gel with a razor blade and placed in eppendorf tubes which had been pre-rinsed with 100% methanol. The tubes containing the protein bands of interest were sent to the Genome B.C. Proteomics Center at the University of Victoria for LC/MS/Mass Spectrometry/trypsin digest analysis and protein identification.

Table 6: Reagents used in the preparation and staining of SDS-PAGE gels

Reagent	**Composition**
1X SDS loading dye	25 mM Tris-Cl pH 7.4, 20% glycerol (v/v) (Sigma), 4% SDS (v/v) (OmniPur/EM Science, Gibbstown NJ), 0.2 % bromophenol blue (w/v) (Sigma), 0.1 % β-mercaptoethanol (v/v) (Sigma)
Coomassie blue staining solution	50% methanol, 10% acetic acid, 1% (w/v) Coomassie Brilliant Blue G
Coomassie blue de-staining solution	50% methanol, 10% acetic acid

2.1.11 Sample Preparation and SDS-PAGE/Coomassie Staining for the Second LC/MS/MASS Spectrometry Analysis

Fractions from gel filtration columns 5 and 7 containing peak endonuclease activity corresponding to an elution volume of 44-50 mL (30-40 kDa protein size range) were pooled. The total volume of 6 ml was measured into 0.5 mL aliquots and pipetted into twelve separate eppendorf tubes. The eppendorf tubes had been thoroughly rinsed with 100% methanol to avoid keratin protein contamination. Due to the sensitivity of LC/MS/MASS Spectrometry analysis, keratin protein contamination prevents accurate identification of target proteins. A standard acetone precipitation procedure was performed as previously described in section 2.1.8. The protein pellets were re-suspended in 10 µL of Milli-Q-dd H_2O and 10 µL of 1X SDS loading dye (composition

shown in Table 6) for a total of 20 µL/ tube. The samples were then boiled for 5 min, allowed to cool to room temperature and loaded onto 15% polyacrylamide SDS-PAGE gel. The samples were electrophoresed at 120V until the bromophenol blue dye front reached the bottom of the gel. The gel was subsequently stained for 3 hours with gently shaking in a solution of Coomassie Brilliant Blue G dye (composition shown in Table 6). The gel was then de-stained (composition of de-stain shown in Table 6) with gentle shaking for 1 hr. The appropriate bands were subsequently excised from the gel and placed in eppendorf tubes which had been pre-rinsed with 100% methanol. The tubes containing the protein bands of interest were sent to the Genome B.C. Proteomics Center at the University of Victoria for LC/MS/Mass Spectrometry/trypsin digest analysis and protein identification.

2.2 Results and Discussion

2.2.1 Protein Purification

The first non-chromatographic/pH precipitation step used to purify a total volume of nine liters of Ribosomal (Liver) Salt Wash (RSW or LSW) generated a seven-fold increase in protein purity and a total increase in units of enzyme activity, as shown in Table 7. The total protein, total volume, specific activity and yield are also shown in Table 7.

Chromatographic purification of two endoribonucleases was successfully accomplished using ion exchange, affinity, and size exclusion chromatography. The column matrices utilized yielded highly reproducible results. The matrices used in this purification scheme were chosen based on previous work done in Dr. Lee's lab (Bergstrom *et al.* 2006). There were, however, two major differences in the purification

used in this research as compared to previous research undertaken to purify these mammalian endoribonucleases. Firstly, the purification described in this research omitted a Reactive-Blue-4 dye affinity matrix. Secondly, a dialysis procedure was performed to remove excess KCl prior to loading pooled elution fractions (with peak endoribonuclease activity) onto subsequent column matrices. To reduce the concentration of KCl, previous work done to purify the endoribonucleases (Bergstrom *et al.* 2006) diluted pooled elution fractions (exhibiting peak endoribonuclease activity) with buffer prior to loading onto subsequent column matrices.

Table 7: Summary of the Partial Purification of Two Mammalian Endoribonucleases from Rat Liver Tissue.

	Total Protein	**Volume**	**Activity**	**Specific Activity**	**Yield**	**Purification**
Step	*mg*	*mL*	*units*	*units/mg*	*%*	*Fold*
Ribosomal Salt Wash	36,000	9,000	4.41×10^7	1225	100	1
pH Precipitation	26,000	9,350	2.15×10^8	8269	100	6.80
Phosphocellulose	679.80	7,590	3.22×10^7	43,367	73	35
Reactive Green-19	21.00	3,250	8.30×10^6	395,238	18.9	323
AffiGel/Heparin	5.33	750	4.15×10^6	778,612	9.4	635.6
Heparin-Sepharose	0.84	45	9.97×10^5	1,186,905	2.3	1069

Each ion exchange column matrix composed of cellulose phosphate (phosphocellulose) with a bed volume of 900 mL was capable of binding approximately 2-3 g of post-pH treated proteins. Endoribonuclease activity eluted from the column at a gradient KCl concentration of 0.45-0.55M (Figure 4, top panel).

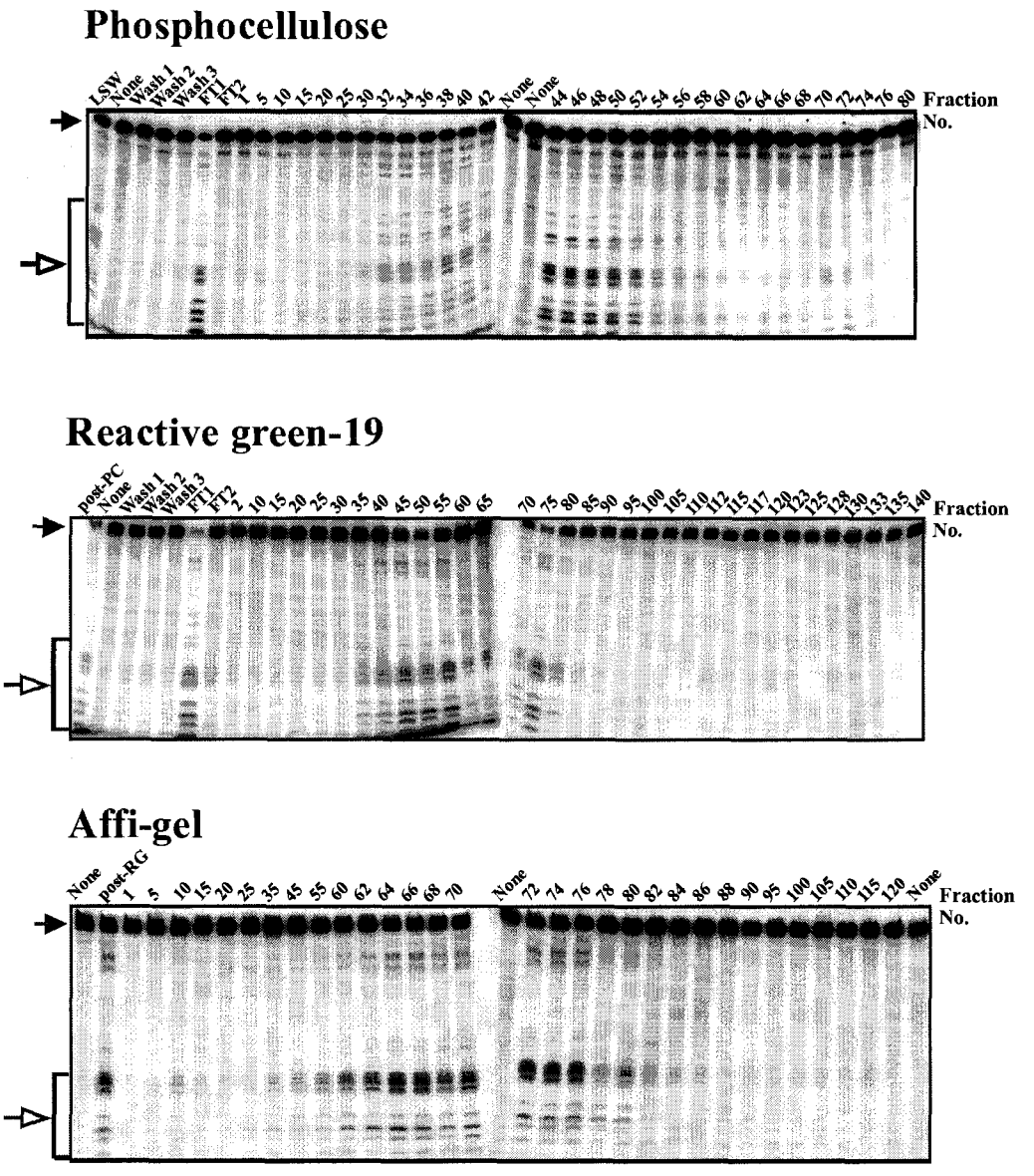

Figure 4: Analysis of endonucleolytic activity of samples from column chromatography purification. All reactions were performed using 5'- γ ^{32}P-radiolabeled *c-myc* CRD (30,000 cpm/lane). RNA was resolved on 12% denaturing polyacrylamide/7M urea gels. Fully intact *c-myc* CRD RNA is shown with a filled arrow. The top panel depicts 4.0 μL (1U) sample aliquots from eluted fractions of phosphocellulose column 5. The middle panel depicts 2.5 μL (1U) sample aliquots from eluted fractions of reactive green-19 column 2. The lowest panel depicts 1.5 μL (1U) sample aliquots from eluted fractions of affi-gel/heparin column #3. Lanes containing no enzyme are labeled 'none'. Lanes used as positive control are labeled LSW (liver salt wash), post-PC (pooled phosphocellulose elution fractions with endonuclease acitivity and post-RG (pooled Reactive Green-19 elution fractions with endonuclease activity) respectively. Filled arrow indicates intact *c-myc* CRD RNA. Bracket and unfilled arrow indicates RNA decay products

Cellulose phosphate chromatography was efficient at binding endoribonuclease proteins; however, there was significant endonucleolytic activity exhibited in the first flow through fraction collected during column loading (Figure 4 top panel, FT-1 lane 6). This was most likely due to overloading the binding capacity of the column matrix. Optimal protein load needed for efficient binding of endoribonucleases to the phosphocellulose column matrix was roughly 1.5 g. Overall, phosphocellulose chromatography yielded a 35-fold increase in enzyme purity as judged by specific activity (Table 7).

The Reactive Green-19 affinity matrix exhibited a high capacity to bind endoribonucleases present in post-phosphocellulose purified sample. The Reactive Green-19 dye affinity matrix (bed volume 160 mL) was capable of binding approximately 50 mg of protein. Endoribonuclease activity eluted from the column at a gradient KCl concentration of 0.35-0.45M (Figure 4, middle panel). The endoribonuclease assay of the fraction collected for flow through 1 (FT-1) during column loading (Figure 4, middle panel, lane 6) exhibited strong endoribonucleolytic activity. Again, this was most likely due to overloading the binding capacity of the column matrix. Optimal protein load needed for efficient binding of endoribonucleases to the Reactive Green-19 dye matrix was 30-40 mg. Overall, Reactive Green-19 affinity chromatography resulted in a 323-fold increase in enzyme purity (Table 7).

Affi-gel/Heparin affinity chromatography also exhibited a high capacity to bind endoribonucleases isolated from rat liver tissue. Optimal protein load concentration for each column run was approximately 1.5 mg. Endoribonuclease activity eluted from the column at a gradient KCl concentration of 0.55-0.65M (Figure 4, lower panel). Overall,

affi-gel/heparin affinity chromatography resulted in a 635-fold increase in enzyme purity (Table 7).

Heparin-Sepharose affinity chromatography exhibited a high degree of binding capability for endoribonucleases present in post affi-gel/heparin pooled elution fractions. Endoribonuclease activity eluted from the column at a gradient KCl concentration of 0.35-0.60M (Figure 5A). Overall, heparin-sepharose affinity chromatography resulted in a 1069-fold increase in enzyme purity (Table 7).

A subset of elution fractions from the first heparin-sepharose column containing endoribonuclease activity (assay shown in Figure 5A) were visualized by SDS-PAGE electrophoresis/silver staining (Figure 5B) to gauge the degree of protein purity within the sample fractions. Not surprisingly, there were several major protein bands remaining in the post-heparin-sepharose elution fractions (Figure 5B, lanes 5-8). Furthermore, the correlation between the fractions assayed in Figure 5A and the proteins visualized by SDS-PAGE in Figure 5B reveals that there is a mixture of proteins present in the eluted fractions with endonucleolytic activity (lanes 5 and 6). There is an increase in the intensity of a protein band at 33 kDa, 37 kDa, and 45 kDa (Figure 5B, lanes 4-8; fractions 32, 38, 41, 44, and 47, respectively); however, when comparing these fractions to the endoribonuclease assay in Figure 5A, it is evident that the increase in the intensity of the aforementioned proteins does not correlate with the observed peak endonucleolytic activity present in fractions 20-42. Moreover, the presence of a mixture of protein bands in the post heparin-sepharose sample coupled with the lack of correlation between protein band intensity (Figure 5B) and endoribonucleolytic activity (Figure 5A) prevented an accurate size estimate of the proteins responsible for endoribonuclease activity.

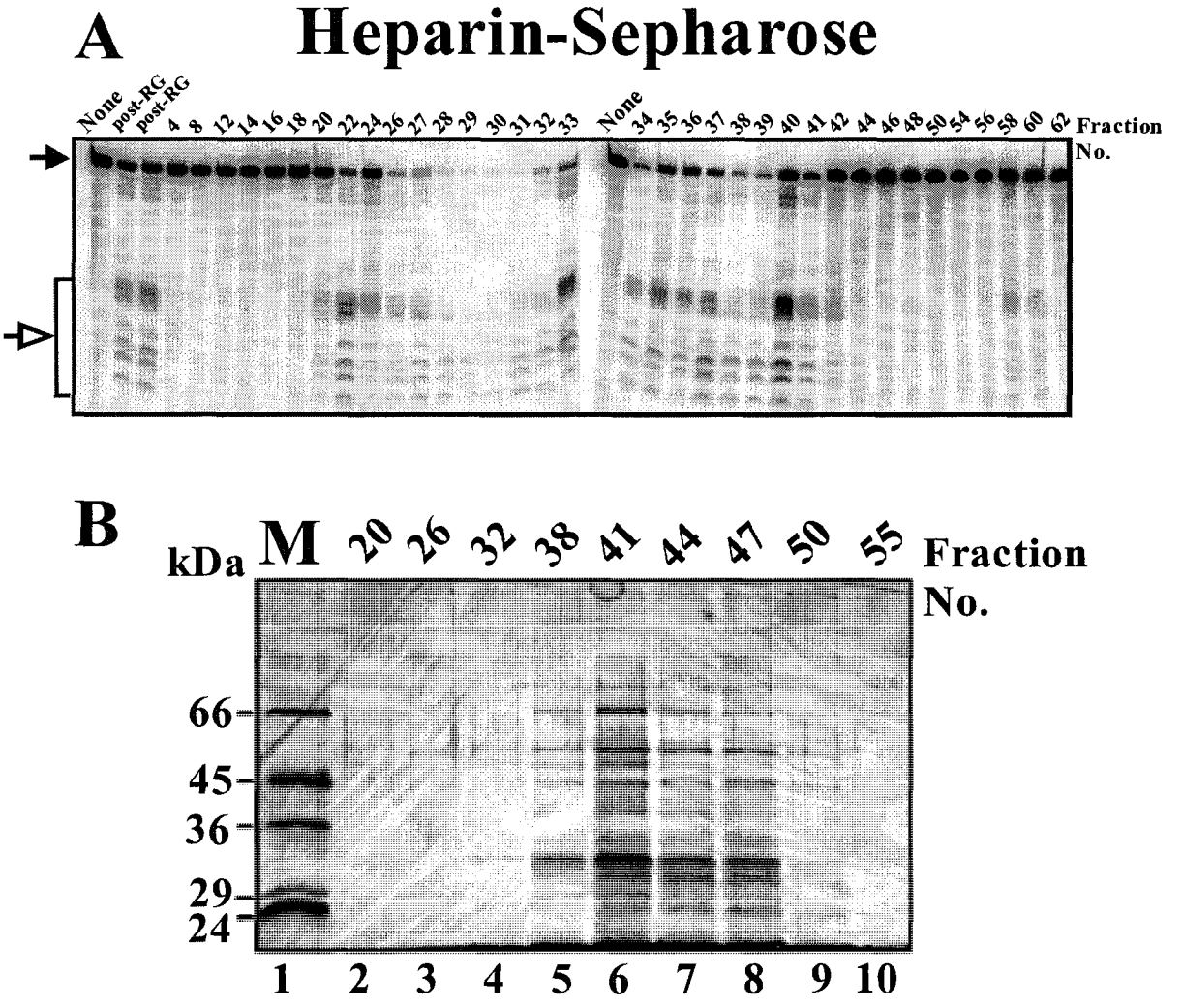

Figure 5: Endonucleolytic activity and SDS-PAGE analysis of post heparin-sepharose purified fractions (A) Autoradiograph depicting sample 1 µL aliquots (1U) taken from eluted fractions and incubated with 5'- γ ^{32}P-radiolabeled *c-myc* CRD RNA. Filled arrow indicates intact *c-myc* CRD RNA. Bracket and unfilled arrow indicates RNA decay products **(B)** 15% polyacrylamide SDS-PAGE gel visualized with silver stain. Lane 1 corresponds to protein marker (M). Lanes 2-10 correspond to selected 0.5 mL elution fractions containing peak endonuclease activity from heparin-sepharose column 1. Molecular weights are indicated on the left.

Gel filtration chromatography was utilized as a means of size separating proteins remaining in pooled post heparin-sepharose elution fractions containing peak

endoribonucleolytic activity. Interestingly and somewhat unexpectedly, standard endoribonuclease assays of gel filtration fractions revealed two distinct regions of endoribonucleolytic activity (Figures 6A and 6B). The first activity was observed within elution volume 44-50 mL (Figure 6A). The second activity was observed within an elution volume of 64-85 mL (Figure 6A). The elution volumes exhibiting endoribonucleolytic activity correspond to proteins of sizes 30-40 kDa and 15-20 kDa, respectively, as calculated from the molecular weight standards used to calibrate the column (section 2.1.7.3).

As shown by Figures 6A, 6B and 7A, gel filtration columns exhibited a high degree of reproducibility. It should be noted, however, that the standard endoribonuclease assay (shown in Figure 6B) of the elution fractions from gel filtration column eight, does not exhibit sharp, clear boundaries between larger molecular weight and smaller molecular weight endonucleolytic activities. Given the larger amount of post heparin-sepharose sample loaded onto this column (approximately 0.4 mg) as compared to the lesser amount of protein loaded onto columns shown in Figures 6A and 7A (approximately 0.10 mg), the observed results are most probably due to excessive amount of protein.

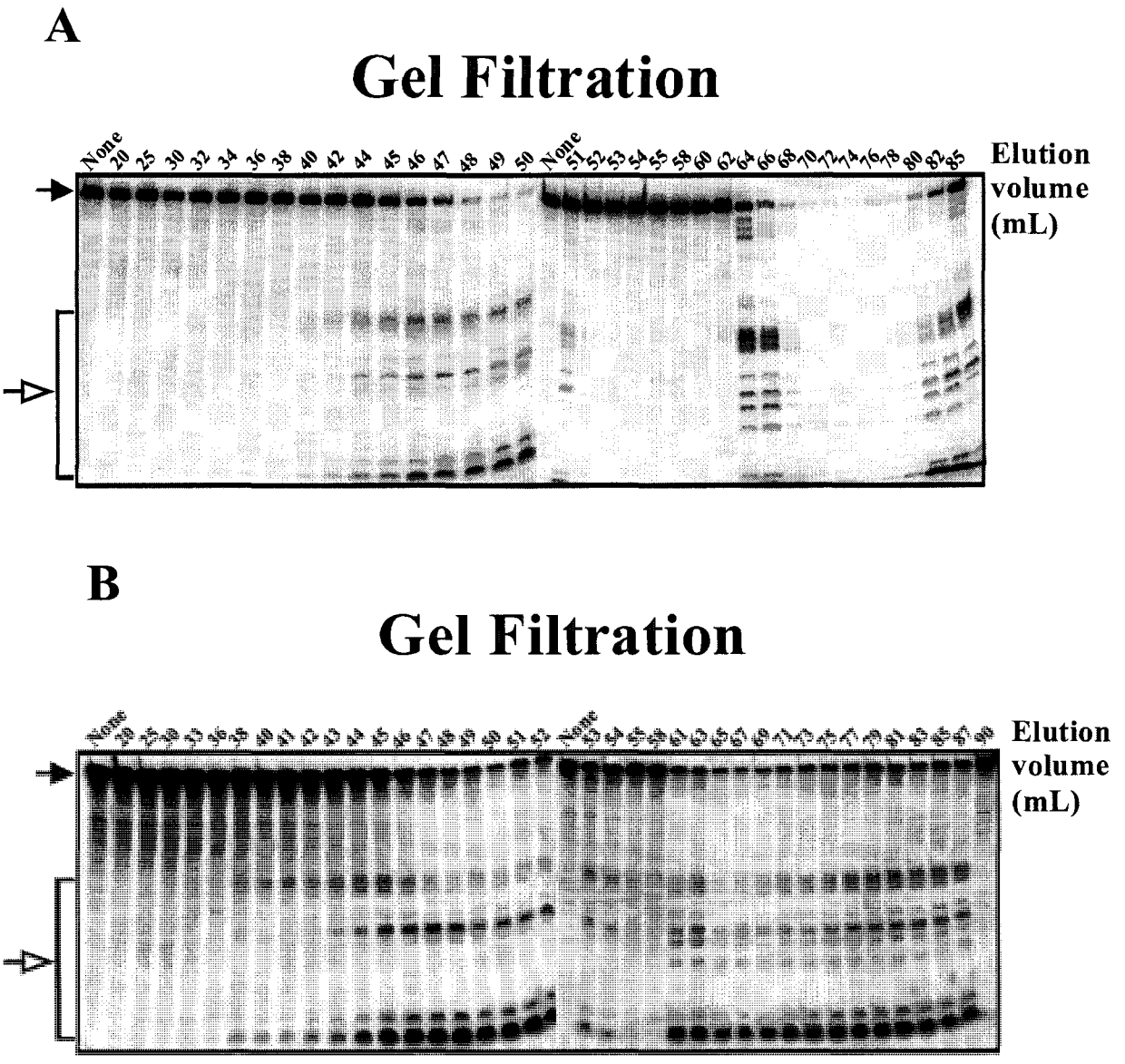

Figure 6: Analysis of endonucleolytic activity of fractions from gel filtration chromatography. (A) Depicts gel filtration column 7. 4.0 µL (0.75 U) sample aliquots taken from the corresponding elution volume was incubated with 5'-γ^{32}P-radiolabeled *c-myc* CRD RNA in a standard endoribonuclease assay. Filled arrow indicates intact *c-myc* CRD RNA. Bracket and unfilled arrow indicates RNA decay products **(B)** Depicts gel filtration column 8. 4.0 µL (0.75U) sample aliquots taken from the corresponding elution volume, labeled above each lane, was incubated with 5'-γ^{32}P-radiolabeled *c-myc* CRD RNA in a standard endoribonuclease assay. Filled arrow indicates intact *c-myc* CRD RNA. Bracket and unfilled arrow indicates RNA decay products

To accurately determine the protein size responsible for endoribonucleolytic activity, a standard endoribonuclease assay was performed on eluted fractions from gel filtration column run five. The fractions from this column were pooled and visualized on an SDS-PAGE/silver stained gel. As shown in Figure 7B (lanes 4-7), there appears to be an increase in intensity of a protein band corresponding to a molecular weight of 35 kDa. In addition, there appears to be an increase in protein bands corresponding to molecular weights of 25 kDa, 18 kDa, and 14 kDa (Figure 7B, lanes 9 and 10). The protein band at 35 kDa in Figure 7B, lanes 4-7 appears to exhibit a slight correlation with endonucleolytic activity in elution volumes 46-50 mL (Figure 7A). The proteins bands at 18 kDa, and 14 kDa (Figure 7B, lanes 9 and 10) appear to correlate with endonucleolytic activity in elution volumes 62-70 mL (Figure 7A).

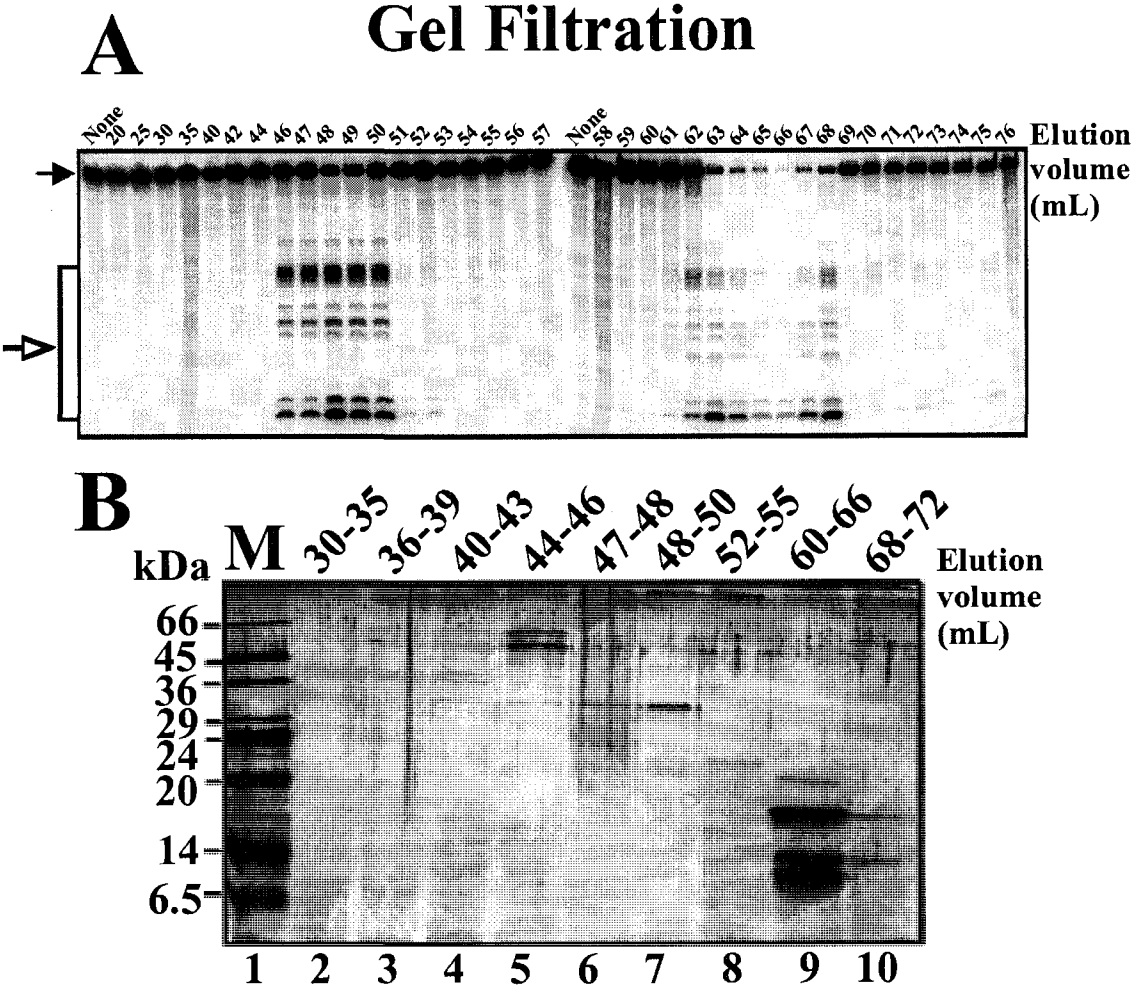

Figure 7: Endonucleolytic activity and SDS-PAGE analysis of elution fractions from gel filtration chromatography. (A) Autoradiograph depicting 4.0 μL (0.75U) aliquots taken from eluted fractions and incubated with 5'- γ ^{32}P-radiolabeled *c-myc* CRD RNA. Filled arrow indicates intact *c-myc* CRD RNA. Bracket and unfilled arrow indicates RNA decay products **(B)** 15% SDS-PAGE gel visualized with silver stain. Lane 1 corresponds to protein marker (M), molecular weights are labeled on the left. Lanes 2-10 depict pooled elution volumes from gel filtration column 5. The pooled elution volumes labeled above lanes 2-10 in (B) correspond to elution volumes labeled above lanes in (A).

To confirm the findings of the aforementioned correlation experiment, a second endoribonuclease assay/SDS-PAGE correlation-type experiment, using elution fractions from gel filtration column runs 7 and 8, was performed. The endoribonuclease assays of

fractions from gel filtration column runs 7 and 8 are shown in Figure 6A and 6B, respectively. The SDS-PAGE/silver stained gel used for the analysis gel filtration column run 7 and the pooled sample from gel filtration column 8 is shown in Figure 8. It is apparent from Figure 8, lanes 4-6, there is an increase in intensity of a protein band at 35 kDa, corresponding to elution volumes of 42-49 mL. Additionally, there is a an increase in intensity of protein bands with molecular weights of 25 kDa, 18 kDa, and 14 kDa which corresponds to gel filtration elution volumes of 62-67 mL (Figure 8, lanes 9 and 10). The protein with apparent molecular weight of 35 kDa exhibited in gel filtration column 7 (Figure 8, lanes 4, 5 and 6) correlates with increasing endoribonucleolytic activity from gel filtration column 7, elution volumes 42-51 mL (Figure 6A). The proteins with apparent molecular weights of 18 kDa and 14 kDa (Figure 8, lanes 9 and 10) correlate with endoribonucleolytic activity from gel filtration column 7, elution volumes 62-85 mL (Figure 6A). The pooled sample of elution volumes 45-50 mL (gel filtration column runs 7 and 8) shown in Figure 8, lane 8 lends further support for the notion that a protein of a molecular weight 35 kDa is responsible for endoribonucleolytic activity in gel filtration elution volumes 40-50 mL. It is evident in Figure 8, lane 8 that there is an intense band of protein with an apparent molecular weight of 35 kDa. Unfortunately, the presence of additional protein bands below and above the 35 kDa band (Figure 8, lane 8) contribute to the uncertainty in determining the precise molecular weight of the protein band responsible for endoribonucleolytic activity in elution volumes 40-50 mL.

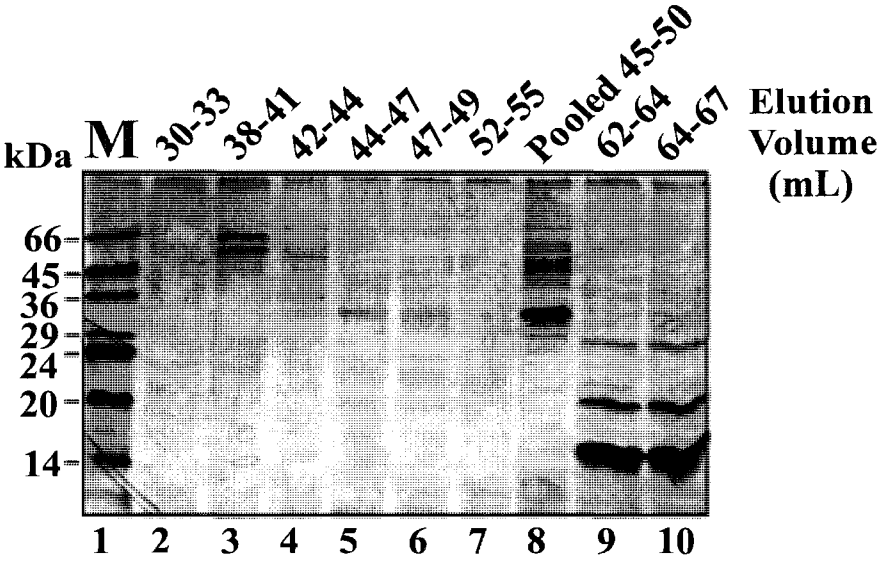

Figure 8: SDS-PAGE analysis of elution fractions from gel filtration chromatography. The gel was silver stained. Lane 1 depicts protein marker with molecular weights labeled to the left of the lane. Lanes 2-7, 9 and 10 depict elution fraction volumes from gel filtration column run 7. Lane 8 depicts a 2.0 mL pooled sample representing elution volumes 45-50 mL from both gel filtration columns 7 and 8.

Overall, the data collected to date suggests that the protein with apparent molecular weight of 35 kDa in Figure 7B (lanes 4-7) and Figure 8 (lanes 4-6 and 8) is the candidate protein responsible for endoribonucleolytic activity in gel filtration elution volumes 40-50 mL. In addition, the data suggests that either the protein band of apparent molecular weight 18 kDa or the protein band of 14 kDa (Figure 7B, lanes 9 and 10; Figure 8, lanes 9 and 10) is responsible for endoribonucleolytic activity in gel filtration elution volumes 60-85 mL.

Post heparin-sepharose purified sample was chosen for protein identification using LC/MS/Mass Spectrometry because of the high abundance of protein present relative to that of gel filtration purified sample. This was particularly important because there is a minimum quantity of protein needed in gel bands for accurate mass spectrometry analysis. Also, the gel staining reagents are required to be non-silver

containing, as silver ions interfere with the mass spectrometry analysis procedure. Given the conditions required for accurate mass spectrometry analysis, Coomassie Brilliant Blue stain was used, although the lower end detection limits of protein using Coomassie Blue stain is far less than the lower end detection limits of protein using silver-based stains. The Coomassie Brilliant Blue-stained gel from which proteins were excised and sent for mass spectrometry analysis is shown in Figure 9. It was decided that the major proteins of sizes corresponding to the general molecular weights ranges were: 40-50kDa (Figure 9, #1), 30-40kDa (Figure 9, #2), 20-25kDa (Figure 9, #3 and #4), and 10-20kDa (Figure 9, #5 and #6). These size ranges were chosen as they best-correlated with endoribonucleolytic acitivities as judged by gel filtration chromatography.

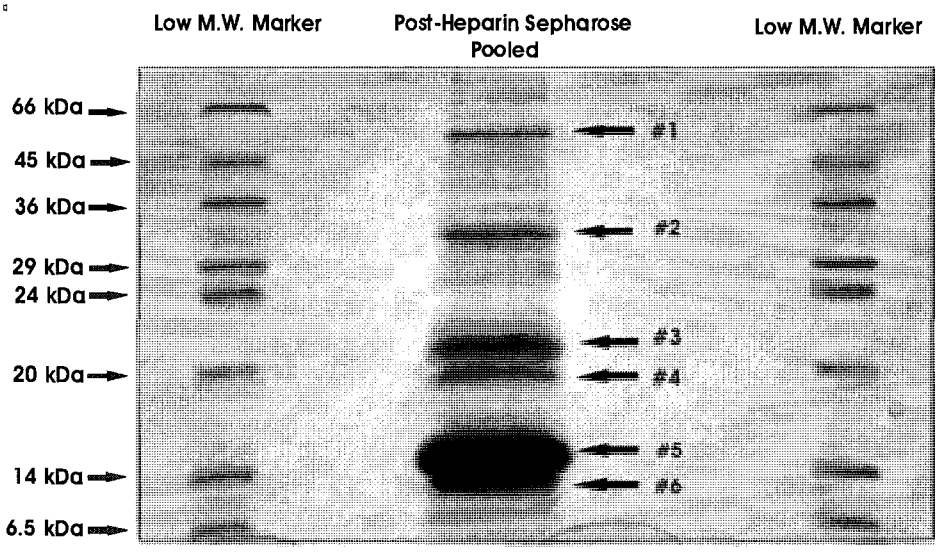

Figure 9: SDS-PAGE analysis of partially purified liver endoribonuclease following heparin-sepharose column chromatography. SDS-PAGE gel was stained with Coomassie Blue. Lane 1 represents protein marker. Lane 2 represents pooled post heparin-sepharose sample. The protein bands indicated with arrows to the right of lane 2 (labeled 1-6) represent the bands that were excised and sent to Genome BC Protemics Center at UVIC for LC/MS/Mass Spectrometry protein identification. Lane 3 represents another sample of protein molecular weight marker. Molecular weights are indicated with arrows to the left.

The results of protein identification using LC/MS/Mass Spectrometry enabled the formulation of a short list of plausible protein candidates which could be responsible for endoribonucleolytic activity as judged by heparin-sepharose chromatography. The list of protein candidates resulting from mass spectrometry analysis is shown in Table 8. There are several possible protein candidates for several of the protein bands. This is most likely due to a mixture of proteins with similar molecular weight within the stained (visible) protein band that were excised. The identity of the largest protein band #1 (Figure 9) was either thioredoxin reductase or glutamate dehydrogenase (Table 8). Neither of these proteins possesses known endoribonucleolytic activity *in vivo* or *in vitro*. Furthermore, the molecular weights of 57 kDa and 61 kDa, respectively, do not correlate with the 35 kDa molecular weight protein associated with endoribonucleolytic activity and were thus excluded as possible endoribonuclease candidates.

Table 8: Summary of LC/MS/Mass Spectrometry data and peptide analysis results used to identify purified proteins from the post heparin-sepharose column shown in Figure 9.

Protein Band #	**Top Protein Matches (*Rodentia* Species) of Relevant**	**Sequence Coverage (%)**	**# of Matched Peptides (Continuous Stretches of Amino Acids)**
1	1) Thioredoxin reductase 2 (57kDa) 2) Glutamate dehydrogenase 1 (61kDa)	1) 34% 2) 41%	1) 12 2) 16
2	1) L-3-hydroxyacyl-CoA dehydrogenase (HADHSC) (34 kDa) 2) Apurinic/apyrimidinic lyase (AP endonuclease/APE1) (35 kDa)	1) 62% 2) 3%	1) 10 2) 1
3	1) Cyclophilin B (Peptidyl prolyl isomerase) (23 kDa)	1) 56%	1) 14
4	1) Pancreatic Ribonuclease A (17 kDa)	1) 45%	1) 5
5	1) Cytochrome C (12.5 kDa)	1) 55%	1) 11
6	1) Small nuclear ribonucleoprotein E (11 kDa) 2) Small nuclear ribonucleoprotein sm d1, chain A (9 kDa) 3) SNRPF (small nuclear ribonucleoprotein F) (10 kDa)	1) 65% 2) 74% 3) 50%	1) 4 2) 4 3) 2

The identity of protein band #2 was confidently narrowed to two choices. As shown in Table 8, the mass spectrometry data for HADHSC exhibited 62% sequence

coverage (10 major peptides identified). The other possible protein candidate was APE 1; however, the mass spectroscopy data for APE1, shown in Table 8, was very weak as there was one peptide match (3% sequence coverage). HADHSC has no known endoribonuclease activity although its molecular weight of 34 kDa corresponds to the largest endoribonucleolytic activity from gel filtration chromatography. Given the high degree of certainty in identifying this protein, the commercially-available recombinant form of HADHSC was obtained for further investigation. Details of the investigation using recombinant HADHSC are provided in Chapter 3.

Mass spectrometry data for protein band #3 was clearly identified as cyclophilin B (Table 8). The mass spectrometry data did not identify any plausible protein alternatives at or near 25 kDa.

Mass spectrometry data for protein band #4 was identified as a known endoribonuclease; rat pancreatic ribonuclease A (RNase 1) (Table 8). Five major peptides were matched which translated into a sequence coverage of 45%. Given the fact that the identity of this band was a known endoribonuclease and the fact that the mass spectrometry peptide sequence data shown in Table 8 was strong, it was tentatively concluded that pancreatic RNase A was responsible for the endoribonucleolytic activity observed in elution volumes 60-85 mL (protein size of 10-20kDa) from gel filtration chromatography. Further evidence to support this conclusion is provided in Chapter 3.

Mass spectrometry data for protein band #5 conclusively identified it as cytochrome C (Table 8). The mass spectrometry data did not identify any plausible protein alternatives at or near 12-14 kDa.

The identity of the final protein band #6 was not entirely clear. The mass spectrometry data (Table 8) identified three possible protein candidates which were all within the small ribonucleoprotein family of proteins. There was no further investigation undertaken to determine the identity of this protein. This is due in large part to the unavailability of specific antibodies against this group of proteins.

In an attempt to conclusively identify the 35 kDa protein responsible for endoribonucleolytic activity, a second set of pooled samples containing peak endoribonucleolytic activity from gel filtration column runs 5, 6, 7 and 8, were sent for LC/MS/Mass Spectrometry analysis. The Coomassie Brilliant Blue-stained SDS-PAGE gel from which candidate stained protein bands were excised, is shown in Figure 10. As shown in Figure 10, lane 2, a range of major protein bands (#1, #2, and #3) corresponding to molecular weights of 38 kDa, 34 kDa, and 28 kDa, respectively, were chosen based largely on the data from gel filtration chromatography.

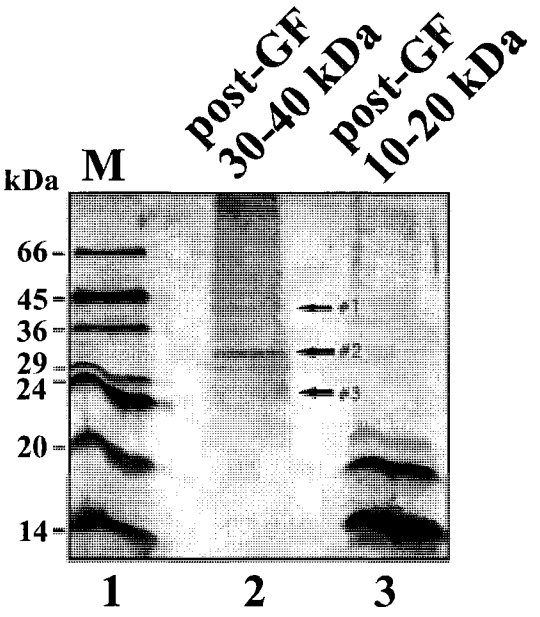

Figure 10: SDS-PAGE analysis of partially purified liver endoribonuclease from gel filtration chromatography. SDS-PAGE gel was stained with Coomassie Brilliant Blue Lane 1 represents protein marker with molecular weight indicated to the left. Lane 2 represents post-gel filtration purified pooled elution volumes of 43-50mL (protein sizes 30-40kDa) from gel filtration column runs. The arrows indicate the protein bands that were excised and sent to Genome BC Protemics Center at UVIC for LC/MS/Mass Spectrometry protein identification. Lane 3 represents post-gel filtration purified pooled elution volumes 65-85 mL (protein sizes 10-20kDa).

The results of LC/MS/Mass Spectrometry protein identification using the second set of samples is shown in Table 9. The largest protein band (#1) was identified as either APE1, annexin III or aldo-keto reductase. The similarity in their molecular weights (shown in Table 9, protein band #1) and the high degree of amino acid sequence coverage from the matching peptides (Table 9, protein band #1) suggests that all three proteins may have co-migrated within the band that was excised.

Interestingly, APE1 was observed in the data from the first mass spectrometry analysis (Table 8, protein band #2). Given its predicted molecular weight of 35 kDa and its known multifunctionality as a DNA-specific endonuclease (Demple and Harrison 1994), redox activator of transcription factor DNA-binding (Xanthoudakis *et al.* 1992;

Evans *et al.* 2000), mediator of parathyroid hormone (PTH) gene (Okazaki *et al.* 1992; Okazaki *et al.* 1994) and additional properties such as 3'-5' exonuclease activity (Richardson and Kroenberg 1964), phosphodiesterase activity (Richardson *et al.* 1964) and RNase H-like activity (Barzilay *et al.* 1995), it was decided to further investigate APE1. The amino acid sequences of the seven matching peptide fragments for APE 1 are shown in Table 10.

Protein band #2 (Figure 10, lane 2) was definitively identified as HADHSC. The mass spectrometry analysis did not present plausible protein alternatives for this protein band. Protein band #3 (Figure 10, lane 2) was not conclusively identified; however, upon closer examination, the most plausible protein listed in Table 9, protein band #3 appears to be Glutathione S-transferase. The predicted molecular weight of Glutathione S-transferase is 26 kDa (Table 9, protein band #3) and the protein band that was excised from the gel (Figure 10, lane 2, #3) corresponded to a protein band of 25kDa-30 kDa.

Table 9: Summary of LC/MS/Mass Spectrometry data and peptide analysis results to identify purified proteins following gel filtration chromatography.

Protein Band #	Top 3 Protein Matches (*Rodentia* Species)	Sequence Coverage (%)	Matched Peptides (Amino Acid Sequences)
1	1) Apurinic/apyrimidinic lyase (AP endonuclease/APE1) (35 kDa)	1) 32%	1) 7
	2) Annexin III (36.5 kDa)	2) 38%	2) 10
	3) Aldo-keto reductase E1 (34.8 kDa)	3) 40%	3) 11
2	1) L-3-hydroxyacyl-CoA dehydrogenase (HADHSC) (34 kDa)	1) 55%	1) 8
3	1) Peroxisomal enoyl hydratase-like protein (36.5 kDa)	1) 46%	1) 12
	2) HADHSC (34 kDa)	2) 20%	2) 3
	3) Glutathione S-transferase (25.6 kDa)	3) 54%	3) 7

Table 10: Matched peptides and the corresponding amino acid sequences of rat Apurinic/apyrimidinic endonuclease (AP endonuclease-APE 1)

Peptide Fragment	Amino Acid Sequence of Peptide Fragment
1	KICSWNVDGLRA (amino acids 61-72)
2	KEEAPDILCLQETKC (amino acids 83-97)
3	KLPAELQELPGLTHQYW (amino acids 101-123)
4	KEGYSGVGLLSRQ (amino acids 124-136)
5	KVSYGIGEEEHDQEGR (amino acids 140-155)
6	RQGFGEMLQAVPLADSF (amino acids 236-252)
7	KALGSDHCPITLYLAL (amino acids 301-316)

Evidence presented in this chapter highlights several candidate proteins that may contribute to native endoribonuclease activity against *c-myc* CRD RNA. Three major protein candidates, HADHSC, annexin III and APE1 were chosen as possibilities for 35 kDa endoribonuclease activity. HADHSC was chosen because it contains a predicted RNA-binding Rossmann fold motif. The Rossmann fold motif is known to bind nucleotides, in particular, the cofactor NAD and its structure is composed of three or more parallel beta strands linked by two alpha helices (Arnez and Cavarelli, 1997; Rao and Rossmann 1973). Annexin III was chosen because another member of the annexin family of proteins (annexin A2) has been shown to bind ribonucleotide homopolymer RNA and human *c-myc* RNA (Filipenko *et al.* 2004). APE1 was the most intriguing candidate since it had known multifunctionality, including DNA-specific endonuclease activity. Consequently, APE1 became the prime candidate for our investigation into the identity of the 35 kDa protein responsible for endoribonuclease activity observed in gel filtration elution volume 40-50 mL.

CHAPTER 3

Identification and Characterization of the 35 kDa and 17 kDa Hepatic Endoribonucleases

This chapter presents the methods and discusses the results of the experiments used to identify 35 kDa and 17 kDa endoribonucleases, including Western blots, standard endoribonuclease assays, electrophoretic mobility shift assays (EMSA) and immunoprecipitation/immunodepletion of native endoribonuclease activity. This chapter also includes characterization experiments and kinetic analysis of purified endoribonucleases with apparent molecular weights of 17 kDa and 35 kDa, respectively.

3.1 Methodology

To conclusively determine the identity of the purified enzymes and to better characterize the properties of each enzyme, numerous experiments were designed and conducted. The following chapter covers the experimental approach used to definitively confirm the identity of two mammalian endoribonucleases. This chapter describes the techniques used and discusses the relevant findings from the variety of protein identification and protein characterization experiments. The biochemical properties of both endoribonucleases are discussed; however, emphasis will be given to the endoribonuclease with an apparent molecular weight of 35 kDa.

3.1.1 Western Blotting to Confirm the Proteins Identified with LC/MS/Mass Spectrometry

Western Blotting analysis was used in an attempt to confirm the identity of the candidate proteins identified by mass spectrometry analysis. The standard SDS-PAGE/Western Blot protocol and reagents outlined below were similar for all samples unless stated otherwise. Pooled samples from post heparin-sepharose chromatography

and gel filtration chromatography were divided into the appropriate number of 1.5 mL eppendorf tubes. Proteins were concentrated using the standard acetone precipitation procedure as outlined in chapter 2, section 2.1.8. Protein pellets were resuspended in 10 µL of 1X SDS/β-mercaptoethanol loading dye (composition shown in Table 6) and 10 µL of Milli-Q-ddH_2O. 8 µL of rainbow marker (GE Healthcare, Montreal) was mixed with 10 µL of 1X SDS/β-mercaptoethanol loading dye. All samples except the rainbow marker were boiled for 5 min and electrophoresed on a 15% SDS-PAGE gel as described in chapter 2, section 2.1.11.

Prior to protein transfer from the SDS-PAGE gel to a nitrocellulose membrane, four pieces of filter paper and one piece of nitrocellulose membrane were soaked in western transfer buffer (composition shown in Table) for 10 min. The SDS-PAGE gel was placed in a 'sandwich' consisting of (in order): one foam spacer, two pieces of filter paper, nitrocellulose membrane, SDS-PAGE gel, two pieces of filter paper, one foam spacer. The 'sandwich' was then placed in a Bio-Rad western blot sandwich cassette, and submerged in transfer buffer, within a Western blot apparatus. An ice block and a stir bar were added to the apparatus. Proteins in the gel were transferred to the nitrocellulose membrane at a constant 190 mA for 100 min.

After protein transfer was complete, the nitrocellulose membrane was removed from the sandwich and placed in Western blocking buffer (composition shown in Table 11) and shaken for 90 min at room temperature. Following the blocking step, the membrane was rinsed twice for 5 min in Western wash buffer (composition shown in Table 11). Primary antibodies used were anti-RNase 1 (GeneTex Inc., San Antonio, TX), anti-cyclophilin B (Abcam Inc. Cambridge MA), anti-cytochrome c (Abcam Inc.

Cambridge MA), anti-HADHSC (GenWay Biotech Inc., San Diego, CA), anti-APE1 (Affinity BioReagents, Golden, CO) and anti-annexin III (GenWay Biotech Inc., San Diego, CA). All primary antibodies were diluted 1:2500 in Western wash buffer. Primary antibody solutions were added to the blot and incubated with gentle shaking at room temperature for 60 min. Blots were then rinsed three times (5 min/rinse) with gentle shaking. Secondary antibodies containing the appropriate Ig chain and the horseradish-peroxidase (HRP) conjugation (all secondary antibodies obtained from Promega Corporation, Madison, WI) were diluted 1:4000 in Western wash buffer. Secondary antibody mixture was added to the blots and incubated at room temperature with gentle shaking for 60 min. The blot was then rinsed for 20 min in Western wash buffer. The wash step was repeated three times. After the final wash, PIERCE SuperSignal West Pico Chemiluminescent visualizing solution (MJS BioLynx Inc. ON, Canada) was prepared. This was accomplished by mixing equal parts (total 8 mL) of the luminal/enhancer solution with the stable peroxidase buffer solution. The Chemiluminescent solution was added to the blot and the blot was shaken vigorously for 1 min. Prior to visualization, excess Chemiluminescent solution was removed from the blot. The blot was visualized with the ChemiImager^{TM} System (Alpha Innotech Corporation, San Leandro, CA).

Table 11: The identity and composition of reagents used for Western Blotting

Reagent	Composition
Transfer buffer	0.050M Tris (w/v), 0.040M glycine (w/v), 20% methanol (v/v) 70% Milli-Q-ddH_2O
Western blocking buffer	7% Skim milk powder (w/v) (Nestle Carnation), 1X TBS, 0.01M Tris, 45 mL Milli-Q-ddH_2O
Western wash buffer	2.0% Skim milk powder (w/v) (Nestle Carnation), 1X TBS, 0.01% Tween 20 (v/v), 900 mL Milli-Q-ddH_2O
Western stripping buffer	100mM β-mercaptoethanol, 2% SDS, 62.5mM Tris pH 6.7

3.1.2 Determining the Identity of the 17 kDa Endoribonuclease

Western Blots were used to confirm the identity (pancreatic RNase A, based on mass spectroscopy data) of the enzyme responsible for endoribonucleolytic activity corresponding to 17 kDa as judged by gel filtration chromatography. Affinity-purified polyclonal antibodies for RNase 1 (GeneTex Inc., San Antonio, TX) were obtained. The RNase 1 antibodies were used to probe post-gel filtration fractions, and post-heparin-sepharose fractions. Sample fractions from post-heparin sepharose and gel filtration exhibiting endoribonucleolytic activity were acetone precipitated using the standard acetone precipitation procedure (chapter 2, section 2.1.8). The samples were then loaded onto 15% SDS-PAGE gel and transferred to a nitrocellulose membrane and visualized with Chemiluminescent substrate as previously described for the standard Western blot protocol (section 3.1.1).

3.1.3 Determining the Identity of the 35 kDa Endoribonuclease

Several approaches were used to conclusively identify the 35 kDa protein responsible for endoribonucleolytic activity exhibited by endoribonuclease assays of

elution fractions from gel filtration chromatography. The following sections describe the methodologies utilized in these approaches.

3.1.3.1 Stripping Antibodies from Western Blots

Western stripping buffer (composition shown in Table 11) was heated to 60°C and 100 mL was added to the specific nitrocellulose blot. The blot was shaken vigorously in a fume hood for 20 min. The stripping buffer was removed and 50 mL of fresh 60°C Western stripping buffer was added to the blot, and the blot was shaken vigorously for an additional 10 min. The Western stripping buffer was then removed. The blot was washed 3 times (5 min each wash) in Western wash buffer (composition shown in Table 11). The blot was then re-blocked in Western blocking buffer (composition shown in Table 11) for 60 min at 37°C. Blots were then re-probed with desired primary antibody appropriate secondary antibody, and visualized as previously described (section 3.1.1).

3.1.4 Characterizing the 35 kDa and 17 kDa Endoribonucleases

To confirm the identity of candidate proteins responsible for endoribonucleolytic activity against 5'-radiolabeled *c-myc* CRD RNA, and to distinguish between endoribonuclease activity corresponding to molecular weights of 17 kDa and 35 kDa as observed with gel filtration chromatography, it was necessary to assess the differences between the 17 kDa and 35 kDa endoribonucleases with respect to cleavage specificity, differences in enzyme kinetic and sensitivity to known RNase inhibitory proteins.

3.1.4.1 Assessing the Sensitivity of the 35 kDa and 17 kDa Enzymes to Ribonuclease Inhibitor Protein (RNasin)

Post-gel filtration purified pooled fractions corresponding to elution volumes 40-50mL (protein sizes 30-40kDa) and 65-80mL (protein sizes 10-20kDa) were utilized for

RNasin experiments. 5 μL (1U) aliquots from elution volumes 40-50mL (protein sizes 30-40kDa) and 5 μL (5U) aliquots from elution volumes 65-80mL (protein sizes 10-20kDa), respectively, were utilized for assay reactions. The reaction incubations and the assay procedures were identical to those previously described for a standard endoribonuclease assay (Chapter 2, section 2.1.6). All RNasin assays were performed using 5'-γ^{32}P-radiolabeled *c-myc* CRD (30,000 cpm/lane) and 1U RNasin (1U=1 μL). RNA was resolved on a 12% denaturing polyacrylamide/7M urea gel.

3.1.4.2 Endoribonuclease Assays of Recombinant Protein Candidates Using 5'-Radiolabeled *c-myc* CRD mRNA

Commercially available recombinant proteins for HADHSC (GenWay Biotech.), annexin III (GenWay Biotech), APE1 (Hickson lab, Oxford, UK) were obtained and tested for endoribonucleolytic activity. A second sample of recombinant APE1 was obtained from Dr. Mitra Sankar's lab (University of Texas Medical Branch [UTMB], Galvestin, TX). Prior to testing recombinant proteins for endoribonucleolytic activity, samples were dialyzed overnight. Dialysis of recombinant protein samples was performed with 10,000 molecular weight cutoff Slide-A-Lyzer dialysis cassettes (PIERCE, Rockford, IL). Dialysis buffer (Dialysis Buffer B, composition is shown in Table 5) was utilized for all recombinant protein samples. Standard endoribonuclease assays using 5'-radiolabeled *c-myc* CRD RNA (nts 1705-1886) were performed as previously outlined in Chapter 2, section 2.1.6.

3.1.4.3 Mapping the Cleavage Sites of the 35 kDa and 17 kDa Endoribonucleases using 5'-Radiolabeled *c-myc* CRD mRNA

Prior to performing the mapping experiments, an RNase T1 digest and an alkaline hydroxyl ladder of *c-myc* CRD RNA were prepared. RNase T1 digests were generated

by incubating 200,000 cpm 5'-radiolabeled *c-myc* CRD RNA (nts 1705-1886) in 10X sequencing buffer (Ambion Inc., Austin, TX) (total volume of 30 μL). 2U of RNase T1 (1U= 1μL) was added to the 30 μL mixture and incubated at room temperature for 10 minutes. The reaction was terminated and the RNA was extracted using a standard phenol/chloroform and ammonium acetate/isopropanol precipitation procedure as outlined in Chapter 2, section 2.1.3. The dried RNA pellet was re-suspended in 10 μL of urea/phenol loading dye (composition shown in Table 4). RNase T1 digest was stored at -20°C until required.

Alkaline hydroxyl ladders were generated by combining 100,000 cpm 5'-radiolabeled *c-myc* CRD RNA (nts 1705-1886) with 1X alkaline hydrolysis buffer for a total reaction mixture of 20 μL. The reaction mixture was heated to 95°C in a heat block for 10 min. The mixture was immediately transferred to ice and 20 μL of formamide loading dye was added. The mixture was stored at -20°C until required.

Mapping of cleavage sites for both the 35 kDa and 17 kDa endoribonucleases was carried out using reaction incubation conditions identical to those that were outlined in the standard endoribonuclease assay (Chapter 2, section 2.1.6). Assays were resolved at 25 mA for 90 min on a 12% polyacrylamide/7M urea gel, dried and visualized using Cyclone Phosphor Imager and Optiquant Software.

3.1.4.4 Assessing the Possibility of N-linked Glycosylation

Additional experiments to conclusively determine the identity of the enzyme responsible for endoribonucleolytic activity (from candidate proteins identified by mass spectrometry corresponding to 35 kDa were performed (Table 8, protein band #2; Table

9, protein band # 1). These experiments were needed to rule out the possibility of post-translational modification within a member of the RNase A family of proteins.

The first such experiment tested the possibility of N-linked glycosidations present on the endoribonuclease. The enzyme N-glycosidase F (removes N-linked protein glycosylations) was utilized. 100 U of recombinant N-glycosidase F (Roche Diagnostics, Mannheim, Germany) was incubated with 3.0 mL of post heparin-sepharose sample overnight at 30°C. The N-glycosidase F-treated post heparin-sepharose sample was aliquoted into separate 1.5 mL eppendorf tubes. The tubes were centrifuged at 10,400 rpm for 10 min. The samples were then pooled and loaded onto a Superdex 75 Hi Load16/60 prep grade gel filtration column (GE Healthcare) at a flow rate of 0.75 mL/min using Buffer F (composition shown in Table 5, Chapter 2). A total of two hundred, 0.5 mL fractions were collected in microcentrifuge tubes (total of 100 mL column/elution volume). A 5 µL aliquot (1U native 35 kDa enzyme) from separate elution fractions was incubated with 5'-radiolabeled *c-myc* CRD RNA (nts 1705-1886) and visualized using the standard endoribonuclease assay as previously described (section 2.1.6).

3.1.4.5 Determining if the 35 kDa Endoribonuclease is Dimeric

To assess whether the endoribonuclease with apparent molecular weight of 35 kDa was a hetero- or homodimeric protein, an experiment using DTT was designed to assess whether the 35 kDa endoribonuclease was composed of multi subunits (with disulfide linkages). 3.0 mL of post heparin-sepharose sample was incubated for 60 min at 4°C in the presence of 250mM DTT. The DTT-treated post heparin-sepharose sample was aliquoted into separate 1.5 mL eppendorf tubes. The tubes were centrifuged at

10,400 rpm for 10 min. The samples were then pooled and loaded onto a Superdex 75 Hi Load16/60 prep grade gel filtration column (GE Healthcare) at a flow rate of 0.75 mL/min in Buffer F (composition shown in Table 5, Chapter 2). A total of two hundred 0.5 ml fractions were collected in microcentrifuge tubes (total of 100 ml column/elution volume). A 5 µL aliquot (1U native enzyme) from separate elution fractions was incubated with 5'-radiolabeled *c-myc* CRD RNA (nts 1705-1886) and visualized using a standard endoribonuclease assay as previously described (section 2.1.6).

3.1.5 Electrophoretic Mobility Shift Assays

EMSA protocols were adopted from the methodologies previously described by Prokipcak *et al.* (1994), with modifications made by Sparanese and Lee (2007). EMSA protocols were designed for CRD-BP; however, similar reaction conditions were adopted for binding of HADHSC, APE1 and annexin III to 5'-γ^{32}P-radiolabeled *c-myc* CRD-1705-1886 RNA. EMSA binding buffers were prepared fresh on ice prior to each experiment. 5'-γ^{32}P-radiolabeled *c-myc* CRD was denatured (heated to 75°C) and renatured (cooled to room temperature) prior to addition in the EMSA binding buffer (composition shown in Table 12). This was done to ensure proper folding of the RNA transcript. EMSA binding buffer containing radiolabeled *c-myc* RNA was incubated in separate experiments with commercially obtained recombinant HADHSC protein (GenWay Biotech., San Diego, CA), recombinant APE1 protein (Dr. Sankar's lab, TX) and commercially obtained recombinant annexin III protein (GenWay Biotech., San Diego, CA). The final reaction mixture for all EMSA experiments was 20 µL and reactions were incubated at 30°C for 10 min, transferred to ice for 5 min and then again incubated at 30°C for 10 min. Following the final 10 min incubation at 30°C, heparin

(Sigma) was added to a final concentration of 5 mg/mL and the reaction was placed on ice for 5 min. 2 µL of EMSA loading dye (composition shown in Table 12) was added to the reaction mixture. The entire reaction mixture was loaded onto a 6% native polyacrylamide gel and resolved at 20 mA for approximately 90 min. Following electrophoresis, the gel was transferred to filter paper and dried using a gel drying apparatus (LABCONO, Kansas City, MO) for 45 min. The dried gel was then exposed to a phosphorimager screen overnight. The autoradiographs were visualized using a Cyclone Storage Phosphor Screen System and Optiquant Software.

Table 12: The identity and composition of reagents used in the EMSA experiments

Reagent	Composition
EMSA binding buffer	5mM Tris-Cl (pH 7.4), 2.5 mM EDTA (pH 8.0), 2mM DTT, 5% glycerol, 0.1 mg/mL (BSA), 0.5 mg/mL yeast tRNA (Ambion), 5U RNasin
EMSA loading dye	250 mM Tris-Cl (pH 7.4), 0.2% bromophenol blue, 0.2% xylene cyanol, 40% sucrose (w/v)

3.1.6 Enzyme Kinetic Analysis of the 35 kDa and 17 kDa Endoribonucleases Using 5'-labeled Oligonucleotide Substrate.

Kinetic analysis of the 35 kDa and 17 kDa endoribonucleases was performed using a synthetic DNA oligonucleotide substrate (Integrated DNA Technologies [IDT], Coralville, IA). The synthetic oligo substrate was designed based on a short stretch of sequence from the CRD region of the *c-myc* mRNA transcript, as shown in Table 13. The substrate was composed of 16 chimeric DNA bases and 1 RNA base. The predicted secondary structure is shown in Table 13. The commercially-obtained oligo was initially lyophilized and required re-suspension in 100 µL of DEPC-treated Milli-Q-ddH_2O. Stock oligonucleotide was quantified using the NanoDrop spectrophotometer. Amount

of oligo was calculated using the formula provided by IDT (Table 13). Oligonucleotide substrate was frozen at -80°C for storage.

Prior to performing kinetic assays, 16 μg (4 μL) of oligonucleotide substrate (stock concentration 4.1 μg/μL) was dephosphorylated and subsequently 5'-γ^{32}P-radiolabeled. The remaining steps used for dephosphorylation reactions were identical to those previously described for *c-myc* CRD RNA, in Chapter 2, section 2.1.5. 5'-γ^{32}P-radiolabeled reactions were performed using half (roughly 8 μg or 2 μL) of the previously generated dephosphorylated oligonucleotide substrate. Preparation and procedures for 5'-γ ^{32}P-radiolabeled reactions using oligonucleotide substrate were performed as previously described for *c-myc* CRD RNA, in Chapter 2, section 2.1.5.

The first step in preparation for assays used to assess Michaelis Menten kinetics involved determining a workable or 'optimal' concentration range of gel filtration-purified 35 kDa and 17 kDa enzyme, respectively, for a given time period. Stop-time assays using various enzymes concentrations over several time periods were performed. Data from the intensities of decayed 5'-radiolabeled oligonucleotide RNA (calculated as DLU/time) was obtained and was subsequently entered into a Microsoft Excel spreadsheet. Of note, DLU intensities were obtained directly from autoradiographs using Optiquant Software. All data was then transferred to KaleidaGraph 3.6.2 (Synergy Software) for linear and nonlinear regression analysis. DLU decay intensities for the different time periods were plotted against enzyme concentration using linear regression analysis. It should be noted that all procedures herein were performed in duplicate; once for the analysis of the native 17 kDa enzyme and once for analysis of the native 35 kDa enzyme.

The next step was performed using an 'optimized' value of native 17 kDa or 35 kDa enzyme. The optimal quantity of enzyme was then incubated with a set concentration of 5'-γ^{32}P-radiolabeled oligonucleotide substrate in a stop-time assay . This procedure was repeated for multiple substrate concentrations. The second set of data was plotted as DLU intensities (at various [substrate]) versus time, and analyzed using linear regression.

To obtain data for the nonlinear regression plots (Michaelis Menten plots) of the respective 17 kDa and 35 kDa enzymes, slope values (rate of appearance of decay product) from the aforementioned linear regression analysis were plotted against the varying substrate concentrations utilized. Nonlinear regression analysis was performed using KaleidaGraph 3.6.2. The values from the nonlinear regression analysis were fit into the Michaelis Menten equation $v = V[S]/(K_m + [S])$ to obtain K_m and V_{max} values for the 17 kDa and 35 kDa endoribonuclease, respectively where v = velocity, [S] is molar amount of substrate, V = maximum velocity, K_m = Michaelis Menten constant ([S] at half-maximal velocity).

Table 13: Sequence, structure and calculation the amount of the synthetic oligonucleotide used to assess kinetic properties of the respective 35 kDa and 17 kDa endoribonucleases. Filled arrow indicates the ribonucleotide UA base-pair that is predicted to be cleaved by native endoribonucleases

Substrate	Data
DNA Oligonucleotide Sequence	5'-CAA GGT AGT $_r$UAT CCT TG-3'
Structure of Oligonucleotide Substrate	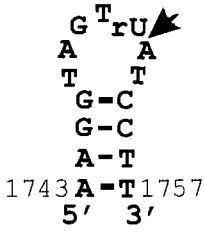
Amount of Oligonucleotide Calculation	11.1 = 66.80 = 0.35 *OD 260 nmoles mg*

3.1.7 Immunoprecipitation of Gel Filtration-Purified Native Extract

Immunoprecipitation experiments were designed to immunodeplete the native 35 kDa endoribonuclease candidate protein, APE1. Pooled post-heparin sepharose and pooled gel filtration elution fractions corresponding to elution volumes of 40-50 mL were utilized for immunodepletion experiments.

Immunoprecipitation reaction preparations and experimental procedures were performed as follows and were identical unless otherwise stated: 400 µL of PIERCE Immunopure Immobilized Protein A slurry (MJS BioLynx Inc. ON, Canada) was placed in a Pierce Seize X kit Handee™ Spin Cup and centrifuged at 3000 rpm for 30 sec. The flow through was discarded and 400 µL of binding/wash buffer (PIERCE; composition shown in Table 14) was added to the beads. The Handee™ Spin Cup Column was capped and inverted 10 times. The spin cup was then centrifuged at 3000 rpm for 30 sec

and the flow through was discarded. The wash/centrifugation steps as previously described were repeated two more times.

The spin cup was placed in a fresh 1.5 mL eppendorf tube and a total volume of 200 µL primary APE1 antibody solution (equivalent to about 25 µg of primary APE1 polyclonal antibody diluted in 175 µL of binding/wash buffer [PIERCE]) was added to the beads contained in the spin cup. Primary antibody solutions were incubated with gentle rocking for 2 hrs at 4°C. The tubes were centrifuged at 3000 rpm for 30 sec. The flow-through was saved and identified as antibody flow through 1. 400 µL of binding/wash buffer was added to the spin cup and mixed by inverting 10 times. The tubes were centrifuged at 3000 rpm for 30 sec and the flow through was saved and termed wash 1. The wash/centrifugation steps were repeated two more times. The spin cup was then transferred to a new 1.5 mL eppendorf tube.

One pre-packaged lyophilized sample of DSS (disuccinimidyl suberate; PIERCE) was opened and re-suspended in 80 µL of DMSO (dimethyl sulfoxide). 25 µL of the DSS crosslinking agent was added to the spin cup. The mixture was incubated with gentle rocking at room temperature for 60 min. The spin cup was then centrifuged at 3000 rpm for 30 sec and the flow through was discarded. 400 µL of binding/wash buffer was then added to the spin cup and mixed by inverting 10 times. The spin cup was centrifuged at 3000 rpm for 30 sec. The flow through was discarded. Addition of wash buffer and centrifugation was repeated two more times. The spin cup was placed in a fresh 1.5 mL eppendorf tube.

In duplicate, a spin cup containing DSS-crosslinked polyclonal syntaxin 18 antibodies was prepared using a procedure identical to that previously described above to

prepare the APE1 monoclonal antibody containing spin cup. The spin cup containing cross-linked polyclonal syntaxin 18 antibodies was used as negative control.

Table 14: Composition and identity of the reagents used in immunoprecipitation experiments

Reagent	**Composition**
Binding/Wash buffer (PIERCE)	0.14M NaCl, 0.008M sodium phosphate, 0.002M potassium phosphate, 0.01M KCl Final pH= 7.4
Elution Buffer (PIERCE)	Primary amine solution, Final pH = 2.8
Antibody Crosslinking Agent (PIERCE)	DSS (disuccinimidyl suberate)
Handee™ Spin Cup Columns (PIERCE)	0.45 µm cellulose acetate filter

One hundred µL of post-heparin sepharose purified sample or 400 µL of pooled gel filtration elution volumes 40-50mL (protein sizes 30-40kDa) were utilized (separate spin cup trials) for immunodepletion experiments. Post-heparin-sepharose purified sample or gel filtration purified sample was pipetted on top of the beads in the spin cup. Spin cups were capped, and incubated with gentle rocking for 2 hrs at 4°C. Spin cups were then centrifuged at 3000 rpm for 30 sec. The flow through was saved and labeled flow through 1 (FT-1). 400 µL of binding/wash buffer was then added to the top of the spin cup. The spin cup was capped, inverted 10 times and centrifuged at 3000 rpm for 30 sec. The wash/centrifugation step was repeated two more times.

Elution of bound proteins was performed as follows. 200 µL of PIERCE Seize X Immunoprecipitation kit Immunopure IgG Elution Buffer (pH 2.8) was added to the spin cups. The cups were capped and inverted 10 times. The cups were then centrifuged at 3000 rpm for 30 sec and the flow through fraction was saved and labeled elution 1.

Elution steps were repeated two more times for a total of 3 times. The elution fractions were immediately neutralized with the addition of an equal volume of Tris-Cl pH 9.5.

A total of one control column using syntaxin 18 polyclonal antibodies and post heparin-sepharose purified sample, two APE1-specific immunodepletion column using post heparin-sepharose sample, and one APE1-specific immunodepletion column using pooled (40-50mL) gel filtration purified sample, were performed.

3.2 Results and Discussion

3.2.1 Identification of Co-purified Proteins by Western Blot

Candidate proteins identified in the first and second LC/MS/Mass Spectrometry analysis were confirmed using Western blot. Co-purified proteins included cytochrome c (lanes 2 and 3, Figure 11-A), cyclophilin B (lanes 2 and 3, Figure 11-B), pancreatic ribonuclease A (RNase A) (lane 2, Figure 12; lanes 2 and 3 Figure 13; lane 5, Figure 15-A; lanes 6-8, Figure 16-A; lanes 6-8, Figure 17-A; lane 3, Figure 18-A), HADHSC (lane 1, Figure 18-B), and APE1 (lane 2, Figure 15-B; lane 6, Figure 16-B; lanes 5-7, Figure 17-B) and annexin III (Figure 18-C). Rabbit affinity-purified polyclonal antibodies for thioredoxin reductase were obtained and used to determine the presence of thioredoxin reductase in post heparin-sepharose purified sample; however, this protein was not detected (data not shown). It was concluded that either thioredoxin reductase was not present in purified heparin-sepharose sample or was present in extremely low concentrations thus preventing detection using Western blot analysis.

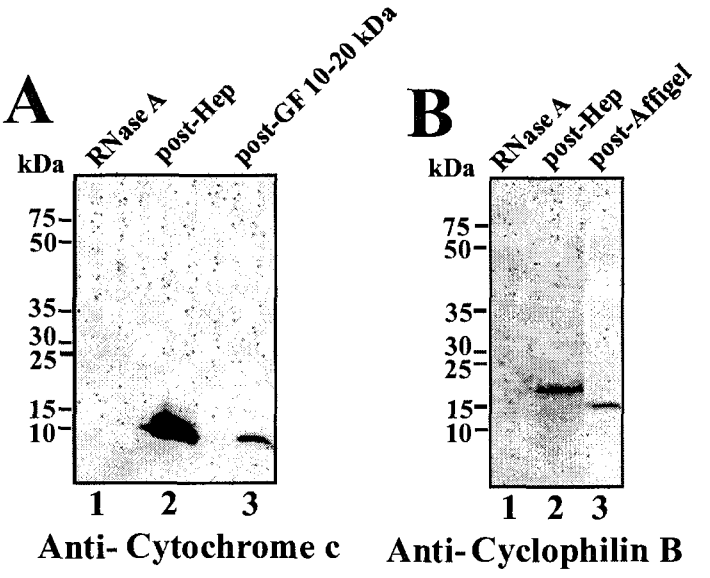

Figure 11: Western blot analysis confirming the presence of cytochrome c and cyclophilin B in partially purified liver extract. (A) Depicts a Western blot for cytochrome c protein using commercially-obtained mouse monoclonal antibody (Abcam Inc, Cambridge, MA). Lane 1 contains 2 μg of recombinant bovine pancreatic RNase A. Lane 2 contains 5 μg of pooled post-heparin-sepharose purified sample. Lane 3 contains pooled post gel filtration purified sample (protein not quantifiable) corresponding to elution volumes 65-85 mL. Molecular weight markers (kDa) are shown to the left of blot **(B)** Depicts a Western blot for cyclophilin B protein using rabbit polyclonal antibody (Abcam Inc., Cambridge, MA). Lane 1 contains 2 μg of recombinant bovine pancreatic RNase A. Lane 2 contains 5 μg of pooled post-heparin-sepharose purified sample. Lane 3 contains 5 μg of post-Affigel purified sample. Molecular weight markers (kDa) are shown to the left.

A summary of the results fromWestern blots used to confirm the presence of co-purified proteins identified using LC/MS/Mass Spectrometry analysis is shown in Table 15. Several of the protein candidates identified with mass spectroscopy analysis including: glutamate dehydrogenase, peroxisomal enoyl hydratase, aldo-keto reductase E1, glutathione S-transferase, and small nuclear ribonucleoprotein E, were not investigated.

Table 15: Summary of results from Western blots used to determine the presence of co-purified proteins identified with LC/MS/Mass Spectrometry analysis one and two.

Protein Candidate from LC/MS/Mass Spectroscopy Analysis	Probed using Western blot analysis	Present in post-heparin-sepharose sample	Predicted molecular weight/Observed molecular weight (kDa)
Glutamate dehydrogenase	No	Not determined	61/-
Thioredoxin reductase	Yes	No	57/-
Peroxisomal enoyl hydratase-like-protein	No	Not determined	36.5/-
Annexin III	Yes *(Figure 33)*	Yes	36.5/ 55
Apurinic/apyrimidinic lyase (AP-endonuclease) –APE 1	Yes *(Figures 15,16,17)*	Yes	35/34.5
Aldo-keto reductase E1	No	Not determined	34.8/ -
L-3-hydroxyacyl-CoA dehydrogenase (HADHSC)	Yes *(Figure 18)*	Yes	34/32
Glutathione S-transferase	No	Not determined	25.6/ -
Cyclophilin B (Peptidyl prolyl isomerase)	Yes *(Figure 11-B)*	Yes	23/ 22
Pancreatic ribonuclease A (RNase A)	Yes *(Figures 12,13, 15-18)*	Yes	17/ 17
Cytochrome C	Yes *(Figure 11-A)*	Yes	12.5/ 13
Small nuclear ribonucleoprotein E	No	No	11/ -

3.2.2 Identifying the 17 kDa Hepatic Endoribonuclease

One of the major challenges of this research was conclusively identifying the proteins responsible for the endoribonuclease activities corresponding to 17 kDa and 35 kDa as observed from endoribonuclease assays of gel filtration-purified fractions. Identification of the 17 kDa endoribonuclease was relatively straight forward as compared to the identification of the 35 kDa endoribonuclease. LC/MS/Mass Spectrometry data for the 17 kDa endoribonuclease in post heparin-sepharose purified sample suggested that it was a member of the RNase A family (RNase 1). Western blot

data using RNase 1 affinity-purified polyclonal antibody, conclusively demonstrated that RNase 1 was present in post-heparin-sepharose purified sample (Figure 12, lane 2) and in post-gel filtration elution volumes of 60–80 mL (10-20 kDa) (Figure 13-B, lane 3; Figure 15-A, lane 5; Figure 16-A, lanes 6-8; Figure 17-A, lanes 6-8; Figure 18-A, lane 3). In addition, correlation between endoribonucleolytic activity in gel filtration elution fractions assayed using the standard endoribonuclease assay (Figure 13-A) and a subset of the same gel filtration elution fractions visualized with Western blot analysis (Figure 13-B, lane 3) support the presence of RNase 1.

Somewhat surprisingly, however, was the presence of multiple bands with molecular weights ranging from 30-37 kDa in several of the Western blot samples. Post heparin-sepharose sample probed with RNase 1 polyclonal antibody (Figure 12, lane 2) exhibit the predicted band at 17 kDa; however, there is a clear band present at 35 kDa. Gel filtration elution fraction volumes corresponding molecular weights of 30-40 kDa (Figure 13-B, lane 2; Figure 15-A, lane 2) probed with RNase 1 antibody clearly exhibit respective bands at 30 kDa and 37 kDa. In addition, anti-RNase 1 Western blot data of pooled gel filtration elution fraction volumes (40-50 mL), without treatment with reducing agent β-mercaptoethanol, exhibits a dark band of protein at 37 kDa (see Figure 18-A, lane 1).

Numerous factors may potentially account for these observations. The polyclonal nature of the commercial RNase 1 antibody source may contribute to cross-reaction with proteins with approximate molecular weights of 30 kDa and 37 kDa, respectively, present in post heparin-sepharose and post gel filtration-purified samples. Alternatively, there has been documented glycosylated (Barrabes *et al.* 2007; Ye *et al.* 2006) and dimeric

(Piccoli *et al.* 2000; Arnold *et al.* 1999) mammalian isoforms of RNase 1-like proteins (within the RNase A superfamily) that migrate with molecular weights larger than the observed standard sizes of 12- 17 kDa (see Table 2, Chapter 1). This topic will be further discussed in section 3.2.4.2.

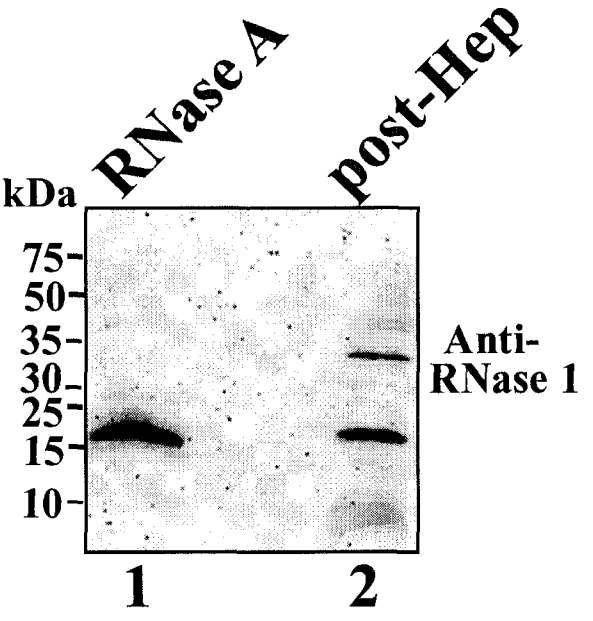

Figure 12: Western blot analysis demonstrating the presence of pancreatic ribonuclease A (RNase 1). Lane 1 contains 2 μg of recombinant bovine pancreatic RNase A. Lane 2 contains 5 μg of pooled post heparin-sepharose purified sample. The blot was probed with commercially obtained RNase 1 polyclonal antibody (GeneTex Inc., San Antonio, TX). Molecular weight markers are shown to the left.

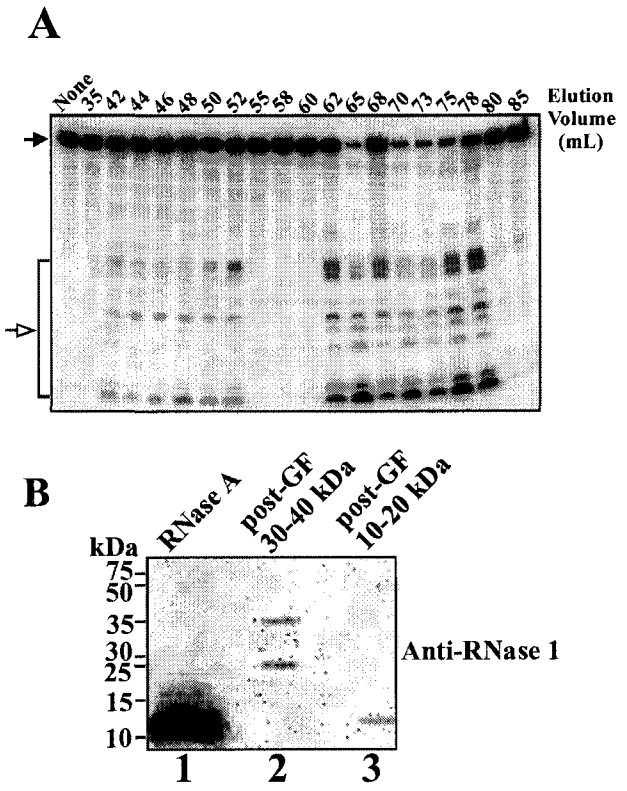

Figure 13: RNase A is present in partially purified rat liver extract from elution volumes following gel filtration chromatography. (A) Depicts an endoribonuclease assay of gel filtration column 9. 3.5 ml of post heparin-sepharose sample was loaded at a flow rate of 1 mL/min. 4.0 µL sample aliquots taken from fractions with the corresponding elution volumes were used for the standard endoribonuclease assay. Filled arrow indicates intact *c-myc* CRD RNA. Bracket and unfilled arrow indicates RNA decay products **(B)** Depicts Western blot analysis of pooled fractions from gel filtration column 9. Lane 1 contains 5 µg of recombinant bovine pancreatic RNase A protein. Lane 2 contains pooled gel filtration fractions (protein not quantifiable) corresponding to elution volumes 40-50 mL. Lane 3 contains pooled gel filtration fractions (protein not quantifiable) corresponding to elution volumes 40 -50 mL.

In summary, substantial evidence gathered using LC/MS/Mass Spectrometry analysis, Western blot analysis, and endonuclease activity/protein identity correlation experiments using standard endoribonuclease assays and Western blotting, coupled with known endoribonucleolytic properties of the RNase A family of proteins, supports the notion that rat pancreatic ribonuclease A (RNase 1) is responsible for the observed endoribonuclease activity in gel filtration elution volumes 60-80 mL (10-20 kDa).

3.2.3 Identifying the 35 kDa Hepatic Endoribonuclease

As previously stated, identification of the 35 kDa endoribonuclease proved to be extremely challenging. Evidence from LC/MS/Mass Spectrometry data, previously discussed in Chapter 2 (Table 8 protein band #2; Table 9 protein band #2) supported HADHSC (native molecular weight 32 kDa (see Figure 18-B, lane 1) as the 35 kDa protein present in both post-heparin-sepharose and gel filtration elution volumes 40-50 mL (30-40 kDa) which best-correlated with endoribonucleolytic activity. Western blot data (Figure 18-B, lane 1) also confirmed the presence of HADHSC in gel filtration elution volumes 40-50 mL (30-40 kDa). However, native HADHSC possesses no known endonuclease activity. Furthermore, as shown in the standard endoribonuclease assay (Figure 14-A, lanes 4-9), the commercial recombinant HADHSC possesses no endoribonucleolytic activity *in vitro*. Standard endoribonuclease reaction cocktail mixtures (see Chapter 2, section 2.1.6) were used to test recombinant HADHSC. Based on this data, alternative routes were explored in an attempt to elucidate the identity of the 35 kDa endoribonuclease.

As shown in Figure 33 (lane 2), the presence of annexin III was confirmed using Western blot analysis. Unexpectedly, the observed molecular weight of annexin III was approximately 55-60 kDa; a significant discrepancy from the predicted molecular weight of 36.5 kDa (see Table 15). Several possible explanations for the observed differences include; post-translational modifications and multi-subunit/covalent interactions (non-disulfide linkages). In addition, annexin III antibodies were rabbit polyclonal in origin, thus it is plausible that the commercially-obtained polyclonal antibody source may have bound non-specifically to one of the proteins present in post-heparin purified sample.

Recombinant commercial annexin III was also tested for endoribonucleolytic activity. As shown in Figure 14-B (lanes 4-6 and 10-12), annexin III did not exhibit endoribonucleolytic capabilities *in vitro*. Once again, standard endoribonuclease reaction cocktail mixtures outlined in Chapter 2, section 2.1.6, were used to test recombinant annexin III.

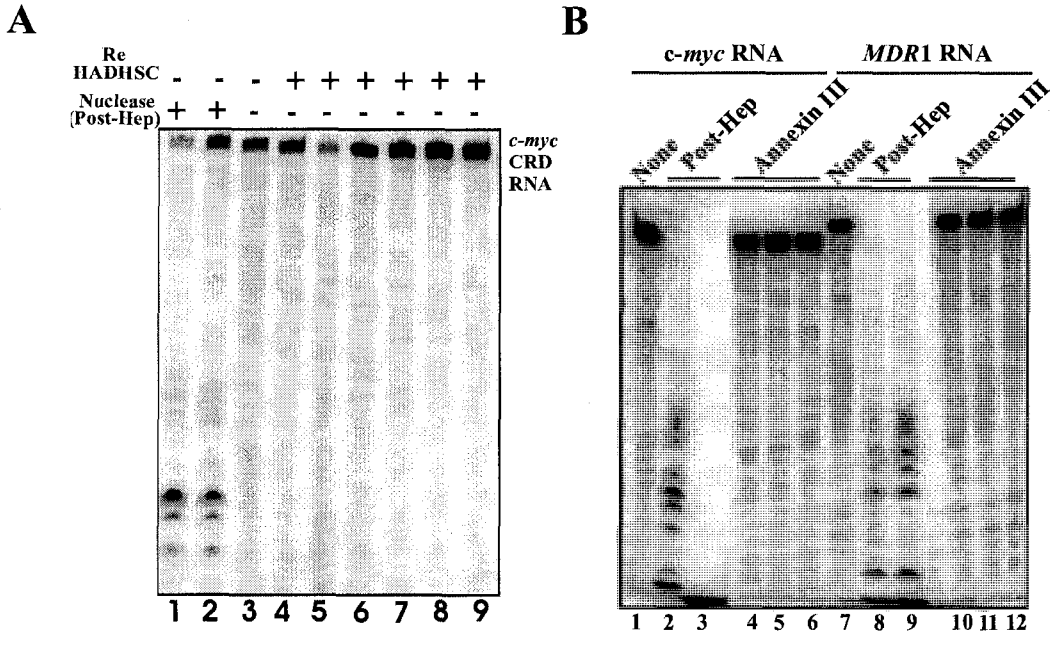

Figure 14: Recombinant HADHSC and annexin III do not exhibit endonuclease activity against *c-myc* CRD RNA. (A) Lanes 1 and 2 contain 1 µL (1U) of post-heparin-sepharose-purified sample. Lane 3 contains *c-myc* CRD RNA alone. Lanes 4-9 contain increasing concentrations (0.5 µL, 1.0 µL, 1.5 µL, 2.0 µL, 2.5 µL, 3.0 µL, respectively) of recombinant HADHSC (stock concentration 3.5 mg/mL) **(B)** Lane 1 contains *c-myc* CRD RNA alone. Lanes 2 and 3 contain 2 µL (2U) and 4 µL (4U) post heparin sepharose purified sample, respectively, incubated with *c-myc* CRD RNA. Lanes 4-6 contain 2 µL commercial recombinant annexin III (stock 1.5 mg/mL; GenWay Biotech., San Diego, CA) with *c-myc* CRD RNA. Lanes 2 and 3 contain 2 µL (2U) and 4 µL (4U) post heparin sepharose purified sample, respectively, incubated with *c-myc* CRD RNA. Lanes 4-6 contain 2 µL commercial recombinant annexin III (stock 1.5 mg/mL; GenWay Biotech., San Diego, CA). Lane 7 contains MDR 1 RNA alone. Lanes 8 and 9 contain 2 µL (2U) and 4 µL (4U) post heparin-sepharose purified sample, respectively, incubated with MDR 1 RNA. Lanes 10-12 contain 2 µL commercial recombinant annexin III (GenWay Biotech., San Diego, CA). All reactions were performed for 7 minutes.

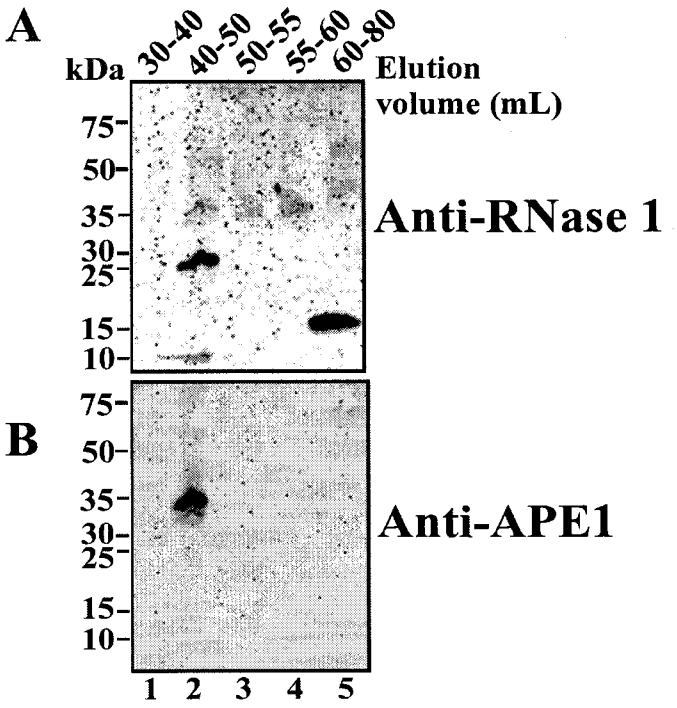

Figure 15: Western blots illustrating the presence of candidate endoribonucleases APE 1 and RNase 1. Elution fractions from gel filtration chromatography #10 were utilized **(A)** Depicts a blot of sequentially pooled elution fractions (lanes 1-5) probed with RNase 1 polyclonal antibody. Molecular weight markers (kDa) are shown to the left. **(B)** Depicts the same blot that has been stripped of RNase 1 antibody and re-probed with APE 1 (mouse monoclonal; Abcam Inc.). Molecular weight markers (kDa) are shown to the left.

APE1 was the final recombinant protein candidate obtained in an attempt to determine the identity of the 35 kDa protein (s) responsible for endoribonuclease activity observed in gel filtration elution volumes 40-50 mL. Western blots that were probed for RNase 1 and subsequently stripped and re-probed for APE1 clearly demonstrate a protein band corresponding to a molecular weight of 34 kDa (Figure 15-B, lane 2; Figure 16-B, lane 6; Figure 17-B, lanes 4 and 5). It should be noted that the protein band exhibited in Figure 17-B, lane 1 is RNase 1 from the corresponding lane (1) in Figure 17-A. The

presence of this band in Figure 17-B was most likely due to incomplete stripping of the antibodies from the Western blot exhibited in Figure 17-A.

In summary, it is evident that APE1 is present in gel filtration elution volumes corresponding to peak endoribonuclease activity (40-50 mL). Consequently, two sources of recombinant APE1 protein were requested. Initially, APE1 was obtained from Dr. Hickson at Oxford University. The second sample was obtained from Dr. Mitrasankar UTMB, Galvestin, TX). Experiments involving recombinant APE1 will be presented and discussed shortly (see section 3.5.2).

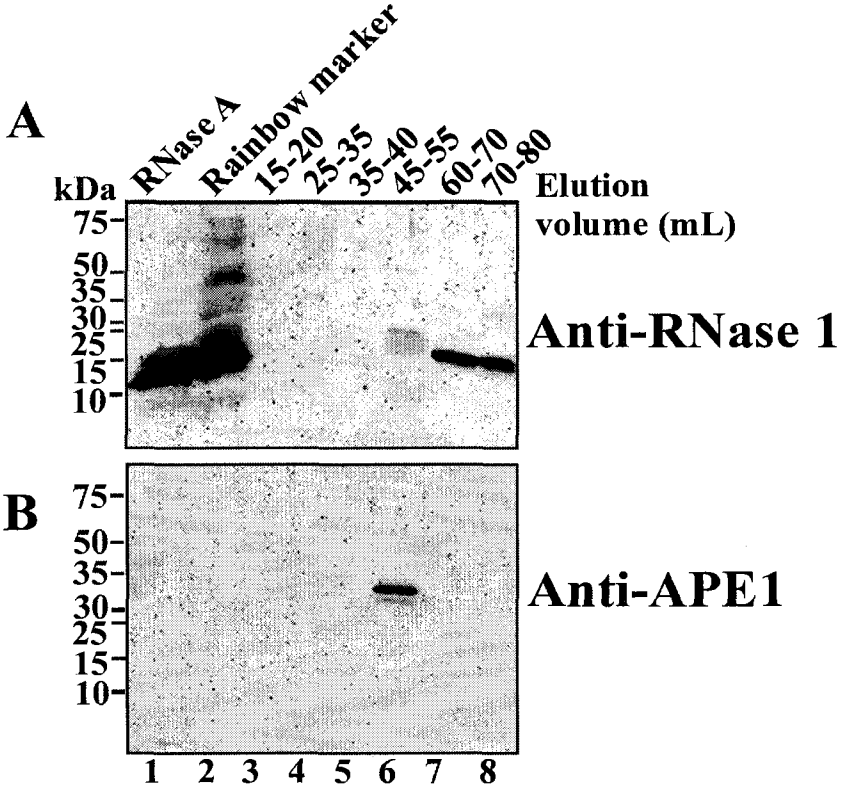

Figure 16: Western blots illustrating the presence of candidate endoribonucleases APE 1 and RNase 1. Elution fractions from gel filtration chromatography #11 were utilized **(A)** Depicts a blot of sequentially pooled elution fractions (lanes 3-8) probed with RNase 1 polyclonal antibody. Lane 1 contains 5 μg of recombinant bovine pancreatic RNase A. Lane 2 contains rainbow marker. Molecular weight markers (kDa) are shown to the left. **(B)** Depicts the same blot that has been stripped of RNase 1 antibody and re-probed with APE 1 (mouse monoclonal; Abcam Inc.). Molecular weight markers (kDa) are shown to the left.

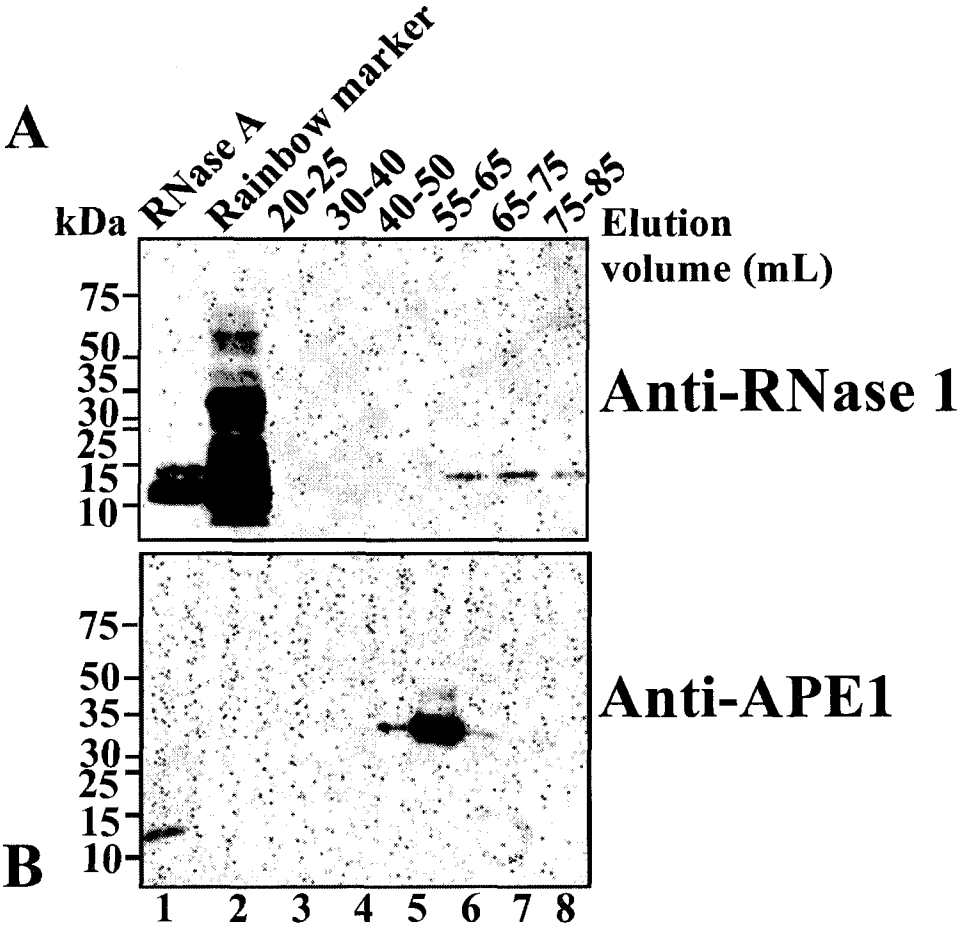

Figure 17: Western blots illustrating the presence of candidate endoribonucleases APE 1 and RNase 1. (A) Depicts a blot of sequentially pooled elution fractions (lanes 3-8) probed with RNase 1 polyclonal antibody. Lane 1 contains 3 μg of recombinant bovine pancreatic RNase A. Lane 2 contains rainbow marker. Molecular weight markers (kDa) are shown to the left. **(B)** Depicts the identical blot, stripped of RNase 1 antibody and re-probed with APE1. Molecular weight markers (kDa) are shown to the left.

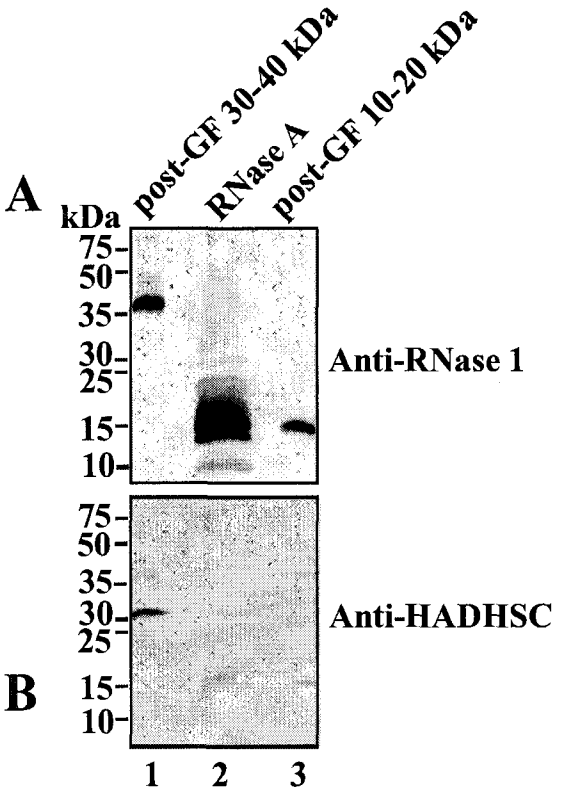

Figure 18: Western blot analysis confirming the presence of candidate endoribonucleases RNase A, HADHSC and Annexin III (A) Depicts a blot of pooled elution volumes from gel filtration column 13 that were resolved on a 15 % SDS-PAGE gel without prior treatment with reducing agent (β-mercaptoethanol). The blot was probed with polyclonal RNase 1 antibody. Lane 1 consists of a total volume of 2.0 mL from pooled fractions corresponding to elution volumes 40-50 mL (protein sizes of 30-40 kDa). Lane 2 represents 5 μg of recombinant bovine pancreatic RNase A. Lane 3 contains a total volume of 2.0 mL from pooled fractions corresponding to elution volumes 65-80 mL (protein sizes of 10-20 kDa). Molecular weight markers (kDa) are shown to the left. **(B)** Depicts the same blot that has been stripped of RNase 1 antibody and re-probed with HADHSC polyclonal antibody (GenWay Biotech., San Diego, CA). Molecular weight markers (kDa) are shown to the left.

3.2.4 Characterizing Native and Recombinant Endoribonucleases

To further distinguish between the 17 kDa and 35 kDa endoribonucleases and to confirm the suspected identities of the proteins identified in the previous sections (3.2.2 and 3.2.3) several characterization experiments were performed. The first such experiment tested the sensitivity to RNase inhibitory protein (commercially available as

"RNasin"). The autoradiograph in Figure 19 demonstrates the results of this experiment. As expected in the absence of the inhibitory protein, pooled samples from gel filtration corresponding to protein sizes 30-40 kDa (lanes 3-6) and 10-20 kDa (lanes 10 and 11), respectively exhibit endoribonuclease activity. In the presence of 1 U of RNasin (per reaction), endoribonuclease activity is significantly diminished for both gel filtration pooled samples (30-40 kDa, lanes 7-9 and 10-20 kDa, lanes 12-14). It should be noted that although RNasin is used in reaction mixtures for standard endoribonuclease assays (0.5 U/reaction; Chapter 2, section 2.1.6) and both 17 kDa and 35 kDa endoribonucleases are sensitive to RNasin, there does not appear to be inhibition of endonucleolytic activity. The most likely explanation for this is the ratio of inhibitory protein (RNasin) to endoribonuclease present in reaction mixtures. Moreover, the concentration of endoribonuclease present in purified samples was sufficiently high enough to mask the inhibitory effects of 0.5U RNasin used in the reaction cocktail mixture.

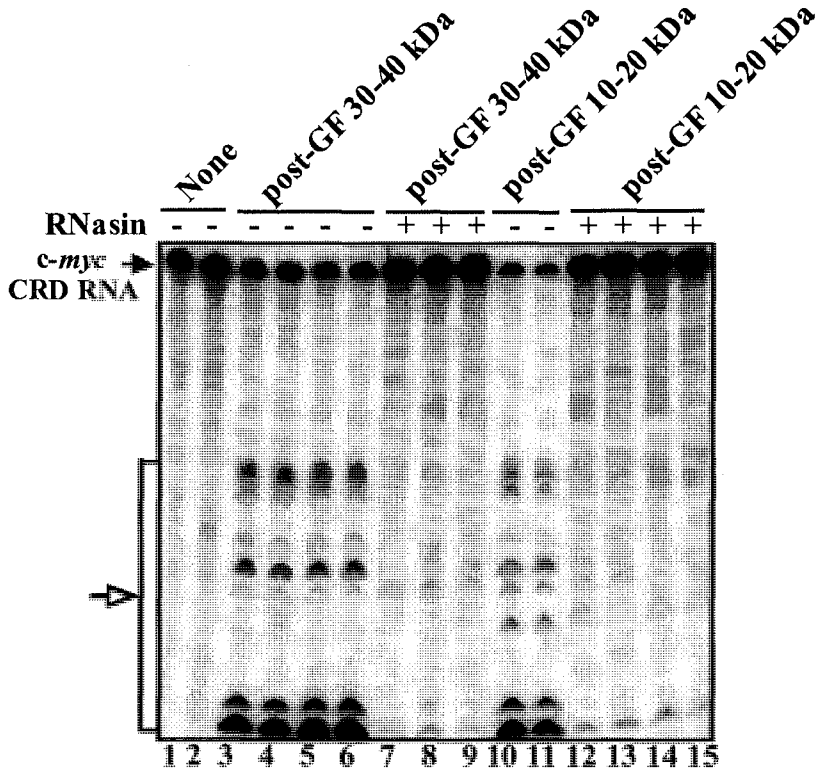

Figure 19: Sensitivity of native 35 kDa and 17 kDa endoribonucleases to commercial recombinant RNasin (Ribonuclease Inhibitor Protein). All assays were performed using 5'- γ ^{32}P-radiolabeled *c-myc* CRD (30,000 cpm/lane). Reactions were incubated for 5 minutes. RNA was resolved on a 12% denaturing polyacrylamide/7M urea gel. Lanes 1 and 2 contain no enzyme. Lanes 3-6 contain 5 μL aliquots (1U enzyme) from pooled fractions corresponding to elution volumes 40-50 mL (protein size of 30-40 kDa) without RNasin. Lanes 7-9 contain 1U RNasin and 5 μL aliquots (1U) from pooled fractions corresponding to elution volumes 40-50 mL (protein size of 30-40 kDa). Lanes 10 and 11 contain 3 μL aliquots (3.0U) from pooled fractions corresponding to elution volumes of 65-80 mL (protein sizes of 10-20 kDa) without RNasin. Lanes 12-15 contain 3 μL aliquots (3.0U) from pooled fractions corresponding to elution volumes of 65-80 mL (protein sizes of 10-20 kDa) with 1U of RNasin. Filled arrow indicates intact *c-myc* CRD RNA. Bracket and unfilled arrow indicates RNA decay products

3.2.4.1 Kinetic Analysis

Optimal enzyme concentrations for both the 17 kDa and 35 kDa native enzymes was found to correspond to the middle of DLU/time versus [Enzyme] linear regression plots (Figure 21-1(A) and 21-1(B)). Approximately 1U of post gel filtration-purified 17 kDa native enzyme and 0.5U of post gel filtration-purified 35 kDa native enzyme were

used for subsequent kinetic studies. A comparative look at the autoradiographs for the 17 kDa and 35 kDa enzymes (Figure 20, lanes 14 and 4, respectively), demonstrate that at the aforementioned concentrations roughly half of the substrate is decayed in a 5 min reaction using the 17 kDa enzyme and in an 8 min reaction using the 35 kDa enzyme.

Analysis of the native 17 kDa and 35 kDa enzymes, using various substrate concentrations (Figure 21-2, (A) and (B), respectively), illustrates that both enzymes exhibit Michaelis Menten-type reaction kinetics. Figure 21-2 (A and B) represents assays of sample 5'-radiolabeled oligonucleotide substrate concentrations over various stop-time periods for the 35 kDa native enzyme. Figure 21-2 (C and D) represents sample oligonucleotide substrate concentrations over various stop-time periods for the 17 kDa native enzyme. Figure 21-2 (B and C), lanes 1-5, demonstrate that reaction rates as a function of time (measured as DLU intensity of decay products) for the 35 kDa native enzyme remain relatively constant using the highest subtrate concentrations (1000 pM and 5000 pM), respectively. A similar finding for the native 17 kDa endoribonuclease, at 5000 pM substrate concentration, is shown in Figure 21-2 (D), lanes 1-5.

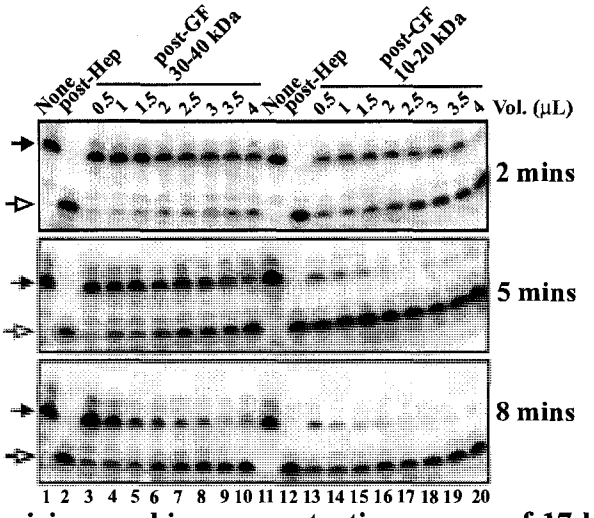

Figure 20: Optimizing working concentration ranges of 17 kDa and 35 kDa native enzyme for kinetic analysis. Autoradiographs using 5'-γ^{32}P-radiolabeled oligonucleotide substrate (all lanes approximately [500 *p*M]) and resolved on 12% denaturing polyacrylamide/7M urea gels. Reaction incubation times are shown on the right. Lanes 1 and 11 contain oligonucleotide alone. Lanes 2 and 12 contain (3 µL) 3 U post heparin-sepharose purified enzyme. Lanes 3-10 contain varying concentrations of 35 kDa native enzyme. Lanes 13-20 contain varying concentrations of 17 kDa native enzyme. Filled arrows represent intact substrate; unfilled arrows represent decay products.

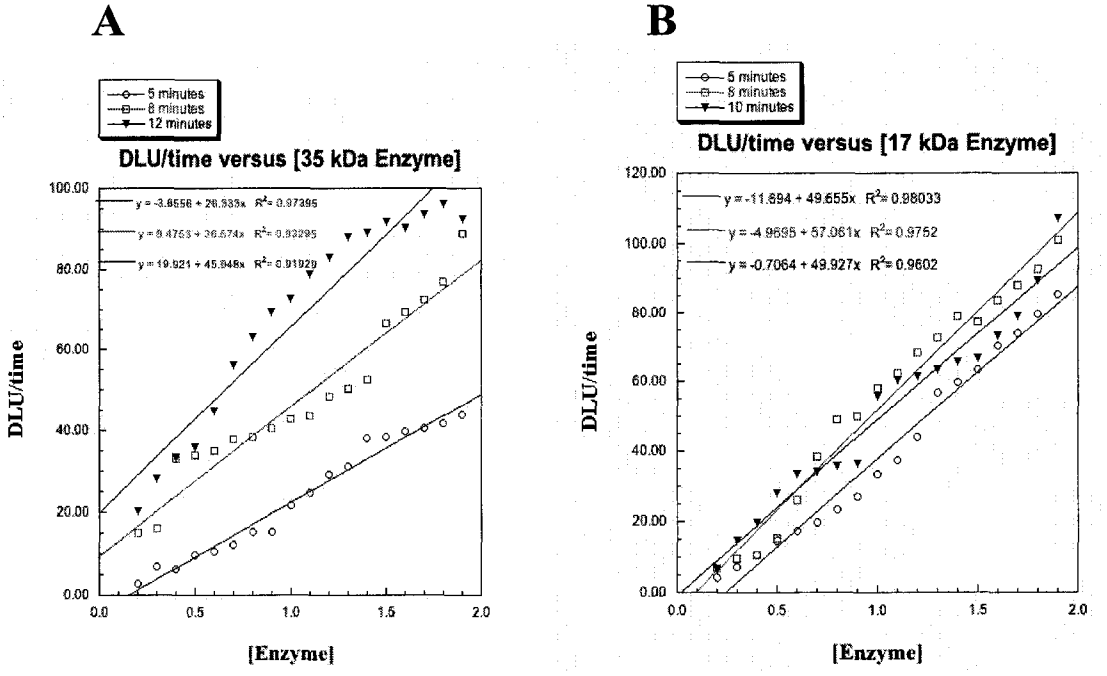

Figure 21-1: Linear regression analysis of optimization experiments. All gels represent stop-time assays using different enzyme concentrations **(A)** Linear regression analysis using various concentrations of native 35 kDa enzyme. Incubation times were 5, 8 and 12 min, respectively **(B)** Linear regression analysis using various concentrations of native 17 kDa enzyme. Incubation times were 5, 8 and 10 min, respectively.

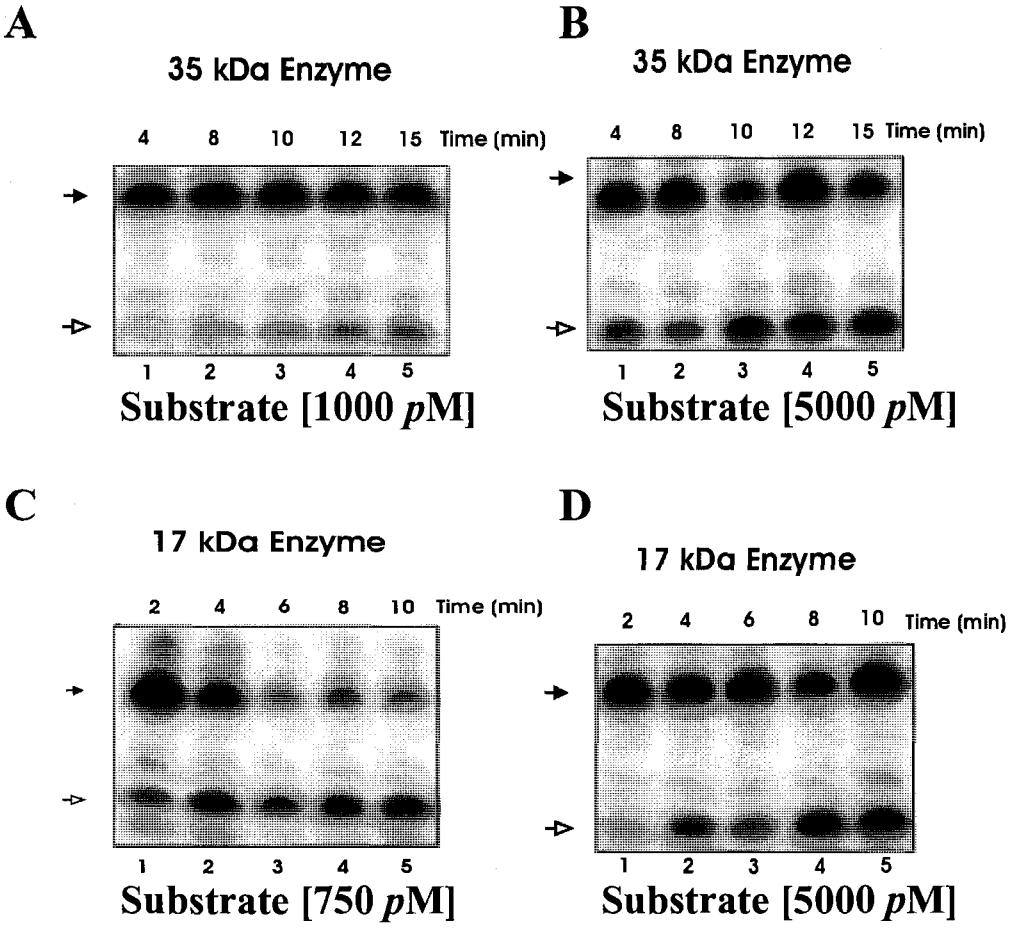

Figure 21-2: A subset of sample stop-time assays used to obtain data for Michaelis Menten kinetic analysis of native 35 kDa and 17 kDa enzymes. Autoradiographs were performed using 5'-γ ^{32}P-radiolabeled oligonucleotide substrate and resolved on 12% denaturing polyacrylamide/7M urea gels. **(A)** Assay of native 35 kDa enzyme using 1000 *p*M concentration of 5'-γ^{32}P-radiolabeled oligonucleotide per lane. Lanes 1-5 represent 4, 8, 10, 12 and 15 minute incubation periods, respectively. **(B)** Assay of native 35 kDa enzyme using 5000 *p*M concentration of 5'-γ^{32}P-radiolabeled oligonucleotide per lane. Lanes 1-5 represent 4, 8, 10, 12 and 15 minute incubation periods, respectively. **(C)** Assay of native 17 kDa enzyme using 750 *p*M concentration of 5'-γ^{32}P-radiolabeled oligonucleotide per lane. Lanes 1-5 represent 2, 4, 6, 8 and 10 minute incubation periods, respectively. **(D)** Assay of native 17 kDa enzyme using 5000 *p*M concentration of 5'-γ^{32}P-radiolabeled oligonucleotide per lane. Lanes 1-5 represent 2, 4, 6, 8 and 10 minute incubation periods, respectively. Filled arrows represent intact substrate; unfilled arrows represent decay product.

A

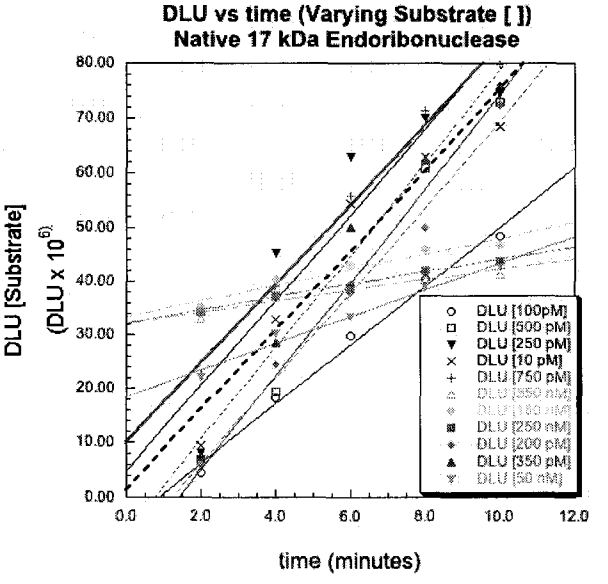

B

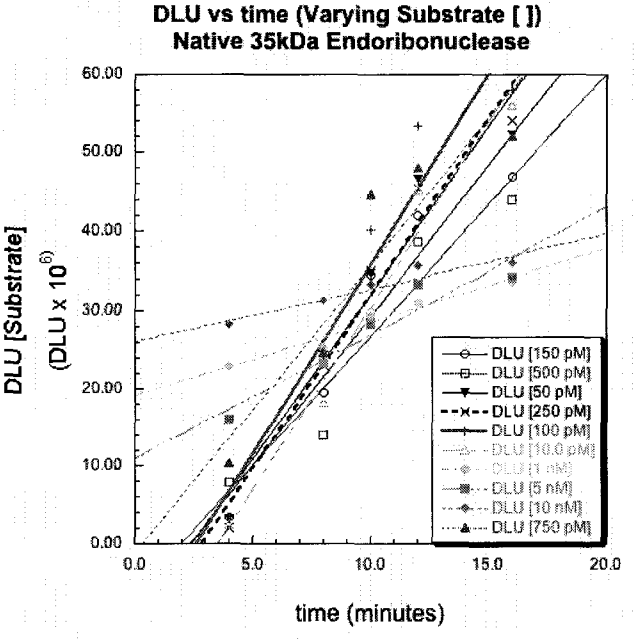

Figure 21-3: Linear regression analysis of stop-time kinetic assays using varying 5'-radiolabeled oligonucleotide substrate concentrations Substrate concentrations are color-coded and shown in the bottom right corner of the plots. **(A)** Results for stop-time assays at 2, 4, 6, 8 and 10 min for eleven respective substrate concentrations using the native 17 kDa enzyme **(B)** Results for stop-time assays at 4, 8, 10, 12 and 15 min for ten respective substrate concentrations using the native 17 kDa enzyme.

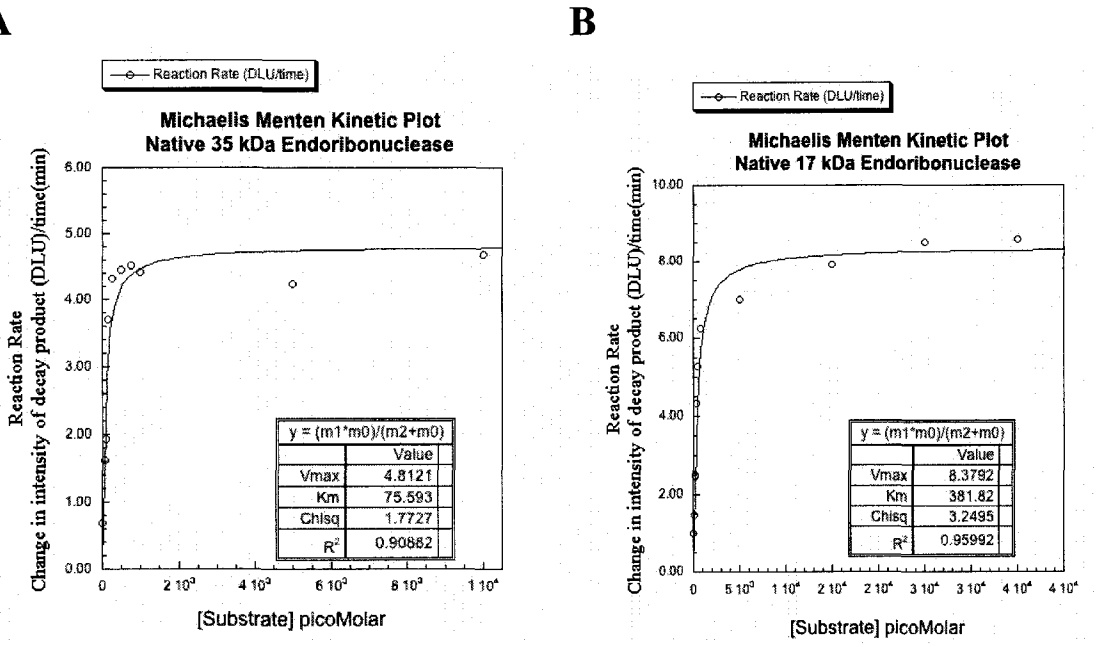

Figure 21-4: Nonlinear regression analysis of Michaelis Menten kinetics for the native 35 kDa and 17 kDa enzymes (A) Was generated from the slope values at the ten respective substrate concentrations in Figure 21-3(B). **(B)** Was generated from the slope values at the eleven respective substrate concentrations in Figure 21-3(A).

Figure 21-3 (A) and 21-3 (B) display reaction rates (DLU intensity versus time of incubation) for the range of substrate concentrations used for both the native 17 kDa and 35 kDa endoribonucleases. The data for the values of the slopes from these linear regression analyses were subsequently plotted as a function of substrate concentration. The results of nonlinear regression analysis using a Michaelis Menten curve fit (KaleidaGraph 3.6.2) for the native 35 kDa and 17 kDa enzymes is shown in Figure 21-4 (A) and (B), respectively.

With increasing oligonucleotide substrate concentration, both the 17 kDa and 35 kDa endoribonucleases exhibited saturation kinetics. Moreover, as substrate RNA is increased to very high levels, the enzymes become saturated and the rate of decay product approaches a constant rate. This is illustrated by a decrease in the slope values

exhibited in Figure 21-3 (A) and 21-3 (B) and by a horizontal flattening of the curves in Figure 21-4 (A) and 21-4 (B). As the enzymes become saturated with substrate (at very high substrate concentrations), V_{max} is approached. However, theoretical V_{max} values are never actually reached. Instead, the characteristic velocity (v) value for the enzymes is defined by the substrate concentration [5'-radiolabeled oligonucleotide substrate] equal to half of the maximum rate ($V_{max}/2$). Moreover, K_m is the concentration of substrate that leads to half-maximal enzyme velocity. This value is is termed the Michaelis Menten constant. It should also be noted that at V_{max} other factors such as pH, and temperature may influence the rate of reaction. K_m values for the 17 kDa and 35 kDa endoribonucleases were 381.82 *p*M and 75.593 *p*M, respectively. V_{max} for the native 17 kDa endoribonuclease was 763.64 *p*M min^{-1}. V_{max} for the native 35 kDa endoribonuclease was 151.2 *p*M min^{-1}.

It should be noted that error bars were not included in Figure 21-3 (A and B), and Figure 21-4 (A and B) because duplicate experiments using the substrate values shown (see Figure 21-3 (A) and 21-3 (B), were not performed, thus no standard deviation values were calculated. Additionally, V_{max} (±) and K_m (±) values were not included as standard deviation values were not calculated. Future experiments designed to fully characterize reaction kinetics of the native 17 kDa and 35 kDa enzymes should repeat endoribonuclease assays two or three times for all substrate concentrations chosen. This will enable calculation of standard deviation values and will improve the accuracy of V_{max} and K_m values.

3.2.4.2 Assessing Structural Features of the Native 35 kDa Endoribonuclease

Previous results from Western blots demonstrate that RNase 1 polyclonal antibody cross-reacts with proteins exhibiting molecular weights of 30 kDa and 37 kDa, respectively (Figure 12, lane 2; Figure 13-B, lane 2; Figure 15-A, lane 2). There are three possibilities to account for such observations: (i) The 17 kDa rat pancreatic RNase A is a monomeric N-glycosylated protein, (ii) 17 kDa rat pancreatic RNase A forms a dimer, or (iii) an RNase 1-like protein within the the molecular weight range of 30-40 kDa can be detected by the RNase 1 polyclonal antibody source used. To test the first possibility, post heparin-sepharose sample was pre-treated overnight with N-glycosidase F and subsequently purified with gel filtration chromatography. Figure 22 clearly demonstrates endoribonuclease activity in elution volumes 45-53 mL (proteins in molecular weight ranges of 25-40 kDa), and elution volumes 62-80 mL. Therefore, it is not likely that the 35 kDa endoribonuclease activity is due to an N-glycosylated isoform of rat pancreactic RNase A. Interestingly, there appears to be endonucleolytic activity in elution volumes 38- 40 mL (corresponding to proteins within the molecular weight range of 60-70 kDa). These results were somewhat surprising given that endonucleolytic activity had not previously been observed in elution volumes 38-40 mL. It was concluded that these observations were most likely the result of elution fraction contamination prior to performing endoribonuclease assays.

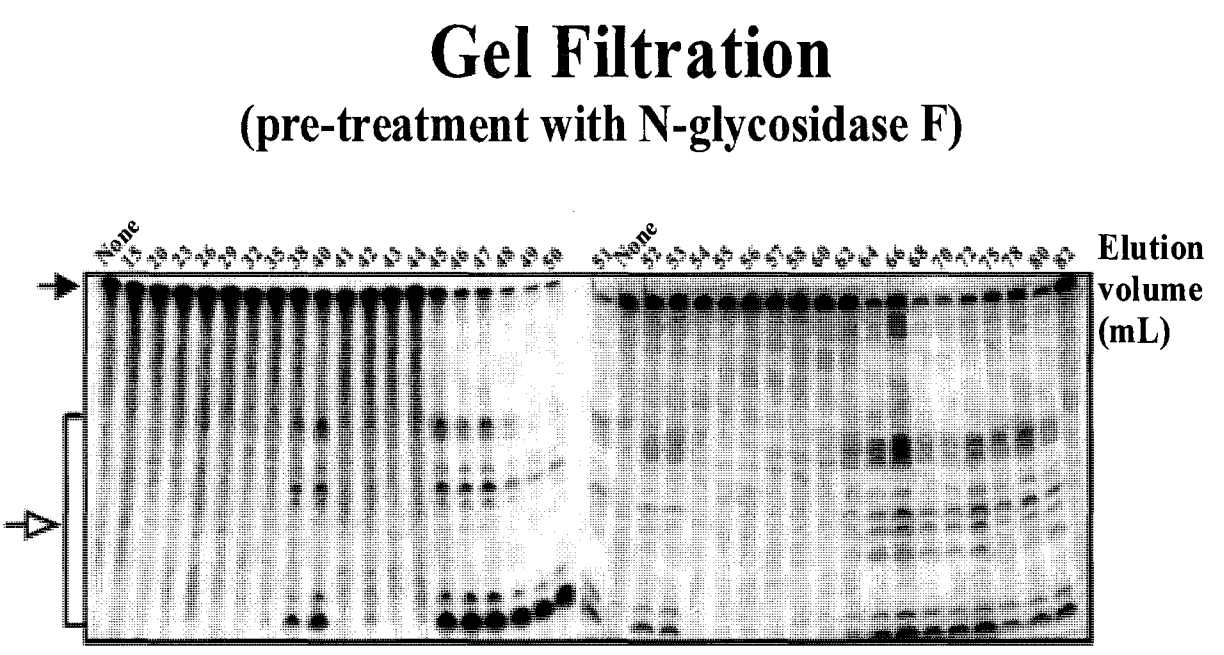

Figure 22: Assessing post-translational modifications of native 35 kDa endoribonuclease using recombinant N-glycosidase F. Autoradiograph depicting a standard endoribonuclease assay using 5'- γ ^{32}P-radiolabeled *c-myc* CRD 1705-1886 of elution fractions from gel filtration chromatography. 3.0 mL of post-heparin sepharose sample was incubated overnight at 30°C with 100 U of N-glycosidase F enzyme mixture (100U; 1 U = 1 μL) prior to loading on gel filtration column. 4 μL aliquots (0.75U enzyme) from 0.5 mL fractions corresponding to the elution volumes shown above each lane were utilized for the endoribonuclease assay. Intact *c-myc* CRD probe is shown with a filled arrow. RNA decay products are shown with a bracket and unfilled arrow.

To test the second possibility, post heparin-sepharose purified sample was incubated with a final concentration of 250 mM DTT to determine if the 35 kDa endoribonuclease was monomeric or dimeric. If the 35 kDa endoribonuclease were dimeric, one would expect treatment with DTT to disrupt subunit linkages (disulfide bridging). Consequently the apparent molecular weight of endoribonuclease activity (if individual subunits retained enzyme activity) would become representative of individual subunit size. Moreover, one would expect a disappearance or a significant decrease in the intensity of endoribonuclease activity in elution volumes 40-50 mL (30-40 kDa molecular weight range).

As illustrated in the autoradiograph below (Figure 23), two distinct endoribonucleolytic activities are still observed. The larger activity suggests that endoribonuclease activity is present in elution volumes 41-49 mL (molecular weight range of 30 kDa-40 kDa) and elution volumes 63-82 mL (molecular weight range of 12-20 kDa). The continued presence of endoribonuclease activity (molecular weight range of 30-40 kDa) indicates that the protein responsible for 35 kDa endoribonuclease activity is most likely monomeric. Given the evidence presented, this hypothesis appears to be most plausible.

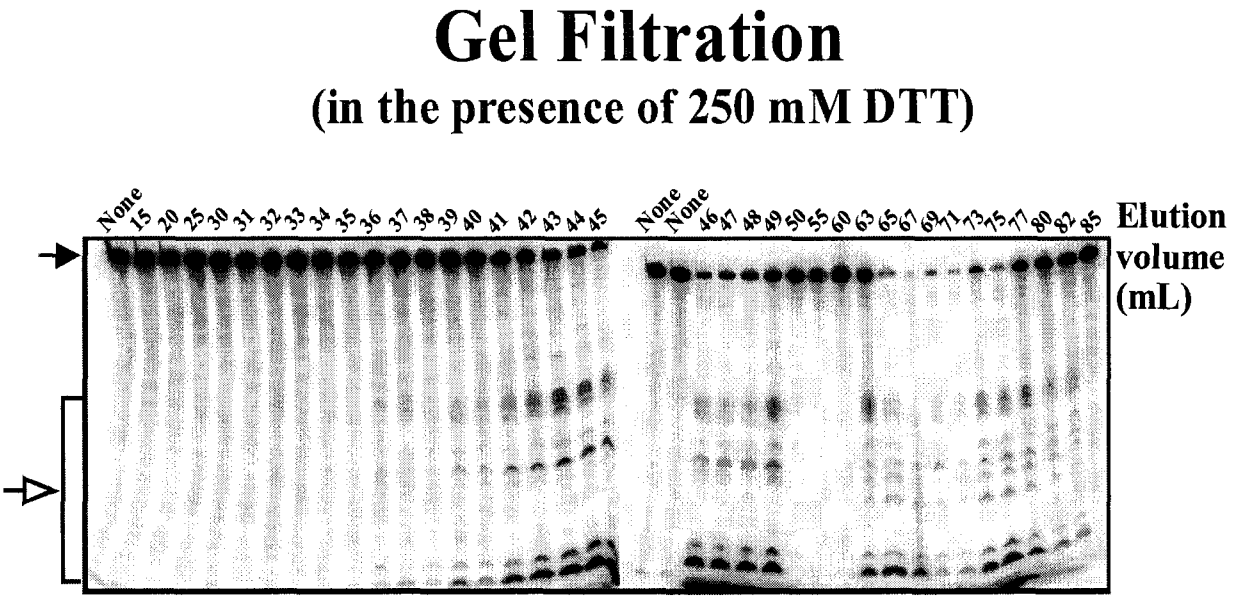

Figure 23: Assessing the properties of native 35 kDa endoribonuclease using DTT. Autoradiograph depicting a standard endoribonuclease assay using 5'- γ ^{32}P-radiolabeled *c-myc* CRD 1705-1886 of elution fractions from gel filtration chromatography. 3.0 mL of post heparin-sepharose sample was incubated for 60 minutes at 4°C in the presence of 250 mM DTT. 4 µL aliquots from 0.5 mL fractions corresponding to the elution volumes shown above each lane were utilized for the endoribonuclease assay. Intact *c-myc* CRD probe is shown with a filled arrow. RNA decay products are shown with a bracket and unfilled arrow.

3.2.5 Recombinant APE1

Recombinant APE1 was obtained from a lab in Texas and from the Hickson lab in the UK. Following dialysis, recombinant APE1 was assayed using standard endoribonuclease assay protocol. Figure 24-A and 24-B depict the results of the assays. It is evident from Figures 24-A, lane 4 (Hickson's lab, UK) and 24-B, lanes 7-9 that both recombinant APE1 samples obtained exhibit endoribonuclease activity. Cleavage sites generated by recombinant APE1 samples appear to exhibit similarity to both post heparin-sepharose sample (Figure 24-B, lanes 2-6) and pooled post-gel filtration elution volumes 40-50 mL (30-40 kDa). In addition, recombinant samples of APE1 appear to generate additional cleavage products near the bottom of the gels (Figure 24-A, lane 4; Figure 24-B, lanes 7-9); however, sequencing gel analysis (shown in Figure 24-C) was required to definitively map endonucleolytic-cleaved RNA products.

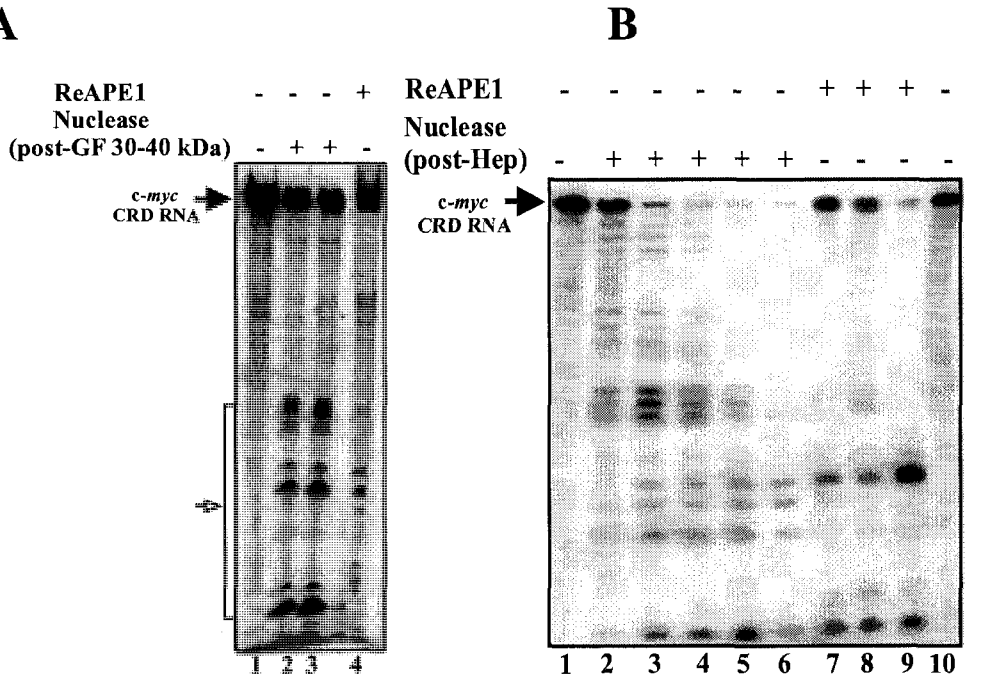

Figure 24: Endoribonuclease assays illustrating the ability of recombinant APE 1 to endonucleolytically-cleave *c-myc* CRD RNA *in vitro*. All assays were carried out using 5'- γ ^{32}P-radiolabeled *c-myc* CRD. Reactions were incubated for 5 minutes **(A)** Autoradiograph of a standard endoribonuclease assay using pooled post gel filtration purified sample and recombinant APE1 protein (obtained from Hickson's lab, UK). Lane 1 contains *c-myc* CRD RNA alone. Lanes 2 and 3 contain 5 μL of pooled gel filtration elution volumes 40-50 mL (protein sizes 30-40 kDa). Lane 4 contains 1 μL dialyzed recombinant APE1 (stock 4 mg/mL). Intact *c-myc* CRD probe is shown with a filled arrow. RNA decay products are shown with a bracket and unfilled arrow. **(B)** Autoradiograph of a standard endoribonuclease assay using pooled post heparin-sepharose purified sample and recombinant APE1 protein (Sankar's lab, TX). Lane 1 contains *c-myc* CRD RNA alone. Lanes 2-6 contain 1 μL (1U), 2 μL (2U), 3 μL (3U), 4 μL(4U) and 5 μL (5U), respectively, of post heparin-sepharose purified sample. Lanes 7-9 contain 1 μL, 2 μL, 3 μL recombinant APE1 respectively (stock 0.3 mg/mL).

Although endoribonuclease assays using recombinant APE1 samples exhibited endoribonucleolytic activity (Figure 24-A, lane 4; Figure 24-B, lanes 7-9) the purity of the recombinant samples to date was unknown. The possibility of contamination, in particular co-purification of RNases during recombinant APE1 preparation, could potentially have occurred. Figures 25-A and 25-B demonstrate the assessment of recombinant APE1 sample purity. As shown in Figure 25-A, lanes 2 and 3, a large

protein band is present corresponding to an approximate molecular weight of 33-35 kDa. Western blots of recombinant APE1 samples shown in Figure 25-B (lanes 1 and 2), clearly demonstrates the presence of a protein band corresponding to a molecular weight of approximately 34 kDa. The blot was probed with anti-APE1 monoclonal antibody, thus it was concluded that the protein bands exhibited at 34 kDa were indeed recombinant APE1. Results to date using two different sources of recombinant APE1 strongly suggest that APE1 is the protein responsible for observed endoribonuclease activity exhibited by the 30-40 kDa purified native enzyme; however, the immunodepletion experiments presented and discussed shortly (see section 3.2.7) were used to further confirm these results.

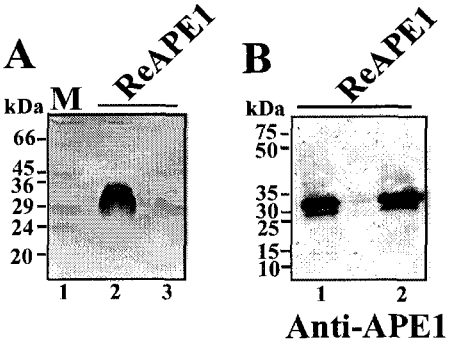

Figure 25: Assessing the purity of recombinant APE 1 samples. (A) 15% SDS-PAGE stained with Coomassie Brilliant Blue. Lane 1 contains low molecular weight protein marker. Lane 2 contains 5 μg of recombinant APE1 (Dr. Sankar's lab, TX). Lane 3 contains 1 μg recombinant APE1 (Hickson's lab, UK). Molecular weight marker sizes (M) are shown to the left of the lane 1 **(B)** Western blot depicting recombinant APE1 samples probed with mouse monoclonal APE1 antibody. Lane 1 contains 3 μg of recombinant APE1 (Dr. Sankar's lab, TX). Lane 2 contains 3 μg of recombinant APE1 (Hickson's lab, UK). Molecular weight markers are shown to the left.

***Note**: Western blot shown in Figure 25-B does not represent the SDS-PAGE gel shown in Figure 25-B

3.2.5.1 Mapping RNA Cleavage Products Generated by Native 35 kDa, 17 kDa and Recombinant Endoribonucleases

A comparison of the RNA cleavage (decay) products generated with purified native enzyme from post heparin-sepharose, post gel filtration chromatography, bovine pancreatic RNase A and recombinant APE 1 are shown in Figure 26 panels A, B and C. The cleavage profile exhibited by post-heparin sepharose purified sample in the presence of *c-myc* CRD RNA 1705-1886 presented in Figure 26-A, lane 3 and Figure 26-B, lane 9 was mapped according to previously reported data (Bergstrom et al. 2006) and using RNase T1 digest of *c-myc* CRD RNA 1705-1886 (Figure 26-A, lane 1; Figure 26-C, lane 1).

RNA cleavage products from post heparin-sepharose (Figure 26-A, lane 3; Figure 26-B, lane 9), gel filtration 10-20 kDa (Figure 26-B, lanes 10-11), gel filtration 30-40 kDa (Figure 26-A, lanes 4-6; Figure 26-B, lanes 12-13; Figure 26-C, lanes 4-5), and recombinant bovine pancreatic RNase A (Figure 26-B, lane 8) exhibited a high degree of similarity. Post heparin-sepharose-purified sample (Figure 26-A, lane 3; Figure 26-B, lane 9) and pooled gel filtration elution sample corresponding to proteins in the molecular weight range of 10-20 kDa (Figure 26-B, lanes 10-11) appeared to generate identical cleavage products. Recombinant bovine pancreatic RNase A appeared to generate nearly identical cleavage products (Figure 26-B, lane 8) with the exception of an additional cleavage product; (illustrated with the bracket, Figure 26-B, lane 8) as compared to both post heparin-sepharose and post gel filtration (10-20 kDa) samples.

Pooled gel filtration elution volumes corresponding to proteins in the molecular weight range of 30-40 kDa (35 kDa endoribonuclease) (Figure 26-A, lanes 4-6; Figure 26-B, lanes 12 and 13; Figure 26-C, lanes 4 and 5) produces several RNA decay products

identical to those observed in post-heparin, post gel filtration (10-20 kDa) and to that of recombinant bovine pancreatic RNase A. The major differences being that the 35 kDa produces fewer decay products and exhibits slightly different dinucleotide cleavage site preference. As shown in Figure 26-A (lanes 4-6) and Figure 26-B (lanes 12 and 13), native 35 kDa endoribonuclease appears to preferentially cleave the dinucleotide UA 1751 shown by asterisks in Figure 26-A and -B. In addition, native 35 kDa endoribonuclease appears to preferentially cleave dinucleotide CA, 1771 and dinucleotide UA, 1773.

If APE1 is indeed the protein that exhibited endonuclease activity in native pooled gel filtration elution volumes (protein sizes 30-40 kDa), one would expect RNA cleavage fragments to have exhibited a high degree of similarity to decay products produced by native 35 kDa endoribonuclease. RNA decay products produced by recombinant APE1 (Figure 26-C, lanes 5-7) and native 35 kDa endoribonuclease (Figure 26-A, lanes 4-6; Figure 26-B, lanes 12 and 13; Figure 26-C, lanes 3 and 4) exhibited one identical cleavage site. As illustrated with the un-filled arrow in Figure 26-C, both native 35 kDa endoribonuclease and recombinant APE1 preferentially cleave dinucleotide 1751 UA. This data does not conclusively prove that APE1 is the protein responsible for 35 kDa endoribonucleolytic activity in native extract; however, it does demonstrate that both recombinant APE1 and native 35 kDa endoribonuclease preferentially cleave 5'- γ ^{32}P-radiolabeled *c-myc* CRD RNA at dinucleotide 1751 UA.

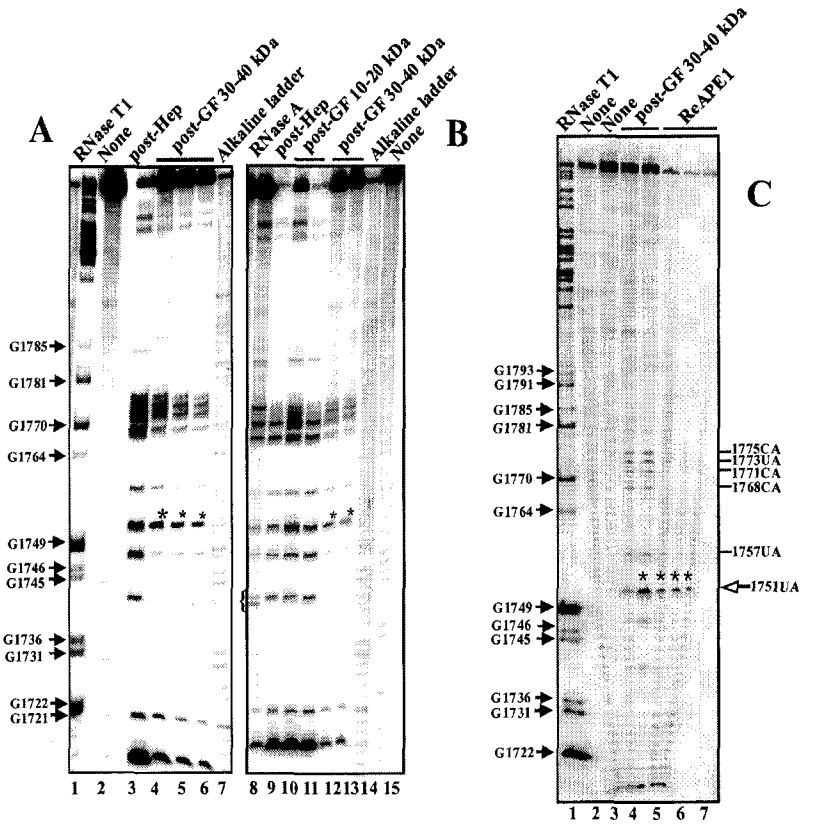

Figure 26: Mapping cleavage products generated with native endoribonuclease samples, recombinant RNase A and recombinant APE1. All mapping experiments were resolved on 12% denaturing polyacrylamide/7M urea sequencing gels. **(A)** Endoribonuclease assay using 5'-γ^{32}P-radiolabeled *c-myc* CRD RNA. Reactions were incubated for 7 minutes. Lane 1 contains RNase T1 digest of *c-myc* CRD RNA 1705-1886. Lane 3 contains 2 μL (2U) of post heparin-sepharose purified sample. Lanes 4-6 contain 4 μL (0.75U), 3 μL (0.6U), and 2 μL (0.4U) of pooled gel filtration elution volumes 40-50 mL (protein sizes 30-40 kDa), respectively. T1 digests are labeled to the left of lane 1. **(B)** Endoribonuclease assay using 5'-γ^{32}P-radiolabeled *c-myc* CRD. Reactions were incubated for 5 minutes. Lane 8 contains 1U (1 U=1 μL) bovine pancreatic RNase A. Lane 9 contains 3 μL of pooled post heparin sepharose purified sample. Lanes 10 and 11 contain 1 μL (1U) and 3 μL (3U), respectively, from pooled fractions corresponding to elution volumes 65-80 mL (protein sizes of 10-20 kDa). Lanes 12 and 13 contain 4 μL (0.75U) and 5 μL (1U), respectively, of pooled gel filtration elution volumes 40-50 mL. **(C)** Autoradiograph of a standard endoribonuclease assay using 5'-γ^{32}P-radiolabeled *c-myc* CRD RNA. Reactions were incubated for 10 minutes. Lane 1 contains RNase T1 digest of 5'-γ^{32}P-radiolabeled *c-myc* CRD 1705-1886. Lanes 4 and 5 contain 3 μL (0.6U) and 4 μL (0.75U), respectively, of pooled gel filtration elution volumes 40-50 mL. Lanes 5-7 contain 1 μL, 2 μL, and 3 μL, respectively, of recombinant APE1 sample obtained from Dr. Sankra's lab (Texas) (stock 0.3 mg/mL). T1 digests are labeled to the left of lane 1.

3.2.6 Electrophoretic Mobility Shift Assays

EMSA experiments were designed to assess the physical interaction between respective recombinant samples of HADHSC, APE1 and 5'-γ^{32}P-radiolabeled *c-myc* CRD 1705-1886 RNA. EMSA protocols were adopted from methods previously used by Sparanese and Lee (2007) and Prokipcak *et al.* (1994). Optimization of binding conditions was based on the *in vitro* interaction between CRD-BP and 5'-γ^{32}P-radiolabeled *c-myc* CRD 1705-1886 RNA. The optimal reaction conditions were identical to those previously outlined by Sparanese and Lee (2007). Optimum binding conditions were measured by the intensity of binding complexes. Figure 27, lanes 12 and 13, illustrate an 'optimal' binding interaction between CRD-BP and 5'-γ^{32}P-radiolabeled *c-myc* CRD 1705-1886 RNA. Optimal binding conditions for CRD-BP/5'-γ^{32}P-radiolabeled *c-myc* CRD 1705-1886 RNA were utilized for EMSA experiments using 5'-γ^{32}P-radiolabeled *c-myc* CRD 1705-1886 RNA /HADHSC and APE1, respectively. Previous work by Sparanese and Lee (2007) demonstrated that recombinant forms of Rpp20, Rpp21 and Rpp40 do not bind 5'-γ^{32}P-radiolabeled *c-myc* CRD 1705-1886 RNA *in vitro*. As such, recombinant forms of Rpp20, Rpp21, and Rpp40 were utilized as negative controls in these experiments. Figure 27 (lanes 9, 10 and 11) and Figure 28 (lanes 5, 6 and 7) demonstrate that at 500 nM Rpp 20, 21 and 40 do not bind 5'-γ^{32}P-radiolabeled *c-myc* CRD 1705-1886 RNA.

Figure 27 illustrates the binding of HADHSC to 5'- γ^{32}P-radiolabeled *c-myc* CRD 1705-1886 RNA. At lowest nanomolar concentrations (100 nM, lane 8), a lower binding complex is formed. As nanomolar concentrations of HADHSC are increased (200nM, 300nM, 500nM; lanes 7, 6 and 5 respectively) a second binding complex is formed and

the intensity of the lower binding complex is greatly reduced. At highest nanomolar concentrations of HADHSC (750 nM, 1000 nM, 1500 nM; lanes 4, 3, and 2, respectively), the lower binding complex disappears whereas the larger binding complex is enhanced. It should be noted, however, that even at highest nanomolar concentrations of HADHSC (1500 nM, lane 2) the intensity of the larger complex is much lower when compared to that of the interaction between CRD-BP (2000 nM) and *c-myc* CRD RNA (lanes 12 and 13).

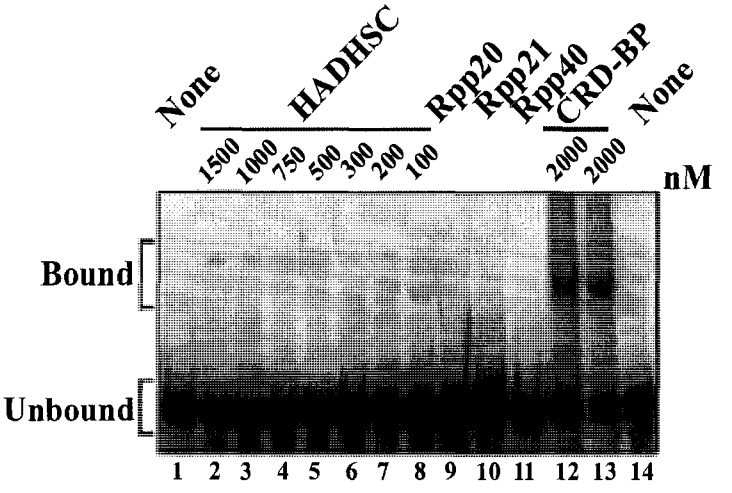

Figure 27: HADHSC is capable of binding to *c-myc* CRD RNA *in vitro*. Lanes 1 and 14 contain *c-myc* CRD RNA alone. Lanes 13 and 14 contain 2000 nanomolar (nM) dialyzed CRD-BP as positive control. Lanes 9-11 contain 500 nM of non-RNA binding proteins Rpp 20, 21 and 40, respectively, as negative control. Lanes 2-8 contain varying nanomolar (nM) concentrations of HADHSC.

As demonstrated in Figure 28, lane 4, 8 and 9, at 1000-2500 nM, recombinant APE1 binds 5'-γ^{32}P-radiolabeled *c-myc* CRD 1705-1886 RNA. Two binding complexes are observed for all micromolar concentrations utilized (1 μM, lanes 4; 2 μM, lane 8; 2.5 μM, lane 9). Somewhat surprisingly, the intensity of the unbound substrate RNA in lanes containing recombinant APE1 (Figure 28, lanes 4, 8 and 9) is significantly diminished. The migration of most *c-myc* substrate RNA appears to have been retarded in the smallest

complex. By comparison, little substrate RNA appears in the larger complex. Given the relative uniformity in intensity of the larger complex across the range of micromolar concentrations utilized, the presence of the larger complex may represent non-specific protein/protein interaction, non-specific protein/RNA interaction or a combination of both. To determine if the *c-myc* CRD-1705-1886/HADHSC and *c-myc* CRD-1705-1886/APE1 associations are specific, competition studies using unlabeled competitor RNA at various molar ratios, would be required.

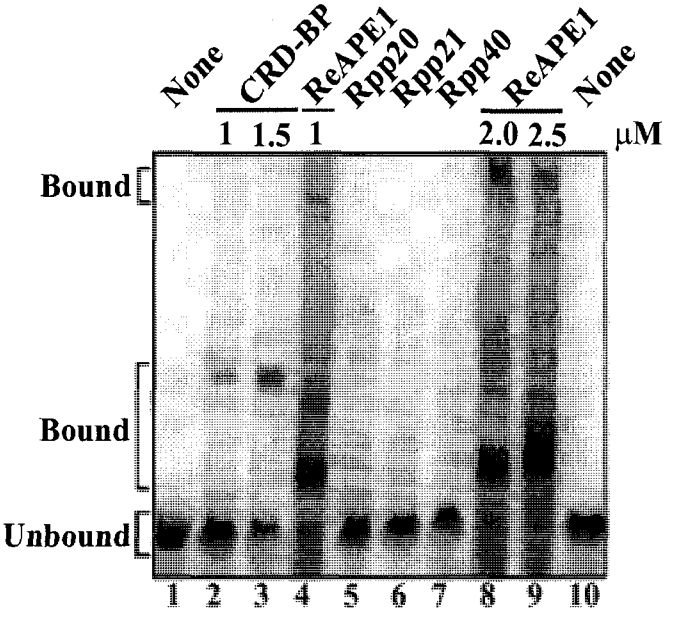

Figure 28: Recombinant APE1 is capable of binding to *c-myc* CRD RNA *in vitro*. All lanes were incubated with 5'- γ ^{32}P-radiolabeled *c-myc* CRD 1705-1886 RNA (50,000 cpm/lane). Lanes 1 and 10 contain *c-myc* CRD RNA alone. Lanes 2 and 3 contain 1.0 μM (micromolar) and 1.5 μM of dialyzed CRD-BP, respectively, as positive control. Lanes 5-7 contain 500 nanomolar (nM) non-RNA binding proteins Rpp 20, 21 and 40, respectively, as negative control. Lane 4 contains 1.0 μM recombinant APE 1 (Hickson's lab, UK). Lane 8 and 9 contain 2.0 μM and 2.5 μM APE 1 (Sankar's lab, TX), respectively. Concentrations (μM) are shown above each lane.

3.2.7 Immunodepletion of Native 35 kDa Endoribonuclease Activity

To further confirm the identity of the 35 kDa endoribonuclease, immunodepletion experiments of native 35 kDa endoribonuclease activity were performed with a PIERCE Seize X Protein A Immunoprecipitation kit. *c-myc* CRD RNA was the primary substrate RNA utilized for endoribonuclease assays of immunodepletion experiments. Of note, due to its availability, MDR1 RNA was utilized as a comparison RNA substrate in one endoribonuclease assay (see Figure 29).

An autoradiograph of the results from the first immunodepletion experiment using the PIERCE Seize X Protein A Immunoprecipitation kit is shown in Figure 29. The spin column was constructed using anti-APE1 monoclonal antibodies. 50 μg of anti-APE1 antibody was cross-linked to the spin column matrix as previously described (section 3.1.7).

Spin column flow-through (FT, lane 3) and pooled wash fractions (Wash, lane 4) exhibit a significant decrease in endonuclease activity. A significant increase in endonuclease activity is once again observed in elution fractions 1 and 2 (lanes 5 and 6). These results suggest that the first attempted immunodepletion of native heparin-sepharose extract, using monoclonal antibodies againt recombinant APE1, was successful. Moreover, an endoribonuclease present in post heparin-sepharose purified sample was bound to the matrix containing cross-linked anti-APE1 monoclonal antibodies.

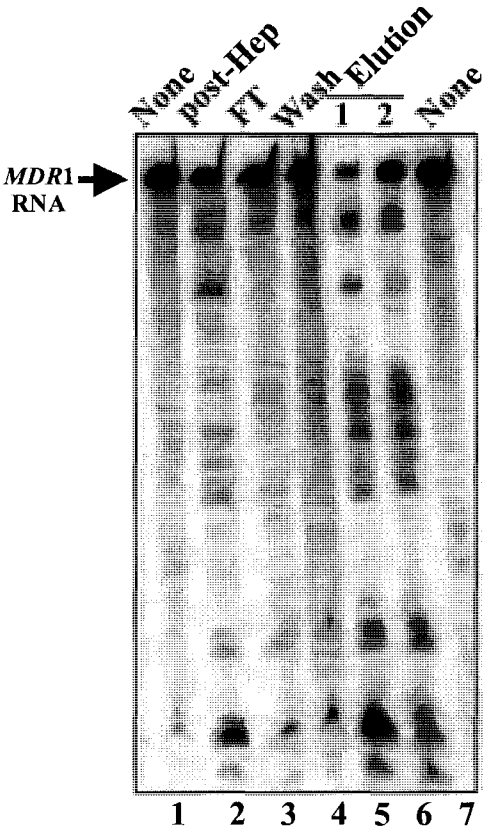

Figure 29: Autoradiograph depicting successful immunodepletion of native heparin-sepharose purified extract using APE1 monoclonal antibodies. The endoribonuclease assay was performed using 5'- γ ^{32}P-radiolabeled MDR 1 RNA. Lanes 1 and 7 contain MDR 1 RNA alone. Lane 2 contains 2 µL (2U) post heparin-sepharose purified sample, prior to loading onto spin column. Lane 3 contains a 4 µL aliquot of flow through fraction 1. Lane 4 contains a 4 µL aliquot from spin column pooled wash (fractions 2 and 3). Lanes 5 and 6 contain 4 µL aliquots from elution fractions 1 and 2 respectively.

A second immunodepletion experiment also using a PIERCE Seize X Protein A Immunoprecipitation spin column was performed. An autoradiograph of the experiment is shown in Figure 30. Post heparin-sepharose purified sample pre-load (lanes 1 and 2) exhibited strong endonuclease activity. Pooled flow-through fraction 1 and wash flow #2 and #3 is shown in 5. There was a clear reduction in observed endonuclease activity in the pooled flow through/wash sample (Figure 30; compare lane 5 to lanes 3 and 4). Elution fractions were hallmarked by the reappearance of strong endonuclease activity

(lanes 6-8). Elution fraction 1 (Figure 30, lane 6) exhibited strongest activity. Elution fractions 2 and 3 (Figure 30, lanes 7 and 8, respectively) contained endonuclease activity; however, it was significantly diminished when compared to elution fraction 1 (Figure 30, lane 6). It should be noted that although endonuclease activity was diminished in pooled flow through/wash fractions (lane 4), activity remained readily apparent.

There are two possible explanations for this observation. First, during loading of the heparin-sepharose sample, the antibodies present on the spin column matrix may have become saturated with protein present in the heparin-sepharose sample load. Consequently, unbound endoribonuclease would have passed directly through the column. Alternatively (bearing in mind that post heparin-sepharose sample contained two distinct (17 kDa and 35 kDa) endoribonuclease activities as previously shown in gel filtration chromatographic purification experiments; Chapter 2, Figure 6-A, 6-B and Figure 7-A), previous results suggested that the 17 kDa (RNase 1) and 35 kDa endoribonuclease (APE1) were distinct proteins. Considering that APE1 monoclonal antibodies were used to construct the immunoprecipitation spin column, it was expected that the 17 kDa RNase 1 protein in heparin-sepharose purified sample would not bind to the column matrix. Consequently, it is not surprising that endonuclease activity is present in pooled wash and flow through fractions (Figure 30; lane 5).

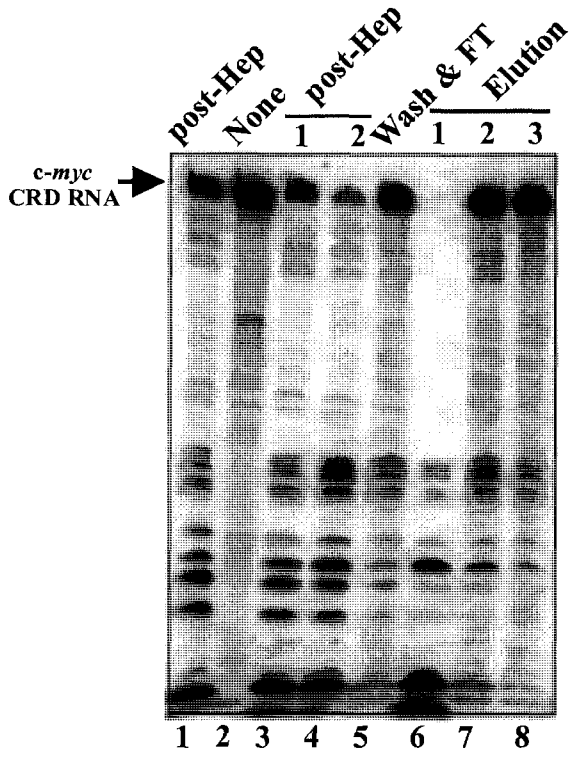

Figure 30: Autoradiograph depicting successful immunodepletion of native heparin-sepharose purified extract using APE1 monoclonal antibody. The standard endoribonuclease assay was performed using 5'-radiolabeled *c-myc* CRD RNA **(A)** Immunodepletion of native 35 kDa endoribonuclease activity. Lanes 1 contains 1 µL (1U) of post heparin sepharose purified sample (positive control). Lane 2 contains *c-myc* CRD RNA alone. Lanes 3 and 4 contain 2 µL (2U) and 3 µL (3U) aliquots of post heparin-sepharose purified sample (spin column pre-load). Lane 5 contains 4 µL of pooled flow through 1 and flow through 2 (wash). Lanes 6, 7 and 8 contain 4 µL aliquots of elution fractions 1, 2 and 3, respectively.

A third spin column (Figure 31-B) was constructed using syntaxin 18 polyclonal antibodies. Thirty µg of syntaxin 18 polyclonal antibody was cross-linked to the protein A spin column matrix as previously outlined (Chapter 3, section 3.1.7). This column was constructed to function as a negative control. A Western blot of the third immunodepletion experiment was also performed (see Figure 32).

Figure 31-A illustrates successful immunodepletion of post gel filtration (30-40 kDa) purified native extract. This was perhaps the most clear-cut evidence supporting successful immunodepletion of post gel-filtration (30-40 kDa) purified native extract.

Flow-through/wash lanes (Figure 31-A, lanes 6 and 7) were marked by the absence of endonuclease activity. Elution fraction 1 (Figure 31-A, lane 8) illustrates the re-appearance of endonuclease activity. Elution fraction 2 (Figure 31-A, lane 9) also exhibited strong activity; however, it was slightly diminished when compared to elution fraction 1 (compare lanes 8 and 9).

The control column shown in Figure 31-B, demonstrated that heparin-sepharose sample activity was not immunodepleted with syntaxin 18 polyclonal antibody. The flow through (FT, Figure 31-B, lane 1) and pooled wash fraction two and three (Wash, Figure 31-B, lane 3) displayed strong endonuclease activity with similar intensity to post heparin-sepharose column pre-load (Figure 31-B, compare lanes 1, 2 and 3). In contrast, elution fractions 1 and 2 (Figure 31-B, lanes 4 and 5, respectively) did not exhibit endonuclease activity. Results from the control column demonstrated that immunodepletion of endoribonuclease activity observed in previous immunodepletion columns (Figures 29, 30, 31-A) was produced specifically by the presence of anti-APE1 monoclonal antibodies.

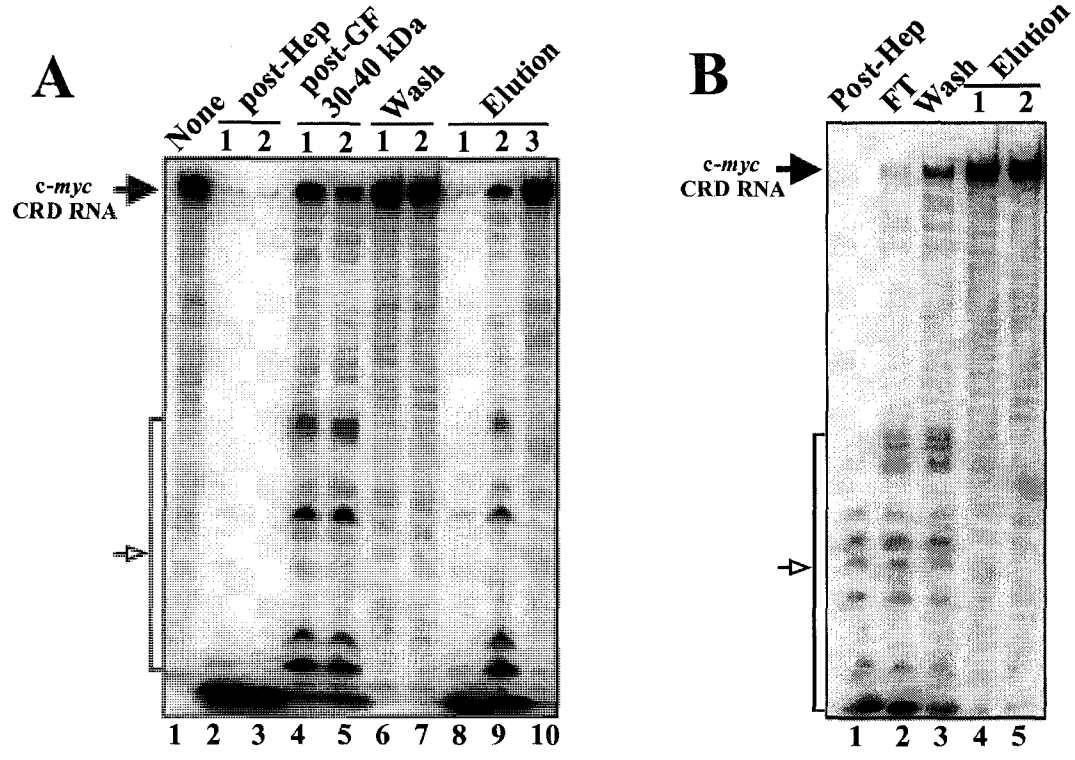

Figure 31: Successful immunodepletion of native 35 kDa endoribonuclease activity. **(A)** Lane 1 contains *c-myc* CRD RNA alone. Lanes 2 and 3 contain 2 µL (2U) and 3 µL (3U) of post heparin sepharose purified sample, respectively. Lanes 4 and 5 contain 4 µL (0.75U) and 5 µL (1U) aliquots of pooled gel filtration elution volumes 40-50 mL (protein sizes 30-40kDa), respectively. Lanes 6 and 7 contain 4 µL aliquots of flow through 1 and flow through 2 (Wash), respectively. Lanes 8 contains 4 µL from elution 1. Lane 9 contains 4 µL from elution 2. Lane 10 contains 4 µL from elution 3. **(B)** Control column using syntaxin 18 polyclonal antibody. Lane 1 contains 2 µL (2U) of post heparin-sepharose purified sample. Lane 2 contains 4 µL of flow through 1. Lane 3 contains 4 µL of pooled flow through fractions 2 and 3 (Wash). Lanes 4 and 5 contain 4 µL of elution fractions 1 and 2, respectively.

Figure 32 demonstrates Western blot analysis of the immunodepletion experiment shown in Figure 31-A. There was a striking similarity between endonuclease activity in post gel filtration (30-40 kDa) purified pre-load (Figure 31-A, lanes 4 and 5), elution fractions 1 and 2 (Figure 31-A, lanes 8 and 9, respectively) and the presence of APE1 in corresponding fractions (Figure 32, pre-load lane 2; Figure 32, elution fractions 1 and 2, lanes 6 and 7, respectively). In addition, the absence of endonuclease activity in wash

fractions (Figure 31-A, lanes 6 and 7) corresponded with the absence of APE1 in flow through (FT) and wash fractions (Wash) on the Western blot shown in Figure 32.

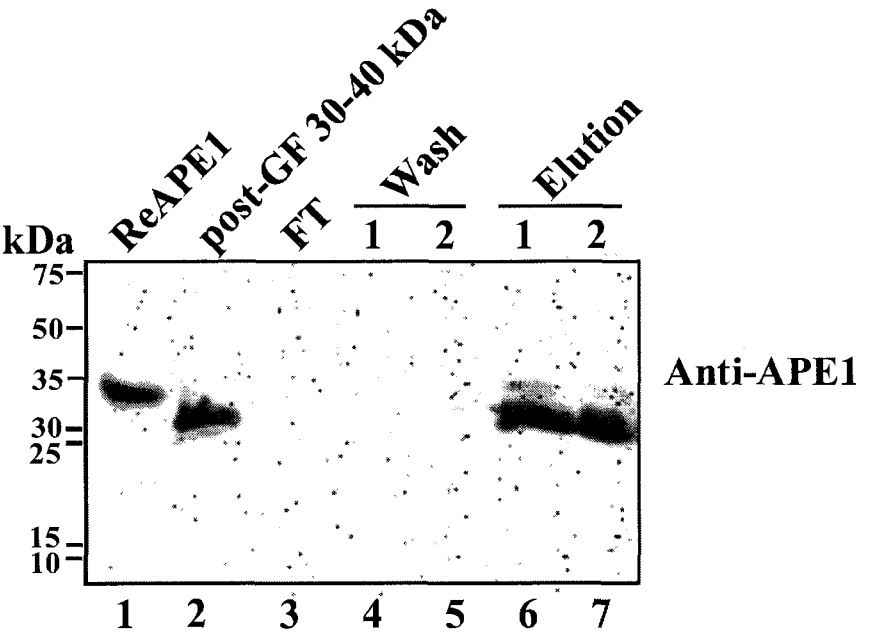

Figure 32: Western blot result of APE 1 immunodepletion experiment. Molecular weight markers are shown to the left of blot. Lane 1 contains 0.5 µg recombinant APE 1 (Sankar's lab, TX). Lane 2 consists of a total volume of 2.0 mL from pooled fractions corresponding to elution volumes 40-50 mL (protein sizes of 30-40 kDa). Lane 3 contains flow through fraction 1. Lanes 4 and 5 contain flow through fractions 2 and 3 (wash). Lanes 6 and 7 contain elution fraction 1 and 2, respectively.

A final experiment was done to test for the presence of annexin III and HADHSC in the immunodepleted native gel filtration (30-40 kDa) sample. The blot shown in Figure 32 was stripped and re-probed with anti-HADHSC and anti-annexin III antibodies, respectively. Figure 33 illustrates that annexin III is present in post gel filtration (30-40 kDa) pre-load sample (lane 2); however, it is not present in flow through (FT, lane3), wash (lanes 4 and 5), or elution (lanes 6 and 7) samples. HADHSC did not appear on the blot (data not shown). These results led to the conclusion that annexin III and HADHSC do not contribute to native 35 kDa endoribonuclease activity.

Overall, this evidence strongly supports the notion that APE1 was the candidate protein responsible for the 35 kDa endoribonuclease activity observed throughout the purification of native rat liver extract.

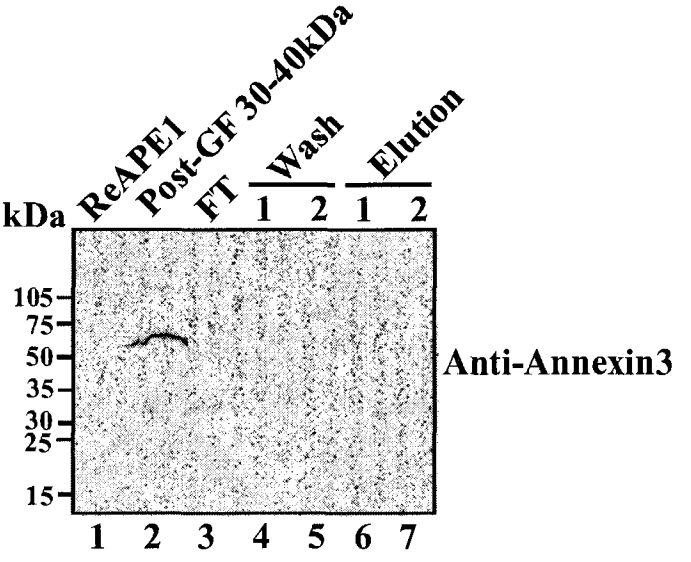

Figure 33: Annexin III is present in post-GF 30-40 kDa sample but does not contribute to endonuclease activity. Lane 1 contains 0.5 μg recombinant APE1 (Sankar's lab, TX). Lane 2 consists of a total volume of 2.0 mL from pooled fractions corresponding to elution volumes 40-50 mL (protein sizes of 30-40 kDa). Lane 3 contains flow through fraction 1. Lanes 4 and 5 contain flow through fractions 2 and 3 (wash). Lanes 6 and 7 contain elution fraction 1 and 2, respectively.

CHAPTER 4

General Discussion

4.1 Introductory Overview-

Multifunctional Mammalian Proteins with Endoribonucleolytic Activity

The role of endoribonucleases in mammalian gene expression has become increasingly evident; in particular, the role of these endoribonucleases in specialized mRNA decay pathways (Dodson and Shapiro 2002; Tourriere *et al.* 2001; Chernokalskaya *et al.* 1998; Hollien and Weissman 2006). However, much is still to be learned about the significance of mammalian endoribonucleases in controlling basal levels of gene expression. Of particular interest is the significance of the discovery that various mammalian proteins exhibit bifunctional or multifunctional capabilities, including endoribonucleolytic function. Often, the known function of a protein family, based largely on primary amino acid sequence, has not provided an adequate predictive measure of endonucleolytic function. Ras-GTPase activating protein SH3 domain binding protein (G3BP), Polysomal Ribonuclease 1 (PMR 1), Inositol-Requiring Enzyme 1 (IRE 1), and Argonaute 2 (Ago 2) are but a few of the clear examples of endoribonucleases where such phenomena are observed.

Recent studies would suggest that multifunctional mammalian proteins that exhibit endoribonucleolytic properties are of paramount importance for cell growth and differentiation (Bisbal *et al.* 2000). This is most clearly shown in current studies that have established a link between external stimuli and direct alteration of mRNA transcript

stability; most notably, the signal transduction pathways and hormonal based regulatory pathways.

Hormonal regulation of mRNA transcripts represents an example of a well-documented mechanism in which the availability of the target cleavage site is determined through *trans*-acting RNA-binding proteins. The effects of estrogen on vitelloginen and albumin mRNA stabilities in *Xenopus laevis* is one of the most extensively studied examples (Blume and Shapiro 1989; Chernokalskaya *et al.* 1998). Hormonal-based regulation of mammalian endoribonucleases has also been observed in the family of RNase A proteins. Studies designed to assess the extracellular distribution of this family of endoribonuclease proteins, performed in rat vaginal and uterine epithelial tissues, suggests that highly elevated levels of estradiol may alter the interaction between pancreatic type RNases and the inhibitory RNase proteins; however, the precise mechanism underlying the alteration is not yet known (Brockdorff and Knowler 1986; Schauer *et al.* 1991; Rao *et al.* 1994).

Structural activation or suppression of proteins with endoribonuclease activity represents an alternate means for controlling their catalytic activity. Prime examples include RNase L and G3BP. It has been proposed that G3BP is targeted to the nucleus through phosphorylation of a serine 149 residue within an N-terminal fragment 2 (NTF-2) like domain which functions as a signal for nuclear import and integration of G3BP into mRNP complexes with the eventual role of degrading *c-myc* mRNA via endonucleolytic cleavage (Tourriere *et al.* 2001). In fact, *c-myc* mRNA decay is delayed in RasGap-deficient mouse fibroblasts that lack the serine 149 phosphorylation site required for nuclear import, providing further support for this hypothesis (Tourriere *et al.*

2001). As such, it is quite plausible that a growth factor-induced change in mRNA decay may be modulated by the nuclear localization of a site-specific endoribonuclease such as G3BP (Irvine *et al.* 2004). The notion that a signal transduction mechanism is required for the activation of G3BPs endonucleolytic function is also supported by its localization in stress granules. Stress granule formation and the induction of heat-shock proteins and various stress-induced transcription factors upon exposure to UV light, elevated temperature and in the presence of oxidative reagents is a well documented pathway; however, the list of players involved in this response is incomplete (Tourriere *et al.* 2003, Tourriere *et al.* 2005). It is entirely possible that G3BP may function in controlling the fate of mRNAs during these cellular stress events. Further evidence of G3BP's role in vertebrate development has been generated through study of G3BP knockout mice. Absence of G3BP in mice during embryonic development has been shown to retard fetal growth and result in neuronal cell death (Zekri *et al.* 2005). Such findings lend support to the possibility that the endoribonucleolytic activity possessed by G3BP *in vitro* may play a significant role in posttranscriptional regulation of selected mRNAs in response to changing growth conditions and extracellular stimuli.

As a testament to the diversity of endoribonuclease proteins, Canete-Soler and colleagues (2005) found that the aldolase A and C isozymes have a possible function as endoribonucleases within specific mRNP complexes, with an ability to cleave the NF transcript at UG sites. These studies suggest that a neuronal-specific mechanism, in response to an extracellular stimulus, functions to activate the endoribonucleolytic activity of aldolases A and C thus promoting cleavage of the NF-L mRNA transcript (Canete-Soler *et al.* 2005). This model of mRNA regulation is similar to the

aforementioned hormonal-type regulation of mRNA transcripts whereby access to the transcript is controlled by competing levels of endoribonuclease and the binding protein(s) that associate with select locations on the mRNA transcript. The neuronal-expressed glycolytic enzymes aldolase A and aldolase C have also been shown to bind the light neurofilament (NF-L) *in vitro* and *in vivo* (Canete-Soler *et al.* 2005). Additionally, they have been shown to compete with poly (A)-binding protein (PABP) within NF mRNPs *in vivo* (Canete-Soler *et al.* 2005). The aldolase A and C isozymes were initially discovered and characterized as proteins functioning in glycolytic, gluconeogenic, and fructose metabolic pathways. Interestingly, cells coexpressing aldolases A and C have heterotetramers that bind to the NF-L mRNA and function differently than the homotetramers present in cells that express one distinctive form of the isozyme (Canete-Soler *et al.* 2005). Consequently, they have hypothesized that the differential expression may represent a mechanism that utilizes structural variation in the A and C isozymes to control gene expression in subsets of neurons, possibly in response to varying environmental stimuli.

Given the wide-ranging implications of *c-myc* overexpression in carcinogenesis (Ioannidis *et al.* 2004), the link between signal transduction pathways/ endoribonuclease activation, and the numerous mammalian proteins that exhibit multiple functions including endoribonucleolytic activity, elucidating the identity of the native mammalian endoribonuclease(s) is of prime importance. In addition, it will provide insight into the mechanisms, players and pathways involved in mammalian mRNA decay.

Aims of this Investigation

There were three aims of this investigation. The first aim was to re-purify the native enzyme(s) and the associated proteins from juvenile rat liver tissue that co-purified with endoribonucleolytic activity against *c-myc* CRD RNA. The second aim of this research was to confirm the identity of the protein(s) responsible for endoribonucleolytic activity against the CRD of *c-myc* mRNA and to immunodeplete native endonuclease activity using appropriate antibodies against the candidate endoribonuclease. The third aim of this research was to characterize recombinant form(s) of the native candidate for endonucleolytic activity.

4.2 Purification and Identification of Candidate Endoribonucleases with LC/MS/Mass Spectrometry Analysis

The primary objective of the first portion of this investigation was to re-purify and identify candidate proteins responsible for native endoribonuclease activity against *c-myc* CRD RNA. Results from the final column chromatography purification step (gel filtration) revealed two distinct endonuclease activities. The larger activity corresponded to a protein of 35 kDa, the smaller activity corresponded to a protein of 17 kDa (refer to section 2.2.1). Two sets of samples, post heparin-sepharose purified and gel filtration purified were sent for LC/MS/Mass Spectrometry analysis. Mass spectrometry results revealed several candidate proteins around 35 kDa and one candidate protein at 17 kDa (refer to section 2.2.1). The 35 kDa protein candidates investigated were HADHSC, annexin III, and APE1. The rationale for investigating these candidate proteins was their known or predicted ability to bind or interact with RNA. HADHSC contains a Rossmann fold motif known to facilitate binding of nucleotides, including RNA (Arnez and

Cavarelli 1997). The annexin family of proteins, namely annexin A2 as been shown to bind several RNA substrates, including human *c-myc* RNA (Filipenko *et al.* 2004). APE1 has multiple documented DNA-specific functionalities including both single-stranded (Marenstein *et al.* 2004) and double-stranded DNA-specific endonulease activity. In addition, APE1 has been shown to bind RNA and to function by cleaving the RNA strand of RNA/DNA duplexes in a manner analogous to RNase H (Barzilay *et al.* 1995). To our knowledge, none of the aforementioned proteins had been shown to possess endoribonucleolytic activity, so the possibility of uncovering a new function for one of these proteins was very exciting. In addition, it was determined that the likely 17 kDa protein responsible for endoribonuclease acitivty was rat pancreatic RNase A (RNase 1).

4.3 Confirming LC/MS/Mass Spectrometry Results and Characterizing Native 35 kDa and 17 kDa Endoribonucleases

The primary objective of this section of the investigation was to test and confirm the identity of native 35 kDa and 17 kDa endoribonucleases. This was accomplished through a variety of Western blot and enzyme characterization experiments. It was determined that HADHSC, annexin III, APE1 and rat pancreatic RNase A (RNase1) were present in native extract (refer to section 3.2.1-3.2.3); however, at this point in the investigation it was not yet known which of these proteins contributed to native 35 kDa endonuclease activity. 17 kDa endonuclease activity was concluded to be the result of rat pancreatic RNase1 as gel filtration data and Western blot data exhibited a high degree of correlation (refer to sections 3.2.1 and 3.2.2). Unexpectedly, anti-RNase 1 Western blots of post-gel filtration purified native sample (30-40 kDa protein sizes) identified a protein

band at approximately 37 kDa. Consequently, further tests were needed to conclusively identify the protein(s) responsible for the native 35 kDa endoribonuclease activity.

To rule out the possibility that the native 35 kDa endonuclease activity was a result of a structural variant of an RNase1-like protein, native post heparin-sepharose and post-gel filtration (protein sizes 30-40 kDa) was treated (in separate experiments) with N-glycosidase F and DTT (Figure 22 and Figure 23, respectively). It was determined that the native endonuclease activity corresponding to a molecular weight of 35 kDa was likely due to a monomeric protein which does not possess N-linked glycosylated residues.

4.3.1 Testing Recombinant Proteins for Endoribonucleolytic Activity

To determine if HADHSC, annexin III, APE1 or a combination thereof were responsible for the native 35 kDa endoribonuclease activity, recombinant forms of these proteins were obtained and tested using standard endoribonuclease assays (refer to section 3.2.4). Results showed that HADHSC and annexin III did not possess endonuclease activity under the conditions utilized. In contrast, recombinant APE1 did exhibit weak endoribonucleolytic activity. The endoribonuclease activity was similar but not identical to the native 35 kDa activity as recombinant APE1 cleaves *c-myc* CRD RNA at one predominant dinucleotide; UA 1751 (Figure 27). By comparison, the native 35 kDa endoribonuclease cleaved *c-myc* CRD RNA at more locations, yet this enzyme exhibited a strong preference for the same UA dinucleotide 1751 (Figure 26-A and 26-B). While the observed pattern of endonucleolytic cleavage from the comparison of the native 35 kDa endoribonuclease and recombinant APE1 RNA was not identical, both exhibit a strong preference for UA dinucleotide 1751.

4.4 Electromobility Shift Assays

Previous studies have in fact shown that APE1 can bind both single- and double-stranded DNA (Mol *et al.* 2000) as well as single-stranded RNA (Barzilay *et al.* 1995). Results confirm that both HADHSC and APE1 bind to *c-myc* CRD RNA contruct (nts 1705-1886). Both APE1 and HADHSC exhibit two binding complexes, respectively, however, at similar protein concentrations it appears as though APE1 binds *c-myc* CRD RNA (nts 1705-1886) more tightly than HADHSC (refer to section 3.2.5).

To our knowledge, there are no previous studies that demonstrate HADHSC ability to bind single-stranded RNA. The presence of an RNA binding motif (Rossmann fold) within the predicted structure of HADHSC, and the multiple documented DNA-/RNA-APE1 interactions led us to perform EMSA experiments to determine if these proteins could bind *c-myc* CRD RNA. In support of the dehydrogenase family of metabolic enzymes with RNA-binding capabilities, GAPDH, another known dehydrogenase contains a predicted Rossmann fold motif. Subsequent studies have revealed that the Rossmann fold of GAPDH provides the molecular basis for RNA recognition (Nagy *et al.* 2000). GAPDH has also been shown to bind single-stranded DNA containing a TAAAT motif. In fact, several dehydrogenase enzymes from multiple domains of life have been shown to possess RNA- and DNA-binding capabilities (Ciesla 2006; Evguenieva-Hackenberg *et al.* 2002). In light of this it would be of interest to test HADHSC's ability to bind both double- and single-stranded DNA. It should be noted that although HADHSC can bind *c-myc* mRNA, it does not appear to affect *c-myc* mRNA in cells. Studies in our lab (Sellers and Lee, unpublished results) have shown that knocking down HADHSC in MCF-7 cells had no effect on levels of *c-myc* mRNA.

4.5 Immunodepletion of Endonuclease Activity in Native Rat Liver Extract

Results of this investigation indicated that APE1 was the protein responsible for 35 kDa endoribonucleolytic activity. To confirm previous data, an immunodepletion experiment was performed using anti-APE1 monoclonal antibodies. Western blot data (Figure 32) indicated that APE1 is indeed present in post-gel filtration elution fractions (30-40 kDa protein sizes) correlating with endoribonuclease activity. Flow-through and wash fractions contained little endonuclease activity (Figure 31-A); however, elution fractions contained activity similar in intensity to pre-load sample (Figure 31-A). Similarly, Western blot analysis of this immunodepletion experiment confirmed that APE1 was present in pooled gel filtration (30-40 kDa protein sizes) pre-load sample (Figure 32), APE1 was absent in flow through and wash fractions and APE1 reappeared in elution fractions (Figure 32).

Comparison of *c-myc* CRD RNA cleavage sites by the native 35 kDa endoribonuclease in immunodepletion pre-load (gel filtration sample, 30-40 kDa) and immunodepletion elution samples (refer to Figure 31-A), reveals an identical pattern; both exhibiting the characteristic preference for dinucleotide UA 1751. This is significant in two respects. Firstly, successful immunodepletion of native gel filtration (30-40 kDa) sample using APE1 monoclonal antibodies confirms that APE1 is likely responsible for native 35 kDa endoribonuclease activity. It should be mentioned that there are differences in the cleavage sites produced by native APE1 and recombinant APE1 against *c-myc* CRD RNA. Previous studies have shown that RNA cleavage specificities are often altered slightly when comparing recombinant and native endoribonucleases. For example, recombinant PMR1 has been shown to cleave a

substrate RNA transcript at identical sites to native PMR1, however, several sites of the RNA transcript that are cleaved by native PMR1 are not cleaved by recombinant PMR1 (Chernokalskaya *et al.* 1998). Chernokalskaya and colleagues (1998) speculate that a specific protein fold achieved by native PMR1, but not by recombinant PMR1, accounts for the observed differences in RNA cleavage (Chernokalskaya *et al.* 1998). Similarly, a specific folding conformation may need to be adopted by native APE1 to achieve the entire set of observed cleavage products against *c-myc* CRD RNA.

Secondly, it confirms that APE1 protein alone generates the observed cleavage pattern of cleavage against *c-myc* CRD RNA. The finding that APE1 is singularly responsible for endonuclease acitivity is important because HADHSC, which was shown to bind *c-myc* CRD RNA, is present in post-gel filtration (30-40 kDa). Binding of HADHSC to *c-myc* RNA during standard endoribonuclease assays may have altered the structure of *c-myc* RNA. Consequently, this may have limited or altered the accessibility of target cleavage sites along *c-myc* RNA. However, this hypothesis is not supported by evidence from endoribonuclease assays of immunodepletion experiments.

Monoclonal anti-APE1 antibodies were used in constructing the immunodepletion spin column, thus the only protein that would have bound to the anti-APE1 antibodies (cross-linked to the column matrix) would have been APE1. Consequently, the cleavage pattern exhibited in spin column elution fractions would result from native APE1. Since the cleavage pattern against *c-myc* CRD RNA in the elution fractions is identical to the cleavage pattern in native pre-load sample from gel filtration elution fractions (protein sizes 30-40 kDa) (see Figure 32) and the fact that HADHSC is not present in the eluted fractions (as determined by Western blot), APE1 alone must be responsible.

4.6 Apurinic/Apyrimidinic Endonuclease-APE1

Human Apurinic/Apyrimidinic Endonuclease (APE1) also named (APEX, HAP-1, Ref-1) is a multifunctional protein homologue of *E. coli* Exonuclease III. It has been characterized as having three principle functions *in vivo*; however, several other properties have been discovered such as 3'-5' exonuclease (Chou *et al.* 2000), phosphodiesterase activity (Izumi *et al.* 2002), and RNase H activity (Barzilay *et al.* 1995).

The first principle function *in vivo* is in repair of abasic sites in single-stranded breaks of DNA. APE1 recognizes damaged DNA and utilizes a hydrolytic Mg^{2+}-stimulated mechanism to execute phosphodiester backbone cleavage 5' to the lesion (Beernink *et al.* 2001; Mol *et al.* 2000). This generates a free 3'-OH terminus which is suitable for priming DNA polymerases (Friedberg *et al.* 1995).

The second function of APE1 has been identified as a redox activator of DNA-binding activity (Xanthoudakis *et al.* 1992). *In vitro* studies have confirmed that APE1 converts the oxidized form (inactive state) of c-Jun into a reduced, active form, which can then bind DNA (Xanthoudakis *et al.* 1994). Recently, APE1 has been shown to function in mediating the activation of additional transcription factors including Pax 5, Pax 8 (Evans *et al.* 2000). In addition, APE1 has been shown to activate the tumor suppressor p53 by redox and non-redox mechanisms, thereby facilitating p53 nuclear translocation and DNA binding (Jayaraman *et al.* 1997).

The third and somewhat distinct function of APE1 is in Ca^{2+} dependent downregulation (repression) of parathyroid hormone (PTH) gene via binding to negative calcium response elements (nCaREs) within the PTH gene promoter (Okazaki *et al.*

1992; Okazaki *et al.* 1994). Experiments have shown that APE1 is a part of nuclear protein complex that binds to nCaRE-A and nCaRE-B (Okazaki *et al.* 1994).

APE1 has been shown to play yet another major role in mammalian cells. APE1 has been identified as a component of a 270-420 kDa endoplasmic reticulum-associated complex, termed SET complex (Fan *et al.* 2002; Fan *et al.* 2003; Lieberman and Fan 2003). SET complex is a target in caspase-independent cell death mediated by the cytotoxic T-lymphocyte protease granzyme-A (Lieberman and Fan 2003). Granzyme-A cleaves Ape1 at a Lys31 residue, thereby destroying its known oxidative repair functions (Fan *et al.* 2003). It is believed by doing so, granzyme-A blocks cellular repair mediated by APE1 and forces apoptosis. In support of this finding, cells with RNAi-induced APE1 knockdown are more sensitive to granzyme-A-induced death, whereas cells overexpressing a mutant non-cleavable form of APE1 are more resistant to granzyme-A-mediated death (Fan *et al.* 2003).

It is hypothesized that APE1 possesses a single catalytic active site for DNA- and RNA-specific nuclease activities (Beernink *et al.* 2001). The active site of the Ape1 contains one Mg^{2+} metal ion which is coordinated predominantly by acidic residues Asp70 and Glu96 (Beernink *et al.* 2001). The coordination of a single Mg^{2+} metal ion is required for efficient phosphodiester bond hydrolysis (Beernink *et al.* 2001). However, structural data shows that Ape1 can bind two Mg^{2+} metal ions in its active site at neutral pH but only one at acidic pH (Beernink *et al.* 2001). This phenomenon at neutral pH may indicate an additional two-metal catalytic functionality.

4.7 Concluding Remarks

This study provides the first documented evidence that APE1 possesses the abililty to hydrolyze a specific site of single-stranded RNA. Furthermore, other DNA specific endonucleases, most notably the structure-specific human Flap Endonuclease 1 (Fen1) which functions as a DNA-specific endonuclease required for cleavage of unannealed 5' arms of template-primer DNA substrates, a processor of Okazaki fragments during DNA synthesis, and a key player in DNA replication and DNA repair, has been shown to hydrolyze several single-stranded RNA substrates (Stevens 1998). Thus there is precedent to suspect that a DNA-specific endonuclease such as APE1 has the ability to hydrolyze single-stranded RNA substrates. Support for this type of dual functionality has been shown. Spinach CSP41 protein functions both as an mRNA-binding protein and cellular ribonuclease (Yang *et al.* 1996). Mammalian GAPDH (isolated from rabbit muscle) has also been shown to bind and cleave RNA (Evguenieva-Hackenberg *et al.* 2002). Interestingly, mammalian GAPDH was found to be sensitive to the ribonuclease inhibitor protein (RNasin) and was found to preferentially cleave between UA and CA dinucleotides, in a manner analogous to RNase A (Evguenieva-Hackenberg *et al.* 2002).

The question remains; however, of what significance, if any, is the finding that a DNA repair enzyme possesses the ability to cleave *c-myc* CRD RNA? Could APE1/RNA interactions result from 'relic' interactions of a primitive 'RNA world' prior to the existence of DNA? Under this scenario, DNA-specific activities may have been acquired as organisms evolved and developed DNA for the storage of genetic materials. Evidence would suggest that multifunctional proteins would be more efficient for

building complex gene regulatory mechanisms in mammalian cells possessing relatively low numbers of protein-encoding genes (Venter *et al.* 2001; Evguenieva-Hackenberg *et al.* 2002).

The preference of APE1 for the dinucleotide 1751 UA may have some *in vivo* significance. AU-rich elements at 3' untranslated regions are well-characterized instability elements. Given the strong cleavage preference of native and recombinant APE1 for dinucleotide UA, it is tempting to speculate that it may function *in vivo* as a cellular endoribonuclease to destabilize particular mRNAs. Consequently, *in vivo* studies, aimed at manipulating cellular expresion of APE1 while monitoring the corresponding changes in levels of specific mRNAs including *c-myc*, is certainly warranted.

Arguably less exciting is the finding that one of the mammalian endoribonucleases purified from rat liver, with the ability to degrade *c-myc* CRD RNA, is a member of the well-studied RNase A superfamily of proteins. Often overlooked, however, is the possible role of this family of proteins in controlling gene expression. Given the known structural capabilities of the RNase A superfamily of proteins such as the formation of higher order structures, one must consider the plausible functional implications of dimeric, trimeric or higher order associations within RNA metabolic processes. Equally intriguing is the discovery of RISBASES (RNases with Special Biological Actions) which have been implicated in tumor cell growth, neurological development, and biological differentiation and the discovery of potential therapeutic cytotoxicity of certain members of the RNase A superfamily such as onconase and Bovine Seminal RNase (BS-RNase). Unfortunately, the physiological role, particularly

the role of RNase A-type endoribonucleases in mammalian RNA decay pathways (if any) remains unclear. Further investigation of this superfamily of enzymes as related to their role in mRNA metabolism, is warranted. With regards to the RNase A superfamily of enzymes, one particular question clearly remain unanswered; Are there any members of the intercellular RNase A family of proteins that perform a physiological function in normal mRNA metabolism?

As more information becomes available about the mechanisms that control the interaction between all endoribonuclease proteins, RNase inhibitory proteins, the elements that are required for activation of endonuclease-mediated pathways, and the RNA-binding proteins that protect RNA from endonucleolytic cleavage, we may uncover new structural features inherent in known and yet-to-be discovered families of endoribonuclease proteins.

Future studies aimed at identifying the significance of multifunctional mammalian proteins with endoribonucleolytic activity should be a priority. In fact, the importance of other known mammalian proteins with endoribonucleolytic function for correct organism development has already been well established. For example, the ER stress response also participates in development of vertebrates. It contributes not only to the expression of ER proteins but of many genes that contribute to the phenotypic changes that characterize secretory cells, such as expansion of the ER and induction of chaperones (Reimold *et al.* 2001). Zhang and colleagues (2005) utilized a gene inactivation approach to show that IRE 1 is required for the development of plasma cells. Given that IRE 1 lies upstream of XBP1, it is hypothesized that the developmental role of XBP1 is coupled to an ER-signaling event which is regulated by the endoribonucleolytic activity of IRE 1. The

CHAPTER 4- GENERAL DISCUSSION

RNase L-mediated endoribonucleolytic activity in response to 2-5A activation, has been shown to influence muscle cell differentiation by lowering murine MyoD mRNA levels (Bisbal *et al.* 2000). In effect, Bisbal and colleagues (2000) demonstrated that RNase L functions to delay the onset of C2 mouse myoblast differentiation via regulation of MyoD mRNA stability. Mutations in the gene encoding RNase L have been recently implicated in the pathogenesis of prostate cancer (Silverman, 2003). In addition, RNase L is hypothesized to function in a role as tumor suppressor suggesting that mutations in the RNase L gene would prevent the necessary RNA cleavage responsible for the antiproliferative and apoptotic activities of the RNase L protein (Silverman 2003).

The value of studying mammalian proteins that possess endoribonucleolytic function including domain identification, key catalytic residue identification and functional interactions required for ribonucleolytic activation, is clear. We can now utilize new and more robust bioinformatic tools to identify new proteins, protein families and to a lesser extent the secondary and tertiary structures required for their respective endoribonucleolytic activities. Additional research into the physiological significance of these proteins is absolutely necessary as it will facilitate our understanding of the mechanisms by which endoribonucleases are differentially and site-specifically activated in RNA processing pathways.

References

Arnez, J.G. and Cavarelli, J. (1997) Structures of RNA-binding proteins. *Q Rev Biophys*, **30**, 195-240.

Arnold, U., Schierhorn, A. and Ulbrich-hofmann, R. (1999) Modification of the unfolding region in bovine pancreatic ribonuclease and its influence on the thermal stability and proteolytic fragmentation. *Eur J Biochem*, **259**, 470-475.

Atchley, W.R. and Fernandes, A.D. (2005) Sequence signatures and the probabilistic identification of proteins in the Myc-Max-Mad network. *Proc Natl Acad Sci U S A*, **102**, 6401-6406.

Baker, K.E. and Condon, C. (2004) Under the Tucson sun: a meeting in the desert on mRNA decay. *Rna*, **10**, 1680-1691.

Barker, R.L., Loegering, D.A., Ten, R.M., Hamann, K.J., Pease, L.R. and Gleich, G.J. (1989) Eosinophil cationic protein cDNA. Comparison with other toxic cationic proteins and ribonucleases. *J Immunol*, **143**, 952-955.

Barnard, E.A. (1969) Biological function of pancreatic ribonuclease. *Nature*, **221**, 340-344.

Barnes, C.J., Li, F., Mandal, M., Yang, Z., Sahin, A.A. and Kumar, R. (2002) Heregulin induces expression, ATPase activity, and nuclear localization of G3BP, a Ras signaling component, in human breast tumors. *Cancer Res*, **62**, 1251-1255.

Barrabes, S., Pages-Pons, L., Radcliffe, C.M., Tabares, G., Fort, E., Royle, L., Harvey, D.J., Moenner, M., Dwek, R.A., Rudd, P.M., De Llorens, R. and Peracaula, R. (2007) Glycosylation of serum ribonuclease 1 indicates a major endothelial origin and reveals an increase in core fucosylation in pancreatic cancer. *Glycobiology*, **17**, 388-400.

Barzilay, G. and Hickson, I.D. (1995) Structure and function of apurinic/apyrimidinic endonucleases. *Bioessays*, **17**, 713-719.

Bashkirov, V.I., Scherthan, H., Solinger, J.A., Buerstedde, J.M. and Heyer, W.D. (1997) A mouse cytoplasmic exoribonuclease (mXRN1p) with preference for G4 tetraplex substrates. *J Cell Biol*, **136**, 761-773.

Beernink, P.T., Segelke, B.W., Hadi, M.Z., Erzberger, J.P., Wilson, D.M., 3rd and Rupp, B. (2001) Two divalent metal ions in the active site of a new crystal form of human apurinic/apyrimidinic endonuclease, Ape1: implications for the catalytic mechanism. *J Mol Biol*, **307**, 1023-1034.

Beintema, J.J., Blank, A., Schieven, G.L., Dekker, C.A., Sorrentino, S. and Libonati, M. (1988) Differences in glycosylation pattern of human secretory ribonucleases. *Biochem J*, **255**, 501-505.

Benner, S.A. and Allemann, R.K. (1989) The return of pancreatic ribonucleases. *Trends Biochem Sci*, **14**, 396-397.

Bergstrom, K., Urquhart, J.C., Tafech, A., Doyle, E. and Lee, C.H. (2006) Purification and characterization of a novel mammalian endoribonuclease. *J Cell Biochem*, **98**, 519-537.

Bernstein, E., Caudy, A.A., Hammond, S.M. and Hannon, G.J. (2001) Role for a bidentate ribonuclease in the initiation step of RNA interference. *Nature*, **409**, 363-366.

Bernstein, P.L., Herrick, D.J., Prokipcak, R.D. and Ross, J. (1992) Control of c-myc mRNA half-life in vitro by a protein capable of binding to a coding region stability determinant. *Genes Dev*, **6**, 642-654.

Binder, R., Hwang, S.P., Ratnasabapathy, R. and Williams, D.L. (1989) Degradation of apolipoprotein II mRNA occurs via endonucleolytic cleavage at 5'-AAU-3'/5'-UAA-3' elements in single-stranded loop domains of the 3'-noncoding region. *J Biol Chem*, **264**, 16910-16918.

Bisbal, C., Silhol, M., Laubenthal, K., Kaluza, T., Carnac, G., Milligan, L., Le Roy, F. and Salehzada, T. (2000) The 2 '-5 ' oligoadenylate/RNase L/RNase L inhibitor pathway regulates both MyoD mRNA stability and muscle cell differentiation. *Molecular and Cellular Biology*, **20**, 4959-4969.

Blume, J.E. and Shapiro, D.J. (1989) Ribosome loading, but not protein synthesis, is required for estrogen stabilization of Xenopus laevis vitellogenin mRNA. *Nucleic Acids Res*, **17**, 9003-9014.

Bonnerot, C., Boeck, R. and Lapeyre, B. (2000) The two proteins Pat1p (Mrt1p) and Spb8p interact in vivo, are required for mRNA decay, and are functionally linked to Pab1p. *Mol Cell Biol*, **20**, 5939-5946.

Bonnieu, A., Piechaczyk, M., Marty, L., Cuny, M., Blanchard, J.M., Fort, P. and Jeanteur, P. (1988) Sequence determinants of c-myc mRNA turn-over: influence of 3' and 5' non-coding regions. *Oncogene Res*, **3**, 155-166.

Brawerman, G. (1987) Determinants of messenger RNA stability. *Cell*, **48**, 5-6.

Bremer, K.A., Stevens, A. and Schoenberg, D.R. (2003) An endonuclease activity similar to Xenopus PMR1 catalyzes the degradation of normal and nonsense-containing human beta-globin mRNA in erythroid cells. *Rna*, **9**, 1157-1167.

Brewer, G. (1999) Evidence for a 3'-5' decay pathway for c-myc mRNA in mammalian cells. *J Biol Chem*, **274**, 16174-16179.

Brewer, G. (2002) Messenger RNA decay during aging and development. *Ageing Res Rev*, **1**, 607-625.

Brockdorff, N.A. and Knowler, J.T. (1986) Oestrogen-induced changes in the relative concentrations of ribonuclease and ribonuclease inhibitor in rat uterus. *Mol Cell Endocrinol*, **44**, 117-124.

Brown, B.D. and Harland, R.M. (1990) Endonucleolytic cleavage of a maternal homeo box mRNA in Xenopus oocytes. *Genes Dev*, **4**, 1925-1935.

Brown, B.D., Zipkin, I.D. and Harland, R.M. (1993) Sequence-specific endonucleolytic cleavage and protection of mRNA in Xenopus and Drosophila. *Genes Dev*, **7**, 1620-1631.

Cairo, G. and Pietrangelo, A. (1994) Transferrin receptor gene expression during rat liver regeneration. Evidence for post-transcriptional regulation by iron regulatory factorB, a second iron-responsive element-binding protein. *J Biol Chem*, **269**, 6405-6409.

Canete-Soler, R., Reddy, K.S., Tolan, D.R. and Zhai, J.B. (2005) Aldolases A and C are ribonucleolytic components of a neuronal complex that regulates the stability of the light-neurofilament mRNA. *Journal of Neuroscience*, **25**, 4353-4364.

Chang, A.C., Sohlberg, B., Trinkle-Mulcahy, L., Claverie-Martin, F., Cohen, P. and Cohen, S.N. (1999) Alternative splicing regulates the production of ARD-1 endoribonuclease and NIPP-1, an inhibitor of protein phosphatase-1, as isoforms encoded by the same gene. *Gene*, **240**, 45-55.

Chang, K.Y. and Ramos, A. (2005) The double-stranded RNA-binding motif, a versatile macromolecular docking platform. *Febs J*, **272**, 2109-2117.

Chen, Y. and Varani, G. (2005) Protein families and RNA recognition. *Febs J*, **272**, 2088-2097.

Chernokalskaya, E., Dompenciel, R. and Schoenberg, D.R. (1997) Cleavage properties of an estrogen-regulated polysomal ribonuclease involved in the destabilization of albumin mRNA. *Nucleic Acids Res*, **25**, 735-742.

Chernokalskaya, E., Dubell, A.N., Cunningham, K.S., Hanson, M.N., Dompenciel, R.E. and Schoenberg, D.R. (1998) A polysomal ribonuclease involved in the destabilization of albumin mRNA is a novel member of the peroxidase gene family. *Rna-a Publication of the Rna Society*, **4**, 1537-1548.

Chou, K.M., Kukhanova, M. and Cheng, Y.C. (2000) A novel action of human apurinic/apyrimidinic endonuclease: excision of L-configuration deoxyribonucleoside analogs from the 3' termini of DNA. *J Biol Chem*, **275**, 31009-31015.

Ciesla, J. (2006) Metabolic enzymes that bind RNA: yet another level of cellular regulatory network? *Acta Biochim Pol*, **53**, 11-32.

Claverie-Martin, F., Wang, M. and Cohen, S.N. (1997) ARD-1 cDNA from human cells encodes a site-specific single-strand endoribonuclease that functionally resembles Escherichia coli RNase E. *J Biol Chem*, **272**, 13823-13828.

Coburn, G.A. and Mackie, G.A. (1999) Degradation of mRNA in Escherichia coli: an old problem with some new twists. *Prog Nucleic Acid Res Mol Biol*, **62**, 55-108.

Cole, J.L., Carroll, S.S., Blue, E.S., Viscount, T. and Kuo, L.C. (1997) Activation of RNase L by 2',5'-oligoadenylates. Biophysical characterization. *J Biol Chem*, **272**, 19187-19192.

Coller, J.M., Tucker, M., Sheth, U., Valencia-Sanchez, M.A. and Parker, R. (2001) The DEAD box helicase, Dhh1p, functions in mRNA decapping and interacts with both the decapping and deadenylase complexes. *Rna*, **7**, 1717-1727.

Coulis, C.M., Lee, C., Nardone, V. and Prokipcak, R.D. (2000) Inhibition of c-myc expression in cells by targeting an RNA-protein interaction using antisense oligonucleotides. *Mol Pharmacol*, **57**, 485-494.

Cunningham, K.S., Dodson, R.E., Nagel, M.A., Shapiro, D.J. and Schoenberg, D.R. (2000) Vigilin binding selectively inhibits cleavage of the vitellogenin mRNA 3'-untranslated region by the mRNA endonuclease polysomal ribonuclease 1. *Proc Natl Acad Sci U S A*, **97**, 12498-12502.

Cunningham, K.S., Hanson, M.N. and Schoenberg, D.R. (2001) Polysomal ribonuclease 1 exists in a latent form on polysomes prior to estrogen activation of mRNA decay. *Nucleic Acids Res*, **29**, 1156-1162.

Czaja, R., Struhalla, M., Hoschler, K., Saenger, W., Strater, N. and Hahn, U. (2004) RNase T1 variant RV cleaves single-stranded RNA after purines due to specific recognition by the Asn46 side chain amide. *Biochemistry*, **43**, 2854-2862.

Demple, B. and Harrison, L. (1994) Repair of oxidative damage to DNA: enzymology and biology. *Annu Rev Biochem*, **63**, 915-948.

Deo, R.C., Bonanno, J.B., Sonenberg, N. and Burley, S.K. (1999) Recognition of polyadenylate RNA by the poly(A)-binding protein. *Cell*, **98**, 835-845.

Deutscher, M.P. (2003) Degradation of stable RNA in bacteria. *J Biol Chem*, **278**, 45041-45044.

Di Donato, A., Cafaro, V., de Nigris, M., Rizzo, M. and D'Alessio, G. (1993) The determinants of the dimeric structure of seminal ribonuclease are located in its N-terminal region. *Biochem Biophys Res Commun*, **194**, 1440-1445.

Dodson, R.E. and Shapiro, D.J. (2002) Regulation of pathways of mRNA destabilization and stabilization. *Prog Nucleic Acid Res Mol Biol*, **72**, 129-164.

Doi, N., Zenno, S., Ueda, R., Ohki-Hamazaki, H., Ui-Tei, K. and Saigo, K. (2003) Short-interfering-RNA-mediated gene silencing in mammalian cells requires Dicer and eIF2C translation initiation factors. *Curr Biol*, **13**, 41-46.

Domachowske, J.B., Bonville, C.A., Dyer, K.D. and Rosenberg, H.F. (1998a) Evolution of antiviral activity in the ribonuclease A gene superfamily: evidence for a specific interaction between eosinophil-derived neurotoxin (EDN/RNase 2) and respiratory syncytial virus. *Nucleic Acids Res*, **26**, 5327-5332.

Domachowske, J.B., Dyer, K.D., Adams, A.G., Leto, T.L. and Rosenberg, H.F. (1998b) Eosinophil cationic protein/RNase 3 is another RNase A-family ribonuclease with direct antiviral activity. *Nucleic Acids Res*, **26**, 3358-3363.

Domachowske, J.B., Dyer, K.D., Bonville, C.A. and Rosenberg, H.F. (1998c) Recombinant human eosinophil-derived neurotoxin/RNase 2 functions as an effective antiviral agent against respiratory syncytial virus. *J Infect Dis*, **177**, 1458-1464.

Dong, B., Niwa, M., Walter, P. and Silverman, R.H. (2001) Basis for regulated RNA cleavage by functional analysis of RNase L and Ire1p. *Rna*, **7**, 361-373.

Dong, B. and Silverman, R.H. (1995) 2-5A-dependent RNase molecules dimerize during activation by 2-5A. *J Biol Chem*, **270**, 4133-4137.

Doyle, G.A., Betz, N.A., Leeds, P.F., Fleisig, A.J., Prokipcak, R.D. and Ross, J. (1998) The c-myc coding region determinant-binding protein: a member of a family of KH domain RNA-binding proteins. *Nucleic Acids Res*, **26**, 5036-5044.

Doyle, G.A., Bourdeau-Heller, J.M., Coulthard, S., Meisner, L.F. and Ross, J. (2000) Amplification in human breast cancer of a gene encoding a c-myc mRNA-binding protein. *Cancer Res*, **60**, 2756-2759.

Evguenieva-Hackenberg, E., Schiltz, E. and Klug, G. (2002) Dehydrogenases from all three domains of life cleave RNA. *J Biol Chem*, **277**, 46145-46150.

Fan, Z., Beresford, P.J., Zhang, D., Xu, Z., Novina, C.D., Yoshida, A., Pommier, Y. and Lieberman, J. (2003) Cleaving the oxidative repair protein Ape1 enhances cell death mediated by granzyme A. *Nat Immunol*, **4**, 145-153.

Felsher, D.W. and Bishop, J.M. (1999) Transient excess of MYC activity can elicit genomic instability and tumorigenesis. *Proc Natl Acad Sci U S A*, **96**, 3940-3944.

Feng, Y. and Cohen, S.N. (2000) Unpaired terminal nucleotides and 5' monophosphorylation govern 3' polyadenylation by Escherichia coli poly(A) polymerase I. *Proc Natl Acad Sci U S A*, **97**, 6415-6420.

Filipenko, N.R., MacLeod, T.J., Yoon, C.S. and Waisman, D.M. (2004) Annexin A2 is a novel RNA-binding protein. *J Biol Chem*, **279**, 8723-8731.

Floyd-Smith, G., Slattery, E. and Lengyel, P. (1981) Interferon action: RNA cleavage pattern of a (2'-5')oligoadenylate--dependent endonuclease. *Science*, **212**, 1030-1032.

Fortin, K.R., Nicholson, R.H. and Nicholson, A.W. (2002) Mouse ribonuclease III. cDNA structure, expression analysis, and chromosomal location. *BMC Genomics*, **3**, 26.

Friedberg, E.C., Bardwell, A.J., Bardwell, L., Feaver, W.J., Kornberg, R.D., Svejstrup, J.Q., Tomkinson, A.E. and Wang, Z. (1995) Nucleotide excision repair in the yeast Saccharomyces cerevisiae: its relationship to specialized mitotic recombination and RNA polymerase II basal transcription. *Philos Trans R Soc Lond B Biol Sci*, **347**, 63-68.

Frischmeyer, P.A., van Hoof, A., O'Donnell, K., Guerrerio, A.L., Parker, R. and Dietz, H.C. (2002) An mRNA surveillance mechanism that eliminates transcripts lacking termination codons. *Science*, **295**, 2258-2261.

Gallouzi, I.E., Parker, F., Chebli, K., Maurier, F., Labourier, E., Barlat, I., Capony, J.P., Tocque, B. and Tazi, J. (1998) A novel phosphorylation-dependent RNase activity of GAP-SH3 binding protein: a potential link between signal transduction and RNA stability. *Mol Cell Biol*, **18**, 3956-3965.

Garneau, N.L., Wilusz, J. and Wilusz, C.J. (2007) The highways and byways of mRNA decay. *Nat Rev Mol Cell Biol*, **8**, 113-126.

Gerlt, J.A. and Gassman, P.G. (1993) Understanding the rates of certain enzyme-catalyzed reactions: proton abstraction from carbon acids, acyl-transfer reactions, and displacement reactions of phosphodiesters. *Biochemistry*, **32**, 11943-11952.

Guhaniyogi, J. and Brewer, G. (2001) Regulation of mRNA stability in mammalian cells. *Gene*, **265**, 11-23.

Guitard, E., Parker, F., Millon, R., Abecassis, J. and Tocque, B. (2001) G3BP is overexpressed in human tumors and promotes S phase entry. *Cancer Lett*, **162**, 213-221.

Hammond, S.M., Boettcher, S., Caudy, A.A., Kobayashi, R. and Hannon, G.J. (2001) Argonaute2, a link between genetic and biochemical analyses of RNAi. *Science*, **293**, 1146-1150.

Hanson, M.N. and Schoenberg, D.R. (2001) Identification of in vivo mRNA decay intermediates corresponding to sites of in vitro cleavage by polysomal ribonuclease 1. *J Biol Chem*, **276**, 12331-12337.

Harrison, A.M., Bonville, C.A., Rosenberg, H.F. and Domachowske, J.B. (1999) Respiratory syncytical virus-induced chemokine expression in the lower airways: eosinophil recruitment and degranulation. *Am J Respir Crit Care Med*, **159**, 1918-1924.

Hermeking, H. (2003) The MYC oncogene as a cancer drug target. *Curr Cancer Drug Targets*, **3**, 163-175.

Herrick, D.J. and Ross, J. (1994) The half-life of c-myc mRNA in growing and serum-stimulated cells: influence of the coding and 3' untranslated regions and role of ribosome translocation. *Mol Cell Biol*, **14**, 2119-2128.

Hoffman, B., Amanullah, A., Shafarenko, M. and Liebermann, D.A. (2002) The proto-oncogene c-myc in hematopoietic development and leukemogenesis. *Oncogene*, **21**, 3414-3421.

Hofsteenge, J., Vicentini, A. and Zelenko, O. (1998) Ribonuclease 4, an evolutionarily highly conserved member of the superfamily. *Cell Mol Life Sci*, **54**, 804-810.

Hollien, J. and Weissman, J.S. (2006) Decay of endoplasmic reticulum-localized mRNAs during the unfolded protein response. *Science*, **313**, 104-107.

Hou, W., Wo, J.E., Li, M.W. and Liu, K.Z. (2005) In vitro cleavage of hepatitis B virus C mRNA by 10-23 DNA enzyme. *Hepatobiliary Pancreat Dis Int*, **4**, 573-576.

Ioannidis, P., Kottaridi, C., Dimitriadis, E., Courtis, N., Mahaira, L., Talieri, M., Giannopoulos, A., Iliadis, K., Papaioannou, D., Nasioulas, G. and Trangas, T. (2004) Expression of the RNA-binding protein CRD-BP in brain and non-small cell lung tumors. *Cancer Lett*, **209**, 245-250.

Ioannidis, P., Mahaira, L.G., Perez, S.A., Gritzapis, A.D., Sotiropoulou, P.A., Kavalakis, G.J., Antsaklis, A.I., Baxevanis, C.N. and Papamichail, M. (2005) CRD-BP/IMP1 expression characterizes cord blood CD34+ stem cells and affects c-myc and IGF-II expression in MCF-7 cancer cells. *J Biol Chem*, **280**, 20086-20093.

Irvine, K., Stirling, R., Hume, D. and Kennedy, D. (2004) Rasputin, more promiscuous than ever: a review of G3BP. *International Journal of Developmental Biology*, **48**, 1065-1077.

Izumi, H., Hara, T., Oga, A., Matsuda, K., Sato, Y., Naito, K. and Sasaki, K. (2002) High telomerase activity correlates with the stabilities of genome and DNA ploidy in renal cell carcinoma. *Neoplasia*, **4**, 103-111.

Jayaraman, L., Murthy, K.G., Zhu, C., Curran, T., Xanthoudakis, S. and Prives, C. (1997) Identification of redox/repair protein Ref-1 as a potent activator of p53. *Genes Dev*, **11**, 558-570.

Jeffery, C.J. (2003) Moonlighting proteins: old proteins learning new tricks. *Trends in Genetics*, **19**, 415-417.

Jing, Q., Huang, S., Guth, S., Zarubin, T., Motoyama, A., Chen, J., Di Padova, F., Lin, S.C., Gram, H. and Han, J. (2005) Involvement of microRNA in AU-rich element-mediated mRNA instability. *Cell*, **120**, 623-634.

Jones, D.J., Ghosh, A.K., Moore, M. and Schofield, P.F. (1987) A critical appraisal of the immunohistochemical detection of the c-myc oncogene product in colorectal cancer. *Br J Cancer*, **56**, 779-783.

Kaufman, R.J. (2002) Orchestrating the unfolded protein response in health and disease. *J Clin Invest*, **110**, 1389-1398.

Kedersha, N., Chen, S., Gilks, N., Li, W., Miller, I.J., Stahl, J. and Anderson, P. (2002) Evidence that ternary complex (eIF2-GTP-tRNA(i)(Met))-deficient preinitiation complexes are core constituents of mammalian stress granules. *Molecular Biology of the Cell*, **13**, 195-210.

Kedersha, N.L., Gupta, M., Li, W., Miller, I. and Anderson, P. (1999) RNA-binding proteins TIA-1 and TIAR link the phosphorylation of eIF-2 alpha to the assembly of mammalian stress granules. *J Cell Biol*, **147**, 1431-1442.

Kennedy, D., French, J., Guitard, E., Ru, K., Tocque, B. and Mattick, J. (2001) Characterization of G3BPs: tissue specific expression, chromosomal localisation and rasGAP(120) binding studies. *J Cell Biochem*, **84**, 173-187.

Khodursky, A.B. and Bernstein, J.A. (2003) Life after transcription--revisiting the fate of messenger RNA. *Trends Genet*, **19**, 113-115.

Kiledjian, M., DeMaria, C.T., Brewer, G. and Novick, K. (1997) Identification of AUF1 (heterogeneous nuclear ribonucleoprotein D) as a component of the alpha-globin mRNA stability complex. *Mol Cell Biol*, **17**, 4870-4876.

Kren, B.T., Trembley, J.H. and Steer, C.J. (1996) Alterations in mRNA stability during rat liver regeneration. *Am J Physiol*, **270**, G763-777.

Kumar, A., Lee, C.M. and Reddy, E.P. (2003) c-Myc is essential but not sufficient for c-Myb-mediated block of granulocytic differentiation. *J Biol Chem*, **278**, 11480-11488.

Langa, F., Lafon, I., Vandormael-Pournin, S., Vidaud, M., Babinet, C. and Morello, D. (2001) Healthy mice with an altered c-myc gene: role of the 3' untranslated region revisited. *Oncogene*, **20**, 4344-4353.

Lee, C.H., Leeds, P. and Ross, J. (1998) Purification and characterization of a polysome-associated endoribonuclease that degrades c-myc mRNA in vitro. *J Biol Chem*, **273**, 25261-25271.

Lee, S.H., Kim, J.W., Lee, H.W., Cho, Y.S., Oh, S.H., Kim, Y.J., Jung, C.H., Zhang, W. and Lee, J.H. (2003) Interferon regulatory factor-1 (IRF-1) is a mediator for interferon-gamma induced attenuation of telomerase activity and human telomerase reverse transcriptase (hTERT) expression. *Oncogene*, **22**, 381-391.

Lemm, I. and Ross, J. (2002) Regulation of c-myc mRNA decay by translational pausing in a coding region instability determinant. *Mol Cell Biol*, **22**, 3959-3969.

Lemmon, M.A. and Schlessinger, J. (1994) Regulation of signal transduction and signal diversity by receptor oligomerization. *Trends Biochem Sci*, **19**, 459-463.

Levens, D.L. (2003) Reconstructing MYC. *Genes Dev*, **17**, 1071-1077.

Levine, T.D., Gao, F., King, P.H., Andrews, L.G. and Keene, J.D. (1993) Hel-N1: an autoimmune RNA-binding protein with specificity for 3' uridylate-rich untranslated regions of growth factor mRNAs. *Mol Cell Biol*, **13**, 3494-3504.

Levy, N.S., Chung, S., Furneaux, H. and Levy, A.P. (1998) Hypoxic stabilization of vascular endothelial growth factor mRNA by the RNA-binding protein HuR. *J Biol Chem*, **273**, 6417-6423.

Li, X.L., Blackford, J.A., Judge, C.S., Liu, M., Xiao, W., Kalvakolanu, D.V. and Hassel, B.A. (2000) RNase-L-dependent destabilization of interferon-induced mRNAs. A role for the 2-5A system in attenuation of the interferon response. *J Biol Chem*, **275**, 8880-8888.

Liao, B., Patel, M., Hu, Y., Charles, S., Herrick, D.J. and Brewer, G. (2004) Targeted knockdown of the RNA-binding protein CRD-BP promotes cell proliferation via an insulin-like growth factor II-dependent pathway in human K562 leukemia cells. *J Biol Chem*, **279**, 48716-48724.

Lieberman, J. and Fan, Z. (2003) Nuclear war: the granzyme A-bomb. *Curr Opin Immunol*, **15**, 553-559.

Liu, C.Y., Xu, Z. and Kaufman, R.J. (2003) Structure and intermolecular interactions of the luminal dimerization domain of human IRE1alpha. *J Biol Chem*, **278**, 17680-17687.

Liu, H., Rodgers, N.D., Jiao, X. and Kiledjian, M. (2002) The scavenger mRNA decapping enzyme DcpS is a member of the HIT family of pyrophosphatases. *Embo J*, **21**, 4699-4708.

Liu, J., Carmell, M.A., Rivas, F.V., Marsden, C.G., Thomson, J.M., Song, J.J., Hammond, S.M., Joshua-Tor, L. and Hannon, G.J. (2004) Argonaute2 is the catalytic engine of mammalian RNAi. *Science*, **305**, 1437-1441.

Lockard, R.E. and Kumar, A. (1981) Mapping tRNA structure in solution using double-strand-specific ribonuclease V1 from cobra venom. *Nucleic Acids Res*, **9**, 5125-5140.

Lykke-Andersen, J. (2002) Identification of a human decapping complex associated with hUpf proteins in nonsense-mediated decay. *Mol Cell Biol*, **22**, 8114-8121.

Ma, W.J. and Furneaux, H. (1997) Localization of the human HuR gene to chromosome 19p13.2. *Hum Genet*, **99**, 32-33.

Mackie, G.A. (1998) Ribonuclease E is a 5'-end-dependent endonuclease. *Nature*, **395**, 720-723.

Marenstein, D.R., Wilson, D.M., 3rd and Teebor, G.W. (2004) Human AP endonuclease (APE1) demonstrates endonucleolytic activity against AP sites in single-stranded DNA. *DNA Repair (Amst)*, **3**, 527-533.

Maris, C., Dominguez, C. and Allain, F.H. (2005) The RNA recognition motif, a plastic RNA-binding platform to regulate post-transcriptional gene expression. *Febs J*, **272**, 2118-2131.

Martinez, J. and Tuschl, T. (2004) RISC is a 5' phosphomonoester-producing RNA endonuclease. *Genes Dev*, **18**, 975-980.

Mastronicola, M.R., Piccoli, R. and D'Alessio, G. (1995) Key extracellular and intracellular steps in the antitumor action of seminal ribonuclease. *Eur J Biochem*, **230**, 242-249.

Meyer, S., Temme, C. and Wahle, E. (2004) Messenger RNA turnover in eukaryotes: pathways and enzymes. *Crit Rev Biochem Mol Biol*, **39**, 197-216.

Mishra, V., Lal, R. and Srinivasan. (2001) Enzymes and operons mediating xenobiotic degradation in bacteria. *Crit Rev Microbiol*, **27**, 133-166.

Mitchell, P. and Tollervey, D. (2001) mRNA turnover. *Curr Opin Cell Biol*, **13**, 320-325.

Mitchell, P. and Tollervey, D. (2003) An NMD pathway in yeast involving accelerated deadenylation and exosome-mediated 3'-->5' degradation. *Mol Cell*, **11**, 1405-1413.

Mol, C.D., Hosfield, D.J. and Tainer, J.A. (2000) Abasic site recognition by two apurinic/apyrimidinic endonuclease families in DNA base excision repair: the 3' ends justify the means. *Mutat Res*, **460**, 211-229.

Mori, K., Kawahara, T., Yoshida, H., Yanagi, H. and Yura, T. (1996) Signalling from endoplasmic reticulum to nucleus: transcription factor with a basic-leucine zipper motif is required for the unfolded protein-response pathway. *Genes Cells*, **1**, 803-817.

Morimoto, R.I. (1998) Regulation of the heat shock transcriptional response: cross talk between a family of heat shock factors, molecular chaperones, and negative regulators. *Genes Dev*, **12**, 3788-3796.

Muhlrad, D. and Parker, R. (1994) Premature translational termination triggers mRNA decapping. *Nature*, **370**, 578-581.

Mukherjee, D., Gao, M., O'Connor, J.P., Raijmakers, R., Pruijn, G., Lutz, C.S. and Wilusz, J. (2002) The mammalian exosome mediates the efficient degradation of mRNAs that contain AU-rich elements. *Embo J*, **21**, 165-174.

Nagy, E., Henics, T., Eckert, M., Miseta, A., Lightowlers, R.N. and Kellermayer, M. (2000) Identification of the NAD(+)-binding fold of glyceraldehyde-3-phosphate dehydrogenase as a novel RNA-binding domain. *Biochem Biophys Res Commun*, **275**, 253-260.

Nagy, E. and Rigby, W.F. (1995) Glyceraldehyde-3-phosphate dehydrogenase selectively binds AU-rich RNA in the NAD(+)-binding region (Rossmann fold). *J Biol Chem*, **270**, 2755-2763.

Nicholson, R.H. and Nicholson, A.W. (2002) Molecular characterization of a mouse cDNA encoding Dicer, a ribonuclease III ortholog involved in RNA interference. *Mamm Genome*, **13**, 67-73.

Nielsen, J., Christiansen, J., Lykke-Andersen, J., Johnsen, A.H., Wewer, U.M. and Nielsen, F.C. (1999) A family of insulin-like growth factor II mRNA-binding proteins represses translation in late development. *Mol Cell Biol*, **19**, 1262-1270.

Nikawa, J. and Yamashita, S. (1992) IRE1 encodes a putative protein kinase containing a membrane-spanning domain and is required for inositol phototrophy in Saccharomyces cerevisiae. *Mol Microbiol*, **6**, 1441-1446.

Niwa, M., Patil, C.K., DeRisi, J. and Walter, P. (2005) Genome-scale approaches for discovering novel nonconventional splicing substrates of the Ire1 nuclease. *Genome Biol*, **6**, R3.

Niwa, M., Sidrauski, C., Kaufman, R.J. and Walter, P. (1999) A role for presenilin-1 in nuclear accumulation of Ire1 fragments and induction of the mammalian unfolded protein response. *Cell*, **99**, 691-702.

Offringa, M., Hazebroek-Kampschreur, A.A. and Derksen-Lubsen, G. (1991) Prevalence of febrile seizures in Dutch schoolchildren. *Paediatr Perinat Epidemiol*, **5**, 181-188.

Okazaki, T., Ando, K., Igarashi, T., Ogata, E. and Fujita, T. (1992) Conserved mechanism of negative gene regulation by extracellular calcium. Parathyroid hormone gene versus atrial natriuretic polypeptide gene. *J Clin Invest*, **89**, 1268-1273.

Okazaki, T., Chung, U., Nishishita, T., Ebisu, S., Usuda, S., Mishiro, S., Xanthoudakis, S., Igarashi, T. and Ogata, E. (1994) A redox factor protein, ref1, is involved in negative gene regulation by extracellular calcium. *J Biol Chem*, **269**, 27855-27862.

Pandey, M. and Rath, P.C. (2004) Expression of interferon-inducible recombinant human RNase L causes RNA degradation and inhibition of cell growth in Escherichia coli. *Biochem Biophys Res Commun*, **317**, 586-597.

Park, J., Kim, C. and Gupta, S. (2000) Differential transcriptional regulation of silencer of death domains in cord blood and peripheral blood lymphocytes. *Int J Mol Med*, **6**, 289-293.

Parker, J.S., Roe, S.M. and Barford, D. (2004) Crystal structure of a PIWI protein suggests mechanisms for siRNA recognition and slicer activity. *Embo J*, **23**, 4727-4737.

Parker, R. and Song, H.W. (2004) The enzymes and control of eukaryotic mRNA turnover. *Nature Structural & Molecular Biology*, **11**, 121-127.

Peng, Y. and Schoenberg, D.R. (2007) c-Src activates endonuclease-mediated mRNA decay. *Mol Cell*, **25**, 779-787.

Perez-Canadillas, J.M. and Varani, G. (2001) Recent advances in RNA-protein recognition. *Curr Opin Struct Biol*, **11**, 53-58.

Piccoli, R., De Lorenzo, C., Dal Piaz, F., Pucci, P. and D'Alessio, G. (2000) Trypsin sheds light on the singular case of seminal RNase, a dimer with two quaternary conformations. *J Biol Chem*, **275**, 8000-8006.

Pillai, S. (2005) Birth pangs: the stressful origins of lymphocytes. *J Clin Invest*, **115**, 224-227.

Prokipcak, R.D., Herrick, D.J. and Ross, J. (1994) Purification and properties of a protein that binds to the C-terminal coding region of human c-myc mRNA. *J Biol Chem*, **269**, 9261-9269.

Rao, K.S., Sirdeshmukh, R. and Gupta, P.D. (1994) Modulation of cytosolic RNase activity by endogenous RNase inhibitor in rat vaginal epithelial cells on estradiol administration. *FEBS Lett*, **343**, 11-14.

Rao, S.T. and Rossmann, M.G. (1973) Comparison of super-secondary structures in proteins. *J Mol Biol*, **76**, 241-256.

Regonesi, M.E., Del Favero, M., Basilico, F., Briani, F., Benazzi, L., Tortora, P., Mauri, P. and Deho, G. (2006) Analysis of the Escherichia coli RNA degradosome composition by a proteomic approach. *Biochimie*, **88**, 151-161.

Reimold, A.M., Iwakoshi, N.N., Manis, J., Vallabhajosyula, P., Szomolanyi-Tsuda, E., Gravallese, E.M., Friend, D., Grusby, M.J., Alt, F. and Glimcher, L.H. (2001) Plasma cell differentiation requires the transcription factor XBP-1. *Nature*, **412**, 300-307.

Ribo, M., Beintema, J.J., Osset, M., Fernandez, E., Bravo, J., De Llorens, R. and Cuchillo, C.M. (1994) Heterogeneity in the glycosylation pattern of human pancreatic ribonuclease. *Biol Chem Hoppe Seyler*, **375**, 357-363.

Richardson, W.H. (1964) Frequencies of genotypes of relatives, as determined by stochastic matrices. *Genetica*, **35**, 323-354.

Rodgers, N.D., Wang, Z. and Kiledjian, M. (2002) Characterization and purification of a mammalian endoribonuclease specific for the alpha -globin mRNA. *J Biol Chem*, **277**, 2597-2604.

Rosenberg, H.F., Dyer, K.D. and Li, F. (1996) Characterization of eosinophils generated in vitro from CD34+ peripheral blood progenitor cells. *Exp Hematol*, **24**, 888-893.

Ross, J. (1995) mRNA stability in mammalian cells. *Microbiol Rev*, **59**, 423-450.

Ross, J. (1996) Control of messenger RNA stability in higher eukaryotes. *Trends Genet*, **12**, 171-175.

Ross, J., Lemm, I. and Berberet, B. (2001) Overexpression of an mRNA-binding protein in human colorectal cancer. *Oncogene*, **20**, 6544-6550.

Rouault, T. and Klausner, R. (1997) Regulation of iron metabolism in eukaryotes. *Curr Top Cell Regul*, **35**, 1-19.

Rudd, P.M., Joao, H.C., Coghill, E., Fiten, P., Saunders, M.R., Opdenakker, G. and Dwek, R.A. (1994) Glycoforms modify the dynamic stability and functional activity of an enzyme. *Biochemistry*, **33**, 17-22.

Saxena, S.K., Rybak, S.M., Davey, R.T., Jr., Youle, R.J. and Ackerman, E.J. (1992) Angiogenin is a cytotoxic, tRNA-specific ribonuclease in the RNase A superfamily. *J Biol Chem*, **267**, 21982-21986.

Schauer, R.C. (1991) Effects of estradiol and progesterone on rat uterine ribonuclease inhibitor activity. *Horm Metab Res*, **23**, 162-165.

Schiavi, S.C., Wellington, C.L., Shyu, A.B., Chen, C.Y., Greenberg, M.E. and Belasco, J.G. (1994) Multiple elements in the c-fos protein-coding region facilitate mRNA deadenylation and decay by a mechanism coupled to translation. *J Biol Chem*, **269**, 3441-3448.

Schoenberg, D.R. and Cunningham, K.S. (1999) Characterization of mRNA endonucleases. *Methods*, **17**, 60-73.

Sen, G.C. and Lengyel, P. (1992) The interferon system. A bird's eye view of its biochemistry. *J Biol Chem*, **267**, 5017-5020.

Sen, G.L. and Blau, H.M. (2006) A brief history of RNAi: the silence of the genes. *Faseb J*, **20**, 1293-1299.

Shamu, C.E. and Walter, P. (1996) Oligomerization and phosphorylation of the Ire1p kinase during intracellular signaling from the endoplasmic reticulum to the nucleus. *Embo J*, **15**, 3028-3039.

Shapiro, R., Riordan, J.F. and Vallee, B.L. (1986) Characteristic ribonucleolytic activity of human angiogenin. *Biochemistry*, **25**, 3527-3532.

Sheth, U. and Parker, R. (2003) Decapping and decay of messenger RNA occur in cytoplasmic processing bodies. *Science*, **300**, 805-808.

Silverman, R.H. (2003) Implications for RNase L in prostate cancer biology. *Biochemistry*, **42**, 1805-1812.

Singhania, N.A., Dyer, K.D., Zhang, J., Deming, M.S., Bonville, C.A., Domachowske, J.B. and Rosenberg, H.F. (1999) Rapid evolution of the ribonuclease A superfamily: adaptive expansion of independent gene clusters in rats and mice. *J Mol Evol*, **49**, 721-728.

Siomi, H. and Dreyfuss, G. (1997) RNA-binding proteins as regulators of gene expression. *Curr Opin Genet Dev*, **7**, 345-353.

Sitia, R. and Braakman, I. (2003) Quality control in the endoplasmic reticulum protein factory. *Nature*, **426**, 891-894.

Sorrentino, S. (1998) Human extracellular ribonucleases: multiplicity, molecular diversity and catalytic properties of the major RNase types. *Cell Mol Life Sci*, **54**, 785-794.

Sorrentino, S. and Libonati, M. (1994) Human pancreatic-type and nonpancreatic-type ribonucleases: a direct side-by-side comparison of their catalytic properties. *Arch Biochem Biophys*, **312**, 340-348.

Sorrentino, S. and Libonati, M. (1997) Structure-function relationships in human ribonucleases: main distinctive features of the major RNase types. *FEBS Lett*, **404**, 1-5.

Sorrentino, S., Tucker, G.K. and Glitz, D.G. (1988) Purification and characterization of a ribonuclease from human liver. *J Biol Chem*, **263**, 16125-16131.

Sparanese, D. and Lee, C.H. (2007) CRD-BP shields c-myc and MDR-1 RNA from endonucleolytic attack by a mammalian endoribonuclease. *Nucleic Acids Res*, **35**, 1209-1221.

Steege, D.A. (2000) Emerging features of mRNA decay in bacteria. *Rna*, **6**, 1079-1090.

Stevens, A. (1998) Endonucleolytic cleavage of RNA at 5' endogenous stem structures by human flap endonuclease 1. *Biochem Biophys Res Commun*, **251**, 501-508.

Stevens, A., Wang, Y., Bremer, K., Zhang, J., Hoepfner, R., Antoniou, M., Schoenberg, D.R. and Maquat, L.E. (2002) Beta -Globin mRNA decay in erythroid cells: UG site-preferred endonucleolytic cleavage that is augmented by a premature termination codon. *Proc Natl Acad Sci U S A*, **99**, 12741-12746.

Stoeckle, M.Y. (1992) Removal of a 3' non-coding sequence is an initial step in degradation of gro alpha mRNA and is regulated by interleukin-1. *Nucleic Acids Res*, **20**, 1123-1127.

Stoecklin, G., Lu, M., Rattenbacher, B. and Moroni, C. (2003) A constitutive decay element promotes tumor necrosis factor alpha mRNA degradation via an AU-rich element-independent pathway. *Mol Cell Biol*, **23**, 3506-3515.

Stoecklin, G., Stubbs, T., Kedersha, N., Wax, S., Rigby, W.F., Blackwell, T.K. and Anderson, P. (2004) MK2-induced tristetraprolin:14-3-3 complexes prevent stress granule association and ARE-mRNA decay. *Embo J*, **23**, 1313-1324.

Tebo, J.M., Datta, S., Kishore, R., Kolosov, M., Major, J.A., Ohmori, Y. and Hamilton, T.A. (2000) Interleukin-1-mediated stabilization of mouse KC mRNA depends on sequences in both 5'- and 3'-untranslated regions. *J Biol Chem*, **275**, 12987-12993.

Tessier, C.R., Doyle, G.A., Clark, B.A., Pitot, H.C. and Ross, J. (2004) Mammary tumor induction in transgenic mice expressing an RNA-binding protein. *Cancer Res*, **64**, 209-214.

Tharun, S., He, W., Mayes, A.E., Lennertz, P., Beggs, J.D. and Parker, R. (2000) Yeast Sm-like proteins function in mRNA decapping and decay. *Nature*, **404**, 515-518.

Tharun, S. and Parker, R. (2001) Targeting an mRNA for decapping: displacement of translation factors and association of the Lsm1p-7p complex on deadenylated yeast mRNAs. *Mol Cell*, **8**, 1075-1083.

Theodorakis, N.G. and Morimoto, R.I. (1987) Posttranscriptional regulation of hsp70 expression in human cells: effects of heat shock, inhibition of protein synthesis, and adenovirus infection on translation and mRNA stability. *Mol Cell Biol*, **7**, 4357-4368.

Thompson, D.C. and Reed, M. (1995) Inhibition of NAD(H)/NADP(H)--requiring enzymes by aurintricarboxylic acid. *Toxicol Lett*, **81**, 141-149.

Tirasophon, W., Lee, K., Callaghan, B., Welihinda, A. and Kaufman, R.J. (2000) The endoribonuclease activity of mammalian IRE1 autoregulates its mRNA and is required for the unfolded protein response. *Genes & Development*, **14**, 2725-2736.

Tourriere, H., Chebli, K., Zekri, L., Courselaud, B., Blanchard, J.M., Bertrand, E. and Tazi, J. (2003) The RasGAP-associated endoribonuclease G3BP assembles stress granules. *J Cell Biol*, **160**, 823-831.

Tourriere, H., Gallouzi, I.E., Chebli, K., Capony, J.P., Mouaikel, J., van der Geer, P. and Tazi, J. (2001) RasGAP-associated endoribonuclease G3Bp: selective RNA degradation and phosphorylation-dependent localization. *Mol Cell Biol*, **21**, 7747-7760.

Tucker, M. and Parker, R. (2000) Mechanisms and control of mRNA decapping in Saccharomyces cerevisiae. *Annu Rev Biochem*, **69**, 571-595.

van Dijk, E.L., Sussenbach, J.S. and Holthuizen, P.E. (2000) Distinct RNA structural domains cooperate to maintain a specific cleavage site in the 3'-UTR of IGF-II mRNAs. *J Mol Biol*, **300**, 449-467.

van Hoof, A., Frischmeyer, P.A., Dietz, H.C. and Parker, R. (2002) Exosome-mediated recognition and degradation of mRNAs lacking a termination codon. *Science*, **295**, 2262-2264.

Varmus, H.E. (1984) The molecular genetics of cellular oncogenes. *Annu Rev Genet*, **18**, 553-612.

Venter, J.C., Adams, M.D., Myers, E.W (2001) The sequence of the human genome. *Science*, **291**, 1304-1351.

Wang, Z. and Kiledjian, M. (2000) Identification of an erythroid-enriched endoribonuclease activity involved in specific mRNA cleavage. *Embo J*, **19**, 295-305.

Wennborg, A., Classon, M., Klein, G. and von Gabain, A. (1995) Downregulation of c-myc expression after heat shock in human B-cell lines is independent of 5' mRNA sequences. *Biol Chem Hoppe Seyler*, **376**, 671-680.

Wickens, M. and Gonzalez, T.N. (2004) Molecular biology. Knives, accomplices, and RNA. *Science*, **306**, 1299-1300.

Wilkinson, M.F. and Shyu, A.B. (2001) Multifunctional regulatory proteins that control gene expression in both the nucleus and the cytoplasm. *Bioessays*, **23**, 775-787.

Wilson, G.M. and Brewer, G. (1999a) Identification and characterization of proteins binding A + U-rich elements. *Methods*, **17**, 74-83.

Wilson, G.M. and Brewer, G. (1999b) The search for trans-acting factors controlling messenger RNA decay. *Progress in Nucleic Acid Research and Molecular Biology, Vol 62*, **62**, 257-291.

Wrana, J.L., Attisano, L., Wieser, R., Ventura, F. and Massague, J. (1994) Mechanism of activation of the TGF-beta receptor. *Nature*, **370**, 341-347.

Xanthoudakis, S., Miao, G., Wang, F., Pan, Y.C. and Curran, T. (1992) Redox activation of Fos-Jun DNA binding activity is mediated by a DNA repair enzyme. *Embo J*, **11**, 3323-3335.

Yang, F. and Schoenberg, D.R. (2004) Endonuclease-mediated mRNA decay involves the selective targeting of PMR1 to polyribosome-bound substrate mRNA. *Mol Cell*, **14**, 435-445.

Yang, J., Schuster, G. and Stern, D.B. (1996) CSP41, a sequence-specific chloroplast mRNA binding protein, is an endoribonuclease. *Plant Cell*, **8**, 1409-1420.

Ye, B., Skates, S., Mok, S.C., Horick, N.K., Rosenberg, H.F., Vitonis, A., Edwards, D., Sluss, P., Han, W.K., Berkowitz, R.S. and Cramer, D.W. (2006) Proteomic-based discovery and characterization of glycosylated eosinophil-derived neurotoxin and COOH-terminal osteopontin fragments for ovarian cancer in urine. *Clin Cancer Res*, **12**, 432-441.

Yoshida, T., Miyazawa, K., Kasuga, I., Yokoyama, T., Minemura, K., Ustumi, K., Aoshima, M. and Ohyashiki, K. (2003) Apoptosis induction of vitamin K2 in lung carcinoma cell lines: the possibility of vitamin K2 therapy for lung cancer. *Int J Oncol*, **23**, 627-632.

Zekri, L., Chebli, K., Tourriere, H., Nielsen, F.C., Hansen, T.V., Rami, A. and Tazi, J. (2005) Control of fetal growth and neonatal survival by the RasGAP-associated endoribonuclease G3BP. *Mol Cell Biol*, **25**, 8703-8716.

Zhang, H., Kolb, F.A., Jaskiewicz, L., Westhof, E. and Filipowicz, W. (2004) Single processing center models for human Dicer and bacterial RNase III. *Cell*, **118**, 57-68.

Zhang, J., Dyer, K.D. and Rosenberg, H.F. (2000) Evolution of the rodent eosinophil-associated RNase gene family by rapid gene sorting and positive selection. *Proc Natl Acad Sci U S A*, **97**, 4701-4706.

Zhang, J., Dyer, K.D. and Rosenberg, H.F. (2002) RNase 8, a novel RNase A superfamily ribonuclease expressed uniquely in placenta. *Nucleic Acids Res*, **30**, 1169-1175.

Zhang, K.Z., Wong, H.N., Song, B.B., Miller, C.N., Scheuner, D. and Kaufman, R.J. (2005) The unfolded protein response sensor IRE1 alpha is required at 2 distinct steps in B cell lymphopoiesis. *Journal of Clinical Investigation*, **115**, 268-281.

Zhao, W., Kote-Jarai, Z., van Santen, Y., Hofsteenge, J. and Beintema, J.J. (1998) Ribonucleases from rat and bovine liver: purification, specificity and structural characterization. *Biochim Biophys Acta*, **1384**, 55-65.

Zhou, H.M. and Strydom, D.J. (1993) The amino acid sequence of human ribonuclease 4, a highly conserved ribonuclease that cleaves specifically on the 3' side of uridine. *Eur J Biochem*, **217**, 401-410.